ASYNCHRONOUS BI-DIRECTIONAL RELAY-ASSISTED COMMUNICATION NETWORKS

By

Reza Vahidnia

A THESIS SUBMITTED IN PARTIAL FULFILLMENT OF THE
REQUIREMENTS FOR THE DEGREE OF
DOCTOR OF PHILOSOPHY
IN
THE FACULTY OF ENGINEERING AND APPLIED SCIENCE
ELECTRICAL AND COMPUTER ENGINEERING
UNIVERSITY OF ONTARIO INSTITUTE OF TECHNOLOGY
FEBRUARY 2014

Abstract

We consider an asynchronous bi-directional relay network, consisting of two single-antenna transceivers and multiple single-antenna relays, where the transceiver-relay paths are subject to different relaying and/or propagation delays. Such a network can be viewed as a multipath channel which can cause inter-symbol-interference (ISI) in the signals received by the two transceivers. Hence, we model such a communication scheme as a frequency selective multipath channel which produces ISI at the two transceivers, when the data rates are relatively high. We study both multi- and single-carrier communication schemes in such networks.

In a multi-carrier communication scheme, to tackle ISI, the transceivers employ an orthogonal frequency division multiplexing (OFDM) scheme to diagonalize the end-to-end channel. The relays use simple amplify-and-forward relaying, thereby materializing a distributed beamformer. For such a scheme, we propose two different algorithms, based on the max-min fair design approach, to calculate the subcarrier power loading at the transceivers as well as the relay beamforming weights.

In a single-carrier communication, assuming a block transmission/reception scheme, block channel equalization is used at the both transceivers to combat the inter-block-interference (IBI). Assuming a limited total transmit power budget, we minimize the total mean squared error (MSE) of the estimated received signals at the both transceivers by optimally obtaining the transceivers' powers and the relay beamforming weight vector as well as the block channel equalizers at the two transceivers.

To my loving parents

Acknowledgements

I would like to express my gratitude to my supervisor Dr. Shahram Shahbazpanahi for all his support, help, and motivation. Dr. Shahbazpanahi has been always ready to support and direct me. He helped me in establishing the research skills and I hope I will carry his inspiration in my future studies and throughout my career. I would also like to thank all my colleagues, friends and classmates whose support, reviews, insights and company will always be remembered.

Of course, I am grateful to my parents for their patience and *love*. Without them this work would have never come into existence (literally).

Oshawa, Ontario — Reza Vahidnia
February, 2014

Table of Contents

List of Figures

List of Acronyms

AF	Amplify-and-Forward
CRLB	Cramer-Rao Lower Band
CSI	Channel State Information
EF	Estimate-and-Forward
EPA	Equal Power Allocation
FF	Filter-and-Forward
FIR	Finite Impulse Response
ISI	Inter-Symbol-Interference
IBI	Inter-Block-Interference
LTE	Long-Term Evolution
MABC	Multiple Access Broadcast
MIMO	Multiple Input Multiple Output
ML	Maximum Likelihood
MPA	Maximum Power Allocation
MSE	Mean Squared Error
OFDM	Orthogonal Frequency Division Multiplexing
SDP	Semi Definite Programming
SNR	Signal to Noise Ratio
SQP	Sequential Quadratic Programming
TDBC	Time Division Broadcast

Chapter 1

Introduction

1.1 Overview

Nowadays, energy conservation is considered as one of the main problems of the world. Energy resources are limited and usage of energy causes many environmental problems such as global warming, air pollution, forest destruction and emission of radioactive substances. Seeking clean and renewable energy sources and increasing the efficiency of power consuming devices are two major solutions for this problem. Since the communication devices are usually categorized as small and low power instruments, one may think that nothing further can be accomplished in order to contribute to saving the energy and maintaining our planet from the threats of global warming by conserving the energy resources for the future generations. However, recently published reports show that in the near future, wireless communication networks will consume a significant amount of energy. Network data rates are expected to increase drastically which results in a huge increase of the consumed power in broadband access technologies. Currently, because of the fact that the communication devices do not utilize the resources to their fullest extent, they appear to be inefficient in terms of spectrum and transmit power. In the recent years, several technologies have

been introduced in order to improve the efficiency of communication devices and to minimize the consumed power in such instruments. One of these technologies is to deploy spatial diversity by using multiple antennas at the transmitters and receivers in multiple input multiple output (MIMO) communication networks.

In many applications such as indoor communications, between a transmitter and the receiver, there is no clear direct link. In these cases, the transmitted signal is reflected in multiple paths before being received at the destination. These signal reflections may introduce destructive attenuations, phase shifts, time delays, and signal distortions when arriving the receiving antenna at the destination. One of the effective methods to mitigate the adverse effects of such multi-path channels is to use antenna diversity at the both transceivers. In multiple antenna transceivers, each antenna experiences a different propagation environment. For instance, if the signal received at one antenna is experiencing a deep fading channel, one can hope that the propagation path to the other antenna has the desirable signal to noise ratio (SNR). Hence, this antenna diversity can lead to a more reliable communication link between the two transceivers by decreasing the probability of occurrence of deep fading and low quality connections in the end-to-end channel. Basically, compared to single-antenna communication schemes, the hardware complexity of multiple-antenna communication networks is higher which in turn results in more complicated processing at the receivers. Therefore, in terms of antenna diversity, there exists a trade-off between complexity and reliability of the communication networks.

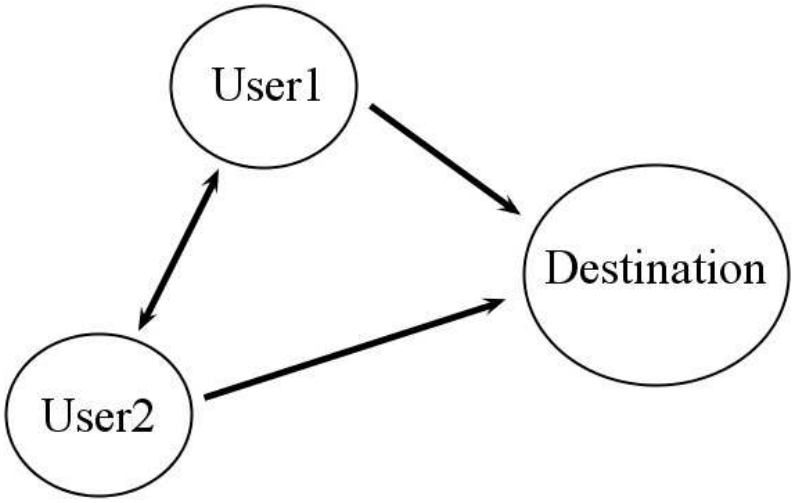

Figure 1.1: A wireless cooperative network with user cooperation.

1.2 Cooperative Communication

Not withstanding the fact that the transmit diversity has many advantages, it may not be applicable in some scenarios due to the size, power, cost and hardware restrictions. For instance, in wireless sensor networks, the size and power of the nodes are limited and this limitation may confine the utilization of the transmit diversity technology.

Recently, for multi-user environments with single-antenna users, in order to achieve transmit diversity, a new technique called cooperative communication has been introduced that enables the users to share their antennas with the other users in the network to generate a multiple-antenna transmitter [1, 2]. In a cooperative communication system, as it is shown in Figure. 1.1, each wireless user is considered to transmit its own data as well as act as a cooperative user for the other user. Users

cooperation results in a trade-off between the reliability and the transmit power. Although, cooperation of the users leads to a more robust communication link between the transceivers, on the other hand, it may be argued that users in average need more power to transmit their own data and the information of the other users. To answer this concern, it should be noted that because of the diversity, the baseline transmit power of all users is reduced. Therefore, the net transmit power of the total network may be reduced if the other factors in the network are constant. Another concern that comes to mind is that since in a cooperative communication network, each node transmits its own data as well as some of the information of the other nodes, the transmission rate of the communication link may be lowered. It is worth mentioning that the cooperation of the users increases the spectral efficiency of each user which in turn pays for the cost of lower transmission rate [1,2]. While designing cooperative communication networks, some other important issues such as hand-off and cooperation assignment, the total interference in the network, fairness of the communication link, and transmit and receive requirements should be considered.

1.3 Relay Networking

Relay network is a class of wireless communication network schemes, where both transceivers (or the source and the destination) are exchanging their information with the help of one or multiple intermediate nodes. In such communication networks, the transceivers (or the source and the destination) may not communicate with each other directly due to the low quality (because of shadowing) or non-existence of the line-of-sight link. In these types of networks, the relay nodes process(or just simply amplify) their received signals and forward them to the destination.

Cooperative relay networks can be considered as two main categories, called full-duplex and half-duplex relaying. In the full-duplex relaying scheme, the data transmission and reception of the nodes of the network is performed at the same time and in the same frequency band, while in the half-duplex scheme, the relaying nodes transmit and receive their information in two different time slots (in time-orthogonal channels).

Compared to half-duplex relaying, the full-duplex scheme has a higher spectral efficiency [3]. However, in full-duplex relaying, the power level difference of the transmit and received signals makes it difficult to implement [4]. On the other hand, although half-duplex relaying protocols are relatively easier for implementation, they have lower spectral efficiency compared to the full-duplex relaying due to the pre-log factor of 0.5 in the sum rate expressions [5].

1.3.1 One-way Relaying Scheme

In a conventional one-way relaying scheme, the transmission of the data is accomplished in two time slots. In the first step, the transmitters send the data to the relays. In the next time slot, the processed signals are forwarded to the receiver. Different approaches can be used to process the data at the relays. One approach is to retransmit the properly scaled and phase-shifted version of the received signal at the relays which is referred to as amplify-and-forward (AF) and is desirable when the noise power at the relays is very low compared to the signal power [6]. The AF technique is of particular interest because it is simple and there is no need to detect the transmitted signals at the relays. However, relay processing is limited to amplifying and adjusting the phase of the received signal before retransmitting it to

the destination(s). Decode-and-forward (DF) is another approach which is usually used when the noise at the relays is relatively high and amplifying the signals will amplify the noise as well [6]. Hence, by decoding the signals and forwarding them to the receiver, the relay noise is avoided to be sent along with the signal. Nevertheless, this process is power consuming and increases the design complexity of the relays [7]. When the channel state information (CSI) is not available at the relay nodes, distributed space-time coding can be used to obtain the cooperative diversity gain [8], [9]. However, when CSI is available, distributed network beamforming can provide better performance [10].

Filter-and-forward (FF) strategy is another relaying approach where all the relay nodes are equipped with finite impulse response (FIR) filters that are used to *equalize* the transmitter-to-relay and relay-to-destination channels.

Estimate-and-forward (EF) method (also known as compress-and-forward or quantize-and-forward) is another relaying protocol (as first introduced by Cover and Gamal [3]). In this scheme, a transformation is applied to the received signals at the relays to provide an estimate of the source signals. This estimate which is known as soft information is then forwarded to the destination.

1.3.2 Two-way Relaying Scheme

In 1961, Shannon introduced the concept of two-way communication channel and studied the communication of two transceivers in both directions at the same time [11]. In a bi-directional relay-assisted communication scheme, two transceivers exchange information with the help of one or multiple relays. Essentially, there are three different protocols to establish a two-way cooperative communication scheme. Figure. 1.2

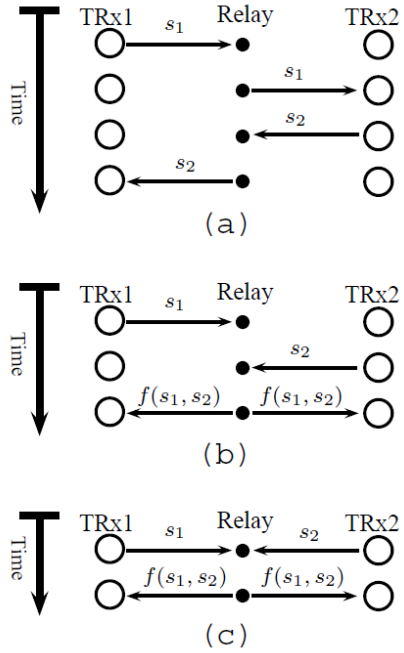

Figure 1.2: Different two-way relaying schemes. (a) Conventional approach. (b) TDBC (c) MABC

illustrates the basic ideas behind each of these three approaches. In the scheme shown in Figure. 1.2-(a), the exchange of two symbols is accomplished in four steps, where two successive one-way relaying approaches are deployed to convey one symbol in each direction.

Figure.1.2-(b) illustrates the so-called time division broadcast (TDBC) two-way relaying scheme, where the number of steps required to communicate two symbols between the two transceivers is three. Figure.1.2-(c) demonstrates the multiple access broadcast (MABC) bi-directional relaying scheme which further reduces the number of steps to two. Based on these three protocols, different bi-directional relaying

schemes have been proposed and analyzed in the literature [12–35]. The MABC approach has been studied in [12–15,19,21–29,31–34] and the TDBC technique in [16,20]. The authors of [17, 18, 30, 35] study both TDBC and MABC approaches.

1.4 Problem Statement and Motivation

In almost all the published results in two-way relay networks, the authors assume that the relays and the transceivers are perfectly time-synchronized or they ignore the fact that the propagation delays for different paths going through each relay can be different. However, considering time asynchronous relay nodes and/or assuming different relay path delays leads to the frequency selectivity of the end-to-end channel. In such scenarios, ISI is inevitable at the transceivers, even if the relay-transceiver channels are frequency flat. For instance, in long-term evolution (LTE) services with sampling 18 million samples per second, the transmitted symbol duration is 0.055 micro seconds. If the difference between the length of the paths through different relays is more than 16.66 meters ($0.055\mu s \times 3 \times 10^8 \frac{m}{s}$), the received signals at the destination will interfere with each other and induce ISI. Therefore, in such practical scenarios, mitigating such an ISI should be considered while designing the network.

In one- and two-way relay networks with frequency selective relay-transceiver channels, there appears to be two competing approaches to combat ISI at the both transceivers: The first approach suggests finite-impulse-response (FIR) filters to be used at the relays [36–43]. This approach, often called filter-and-forward (FF) technique, implements the channel equalization in a distributed manner, i.e., the relays collectively accept the burden of equalization by deploying FIR filters. The FF approach can be viewed as a single-carrier equalization scheme. In the second approach,

a multi-carrier equalization technique is used to compensate the frequency selectivity of the relay-transceiver channels [44]. More specifically, all the relays and the transceivers are equipped with orthogonal frequency division multiplexing (OFDM) technology to diagonalize the end-to-end channel into multiple parallel flat fading channels. While the goal in the FF approach is to optimally design the relay FIR filters (and possibly the transceiver transmit powers), the objective in the OFDM-based method is to allocate power judiciously across different subcarriers as well as among different nodes including the relays and the two transceivers. Although these two schemes combat the ISI (caused by the frequency selectivity of relay-transceiver channels) in two seemingly different ways, they both require the relays to undertake a rather complicated processing, let it be deploying OFDM schemes or using FIR filters at the relays. Such complicated relay processing may not be needed, in particular, when the relay-transceiver channels are frequency flat but the end-to-end channel exhibits frequency selectivity due to the difference in the arrival times of the relay signals to each of the two transceivers. In fact, the relay nodes may not be perfectly time-synchronized and/or the signal paths going through different relays could be subject to different propagation delays. These two phenomena will cause the relay signals arrive at each transceiver at different times, thus leading to the frequency selectivity of the end-to-end channel, even though the relay-transceiver channels are frequency flat. In this thesis, considering a frequency selective end-to-end channel between the two transceivers, we study the single- and multi-carrier asynchronous two-way relay networks where the relays are simply amplifying their received signals and the equalization is performed at the two transceivers. Since to the best of our knowledge, the concept of bi-directional asynchronous relay networks is new and has

not been widely studied in the literature, we are motivated to improve the performance of such communication links by modeling these networks and then optimizing metrics such as SNR and MSE under the individual and total power constraints. We aim to perform this improvement in the networks by optimally obtaining the relay beamforming weight vector and the transceivers' powers as well as designing the required equalizations at the both transceivers.

1.5 Methodology

For both multi-carrier and single-carrier communication schemes, we develop our system model of a two-way relay network, where different relay paths have different propagation/processing delays. Such a two-way relay channel can be viewed as a multipath end-to-end channel whose impulse response can be optimally designed by judiciously obtaining the relay beamforming weights.

For the multi-carrier communication scheme, we study the application of OFDM at the two transceivers, while the relays use simple AF relaying protocol. Doing so, we then consider the problem of joint subcarrier power allocation and distributed beamforming. This aspect of our work is new and has not been studied in the literature. We present two different optimization problems with two different objective functions, each of which targets a different optimality criterion. Each of these optimality criteria is well-justified for a certain scenario. We then show how each optimization problem can be solved using efficient optimization techniques. Obtaining the solutions to these optimization problems is by no-means trivial as we need to carefully examine the structure of each problem.

For the single-carrier communication using block transmission/reception scheme,

we model the transceivers received signals, the end-to-end channel and the total received noise at each transceiver for an asynchronous two-way AF relay network, where the transceivers are equipped with post-channel equalizers to combat ISI. We then present an optimization problem to optimally obtain the block channel equalizers as well as the relay weight vector and the transceivers' transmit powers under a total power budget in order to minimize the total MSE at the both transceivers.

In a single-carrier communication scheme similar to the one described above, we deploy pre-channel equalization at the two transceivers. Then, we formulate and solve the problem of minimizing the total MSE at the two transceivers under a total transmit power budget. We also analyze and compare the performance of the pre- and post-channel block equalizer schemes and show the advantages of each approach.

1.6 Outline of Dissertation

In this thesis, we focus on asynchronous two-way relay networks over multi- and single-carrier communication schemes. The remainder of this thesis is organized as follows: In Chapter 2, we first review the recent research results on power allocation with perfect channel state information. Then, we proceed to the recent solutions to obtain channel estimation in two-way relay networks. In Chapter 3, we study joint subcarrier power allocation and network beamforming in asynchronous bi-directional relay networks using a multi-carrier comunication scheme. For such a scheme, we propose two different algorithms, based on the max-min fair design approach, to calculate the subcarrier power loading at the transceivers as well as the relay beamforming weights. We develop computationally efficient solutions to these two approaches. Simulation

results are presented to show that our proposed schemes outperform equal or maximum power allocation schemes. In Chapter 4, we develop our data model for a single-carrier communication scheme. We optimally obtain the transceivers' powers and the relay beamforming weight vector as well as the post-channel block equalizers at the two transceiver. We also provide simulation results to represent the performance of our proposed algorithm. In Chapter 5, designing a pre-channel block equalizer and optimally obtaining the relay beamforming weights as well as the transceivers' powers are studied for a single-carrier communication scheme. In the simulation section of this chapter, we compare the performance of the proposed algorithm with the one introduced in Chapter 4 for the post-channel equalization scheme and explain the advantages of each method. In Chapter 6, we present the concluding remarks as well as the potential future work in this area of research.

1.7 Notation

We represent the statistical expectation by $\mathrm{E}\{\cdot\}$ and use $\mathrm{tr}\{\cdot\}$ to denote the trace of a matrix. We use lowercase and uppercase boldface letters to represent the vectors and matrices, respectively. Complex conjugate, transpose, and Hermitian transpose are denoted as $(\cdot)^*$, $(\cdot)^T$, and $(\cdot)^H$, respectively. The l_2 norm of a vector $\mathbf{v}$ is represented as $\|\mathbf{v}\|$. Also, $|z|$ stands for the amplitude of the complex number z. The $N \times N$ identity matrix and the $M \times N$ all-zero matrix are denoted as $\mathbf{I}_N$ and $\mathbf{0}_{M\times N}$, respectively. We use $\mathrm{diag}(\mathbf{v})$ to represent the diagonal matrix whose diagonal entries are the elements of the vector $\mathbf{v}$. We use $\star_{\mathrm{c}}$ and $\star_{\mathrm{d}}$ to denote the continuous- and the discrete-time convolution operations, respectively. The notation $\mathbf{a} \preceq \mathbf{b}$ ($\mathbf{a} \succeq \mathbf{b}$) indicates that all entries of the vector $\mathbf{a} - \mathbf{b}$ are non-positive (non-negative).

Chapter 2

Literature Review

In this chapter, the recent studies in relay network wireless communications are discussed and the development of new approaches with their advantages and drawbacks is reviewed. Through this section, we have a look at the similar researches regarding power allocation and distributed beam-forming and rate maximization in one-way and two-way relaying schemes considering perfect and imperfect channel state information. We also review different approaches used in the papers in order to combat ISI in multi- and single-carrier modulation schemes. Moreover, we study some similar works which lead to relay selection schemes. Channel estimation techniques in bi-directional relay networks are also included in our literature survey.

Many cooperative schemes have been proposed in literature [2, 5, 8, 9, 45–50]. In some papers such as the differential transmission methods introduced in [49] and [50] it is assumed that no node in the network knows the channel information. In some other works, it is considered that the channel information at the receiver is known, but not at the relays and the transmitter. For instance, we can mention the non-coherent amplify-and-forward method studied in [46] and distributed space-time coding of [9]. Some researches have been performed assuming channel information at the receiving

side of each transmission, such as the decode-and-forward scheme introduced in [46] and [8] and the coded cooperation of [48].

The coherent amplify-and-forward scheme in [47] assumes full channel information at both relays and the receiver. Yet, only channel direction information is used at the relays. In all these cooperative methods, the relays always cooperate using their highest powers. In none of the above papers it is allowed for the relays to adaptively adjust their transmit powers in accordance with the channel magnitude information. This concern has been studied in [51].

2.1 Power Allocation with Perfect Channel State Information

Optimal power allocation (OPA) in AF networks has been studied recently in many literatures [52–55]. Most of these papers (e.g., [52–54]) focus on the single-relay networks, and solve for the optimal power division between the source and the intermediate relay nodes. OPA in multi-hop systems was discussed in [55], where the relay nodes are employed for the purpose of extending the coverage area, and not for the sake of diversity.

2.1.1 Distributed Beamforming

For different relaying strategies, the problem of power allocation between the source and the relay node(s) has been well studied in the literature [56].

In [10] and [51], considering cooperative one-way relays, a distributed beamforming

strategy is proposed with individual relay power constraints. Relays are assumed to simply amplify their received signal with an adjusted complex weight. In [51] it is assumed that the relays know the instantaneous CSI for both transmitter to the relay and relay to the receiver links which makes the relays match their weight's phase with the total phase of the link. Hence, the only parameter which needs to be determined is the amplitude of the weights of the relays and therefore, the researchers are dealing with a distributed power control problem where they maximize the SNR at the receiver, while guaranteeing that the individual relay powers meet the required constraints.

Assuming frequency selective channels, a relay network of one transmitter, one destination, and multiple relay nodes is considered in [36]. In the literature, researchers have proposed a filter-and-forward relaying protocol in order to compensate the effect of such frequency selective channels. Hence, for the purpose of compensating the transmitter-to-relay and relay-to-destination channels, all the relay nodes are equipped with FIR filters . In [57] a network modeled as an artificial multipath channel, where each path corresponds to a particular relay is considered. While the relays use amplify-and-forward technique, OFDM processing is applied only at the source and destination nodes. Thus, compared to [36] the relays remain simple and inexpensive. In contrast with the conventional multipath channel models where there exists no control on the channel impulse response, in this model by adjusting the relays complex weights, the channel taps can be controlled.

In [58] having a one-way relay network with a source, a destination and R relays and with the assumption of known second-order statistics of the channel coefficients, two different beamforming designs are proposed in a distributed manner. In their

first approach, researchers minimize the total transmit power subject to a certain guaranteed quality of service for the receiver and obtain a closed-form solution. In their second proposed approach, they design the beamforming weights such that the receiver SNR is maximized, subject to the total transmit power (with a closed-form solution) and individual relay power constraints. It is shown that the SNR optimization problem with individual relay power constraints leads to a sequential quadratic programming (SQP) optimization problem which using a semi-definite relaxation, can be converted into a convex feasibility semi-definite programming (SDP). The provided simulation results show that satisfying the quality of signal becomes much more difficult when the uncertainty in the channel state information is increased.

In [59] an SNR balancing approach has been developed for a bi-directional AF relay network where all nodes are equipped with single antenna. In the proposed SNR balancing technique introduced in this paper, the smallest of the two transceiver SNRs is maximized subject to the total transmit power budget and using an iterative procedure a unique solution has been obtained for this optimization problem. The researchers have proved that for any channel realization, half of the maximum power budget is allocated to the both transceivers and the remaining half is shared among all the relays. For the aforementioned network, a semi-closed-form solution has been presented in [27]. A simple bi-section method is used to obtain the transmit power of one of the two transceivers. Then, it has been shown that the relay beamforming weight vector has a closed-form solution. Numerical results demonstrate that by using the proposed solution, the computational complexity is much lower.

2.1.2 Sum-Rate Maximization

Maximizing the capacity of the relaying networks has attracted a significant amount of interest, where researchers try to maximize the sum-rate of the network, subject to different constraints. In [60] a beamformer has been designed for an amplify-and-forward bi-directional network with two transceivers and several relays, considering MABC relaying scheme. The channel between the nodes are assumed to be flat fading and mutually uncorrelated. Moreover, the channels are assumed to be reciprocal. The beamforming coefficients are designed in such a way that sum-rate of the network is maximized under the total relay power constraint. It is shown that since the objective function of the optimization problem introduced in this work, is the product of the two fractional quadratic functions, it is neither convex nor concave. The researchers use a so called branch-and-bound algorithm to obtain the global optimal solution for this optimization problem. They also address a sub-optimal solution which has less complexity and optimizes the cost function only over one real variable. In their simulation results they show that this sub-optimal solution suffers small sum-rate losses in comparison with the optimal solution.

In [28], for the same system setup described in [60], the sum-rate maximization problem has been solved under the total transmit power constraint. Based on the shape of the obtained achievable rate region, the researchers have proved that the sum-rate maximization problem is equivalent to an SNR balancing approach where the minimum SNR of the two transceivers is maximized under the assumption that the total transmit power of the network is limited.

In [61], again for the same system model described in [28], three different relaying schemes on the basis of their maximal capacity have been studied. In the first

scenario, one-directional transmission with two time stages is considered. In the first time slot, the signal is transmitted to the relays and in the next phase, the relays retransmit the signal to the destination. The authors have considered the problem of maximizing the SNR by obtaining the relay weight vector, subject to a limited power for the transmitter and the relay nodes. This problem is shown to be equivalent to maximizing the sum-capacity of the two-phase scheme introduced in [27], and it can be solved using a simple bi-section search. In the second scenario, the authors of the paper, maximize the capacity of a traditional four-phase scheme which consists of two sequential one-directional transmissions. Moreover, they show that if the total available power of the two time slots is the half of the total available power of the four time slots, the maximum sum-capacity of the fair four-phase scheme is equal to the maximal capacity of the one-directional scheme. In the third scenario introduced in the paper, an upper bound for the maximum sum-capacity for the three-phase scheme (TDBC) is derived. Through the simulation results, it has been shown that if the total available power is high, the two-phase scheme gives the highest sum-capacity in comparison with the traditional four-phase and the three-phase schemes.

2.1.3 Relay Selection

In many publications, with a known and fixed channel information, the researchers aim to design and/or obtain a relaying method for the purpose of optimizing the outage probability or the throughput of a communication network, or as it is performed in [5], [62] and [63], they are looking to minimize the error rate for a certain cooperative coding scheme. In the aforementioned papers, the relays are assumed to act as both the relay and the source or the cooperation of the relays is already

determined [64]. Nonetheless, this is not always the case and the cooperation of the relays may not necessarily be known and the active relays can be selected among the available nodes of the communication network.

The researchers in [65] and [66], have introduced relay selection methods, to optimize the frame error rate and/or the outage probability of the communication network by choosing a selection of relays among a specific number of relays. In [64] assuming a single source and destination and N uniformly distributed relays, a relay selection in a wireless cooperative network has been studied in order to minimize the total transmission time of a fixed amount of data. Assuming flat fading channels between the terminals and the relays and considering decode-and-forward transmission at the relays, a cooperative transmission protocol consisting of two phases can be considered. In the first phase which is called the listening phase, the data is transmitted to the relays with the assumption that no information can be received at the destination (There is no direct link between the source and the destination). According to an appropriate relay selection criterion, the source determines the cooperation of each relay and thus the time allocated to the listening phase is set to guarantee that all selected relays can correctly decode the transmitted data from the source. In the next phase (cooperative phase), the source and the selected relays cooperate to transmit the data to the destination. It is assumed that each relay has the same average transmit power P as the source terminal. In this paper, a so called best expectation criterion is proposed which selects the optimal set of relays which minimizes the total transmission time.

Using a dynamically selected best relay to decode and forward the data from a

source to a destination, is a practical and common paradigm in cooperative communication systems. Such systems consist of two phases, called the relay selection phase and the data transmission phase. In the relay selection phase, the system selects the best relay by using transmission time and energy. In the data transmission phase, the system transmits the data using the spatial diversity benefits of relay selection. A closed-form expression for the overall throughput and energy consumption is derived in [67]. A baseline non-adaptive system and several adaptive systems are analyzed which adapt the selection phase, relay transmission power, or transmission time. The time and energy trade-off between the selection and data transmission phases is also studied. The results presented in this paper, show that the selection phases time and energy overhead can be significant while selection gives great benefits. Indeed, at the optimum, the selection depends on the mode of adaptation and number of the relays and can be imperfect. The represented results also provide guidelines about the optimal system operating point for different modes of adaptation.

The idea of single relay selection to multiple relay selection has been generalized in [68] considering a one-way AF relay network. The researchers have assumed that each relay only knows its own channels, while the receiver knows all the channel values through training. Under the assumption that each node of the communication network has a power limit, the achievable diversity of some existing single relay selection schemes is derived and multiple relay selection schemes including SNR-maximizing and SNR-suboptimal have been discussed. It has been shown that these schemes achieve full diversity and low error rates. The number of cooperating relays of these schemes varies with the channel values. However, unlike the selection DF in [8], whether a relay cooperates depends on not only its own channels but also all others.

Moreover, unlike the proposed scheme in [69], all relays share the same communication channel.

2.2 Power Allocation and Channel Estimation

A significant amount of work on channel estimation in one-way relay networks have been done [70–75]. However, as two-way relay networks are being more studied in the literature, it seems that different channel estimation methods need to be investigated. compared to one-way relaying networks, channel estimation in bi-directional relay systems is more complicated due to the fact that the estimates are not only needed for coherently detecting the transmitted signals, but also for cancelling the self-interference signals at the both transceivers.

Many works in the field of relay-assisted communication, assume perfect channel knowledge. Nonetheless, obtaining the accurate channel state is crucial. In [76], two terminals are considered to exchange their data through a relay node in a bi-directional manner where the terminals and the relay are equipped with a single antenna. The authors aim at maximizing the effective received SNR after considering the channel estimation errors. In order to estimate the channel state information under amplify-and-forward relaying scheme, a two-phase training protocol is proposed in this paper. First, the training signals are sent to the relay by both transceivers. Then, the signal is amplified and retransmitted to the transceivers. Each transceiver estimates the required channel parameters for data detection. Since the maximum likelihood (ML) estimation in the two-way relay networks is shown to be nonlinear, the corresponding optimal training design seems difficult to be obtained. Therefore,

the researchers resort to the Cramer-Rao lower bound (CRLB)-based design.

In [77], considering a bi-directional amplify-and-forward relay network with a single node relay, a channel estimation prototype is proposed such that the relay, first, estimates the channel parameters during a training phase by means of the adopted maximum likelihood (ML) channel estimation. Then, the power is allocated for these estimated parameters in such a way that the average signal to noise ratio of the detection data is maximized and the mean square error of the channel estimation is minimized. Note that in this work, the channels have been assumed to be flat fading. However, frequency selective channels can be considered by equipping the transceivers with OFDM. Employing OFDM for transmission over time-dispersive channels in the two-way relay network is studied in [78].

The effect of the training-based channel estimation error upon individual and sum-rate of the two transceivers communicating in AF two-way relaying network is studied in [79]. In the multiple-access (MA) phase, both transceivers send their training symbols to the relay and in the broadcasting (BC) phase the relay retransmits its own training symbols, followed by an amplified version of the signal, received in the MA phase. This training symbol facilitates the transceivers to perform the self-interference suppression and to estimate the cascaded overall relay channel, required for the recovery of the data of interest. Lower bounds on the training-based individual rates and sum-rate of the two users are derived and the effect of channel estimation errors upon the sum-rate lower bound is investigated.

Under the assumtion that the total transmit power of the network is constrained, in order to maximize the lower bound of the sum-rate, the power is optimally allocated to the three nodes and also an optimal solution to allocate the power between the

data and training symbols is obtained. Moreover, the relationship between the relay location and the optimal solutions is studied. The authors in their other work, have discussed the sum-rate maximization of the two-way AF relay networks with imperfect channel state information [80]. In this research, the optimal power allocation for the transceivers and the relay as well as the optimal power allotment between the training and data symbols that maximize the average sum-rate lower bound is investigated. Furthermore, the variation of the power allocations by changing the position of the relay is discussed. It has also been shown in this paper that the orthogonality of the training vectors transmitted by the transceivers results in the minimum MSE of the channel estimation.

Chapter 3

Multi-carrier Asynchronous Two-way Relay Networks

3.1 Introduction

In this chapter, we focus on an MABC-based two-way relaying scheme, as this scheme is the most bandwidth efficient bi-directional relay beamforming method, compared to the other two counterparts, when the direct link between the two transceivers does not exist [35]. Assuming simple AF relaying, we consider asynchronous bi-directional relay networks, consisting of two single-antenna transceivers and multiple single-antenna relays, where the transceiver-relay paths are subject to different relaying and/or propagation delays. As such, we model the end-to-end channel as a frequency selective multipath channel which produces ISI at the two transceivers, when the data rate is sufficiently high. In order to combat ISI caused by different relaying and propagation delays in the network, the OFDM approach is used at the two transceivers. However, in order to avoid complexity at the relays, each relay simply amplifies and forwards its received signal by multiplying it with a complex

beamforming weight. As such, the relays do not even need perfect frequency synchronization, as unlike the method of [44], they do not employ any OFDM decoding and coding. *For such a communication scheme, our goal is to optimally obtain subcarrier powers at the two transceivers as well as the beamforming weights at the relays.* To do so, we design two different MABC-type methods based on two different max-min design approaches.

In the first approach, for any given set of transceivers' transmit powers, we first obtain a set of relay beamforming weight vectors such that each member of this set maximizes, per-relay power constraints, the power-normalized signal-to-noise ratio (SNR) at one of the transceivers on one of the subcarriers. This set will have twice as many members as the number of subcarriers, each of which corresponds to one possible impulse response for the multipath end-to-end channel. The transceivers' subcarrier powers are then obtained through the maximization of the smallest subcarrier SNR at both transceivers for all such possible choices of the end-to-end channel impulse response.

In the second approach, we aim to maximize the worst SNR across all subcarriers as well as for both transceivers, subject to a total power constraint, by simultaneously adjusting the transceivers' transmit powers and the relay beamforming coefficients. We show that this approach is equivalent to an SNR balancing technique, and then, we rigorously prove that this technique leads to a relay selection solution, where only the relays corresponding to one of the taps of the multipath end-to-end channel, are turned on and the other relays do not participate in the communication scheme. We propose a simple technique to determine which tap of the multipath end-to-end channel should be non-zero. We also present a semi-closed-form solution to obtain

the relay beamforming weights and transceivers' subcarrier powers.

The contribution of this chapter is highlighted below:

- We develop the data model for a two-way relay network, where different relay signals are subject to different propagation/processing delays. This aspect of our work is novel, and to the best of our knowledge, it has not been studied in the literature. Basically, *we clearly show that from the stand point of the two transceivers, the two-way relay channel can be viewed as a multipath end-to-end channel whose impulse response can be optimally designed by judiciously obtaining the relay beamforming weights.*

- Based on the above interpretation of asynchronous two-way relay networks, we study the application of OFDM at the two transceivers, while the relays use simple amplify-and-forward relaying protocols. Doing so, we then consider the problem of joint subcarrier power allocation and distributed beamforming. This aspect of our work is also new and has not been studied in the literature.

- We present two different optimization problems with two different objective functions, each of which targets a different optimality criterion. Each of these optimality criteria is well-justified for a certain scenario. We then show how each optimization problem can be solved using efficient optimization techniques. Obtaining the solutions to these optimization problems is by no-means trivial as we need to carefully examine the structure of each problem.

3.2 Signal Model

We consider a network of L single-antenna relay nodes, which are participating in a collaborative communication scheme to establish a two-way connection between two transceiver nodes. Let $\tau_{l_{pq}}$ denote the propagation delay of the signal transmitted by Transceiver p, relayed by the lth relay node and received by Transceiver q, for $p, q \in \{1, 2\}$ and $l \in \{1, 2, \ldots, L\}$. Note that for $p = q$, the value of $\tau_{l_{pp}}$ represents the propagation delay of the signal transmitted by Transceiver p which goes through the lth relay and is received back by Transceiver p. In this work, to avoid a significant computational complexity at the relays, we assume that the relays adopt a simple amplify-and-forward relaying protocol.

3.2.1 End-to-End Channel Modeling

Assuming that the channel between each transceiver and each relay is frequency flat and reciprocal, the effective linear time-invariant channels between the two transceivers (including the self-interference channels) can be represented by a 2×2 *channel impulse response matrix*, denoted as $\mathbf{H}(t)$, which is given by $\mathbf{H}(t) = \begin{bmatrix} h_{11}(t) & h_{12}(t) \\ h_{21}(t) & h_{22}(t) \end{bmatrix}$. Note that for $p \in \{1, 2\}$, the impulse response $h_{pp}(t)$ represents the effective channel that the signal transmitted by Transceiver p goes through, when it is received back by the same transceiver. This signal is often called self-interference. Based on these assumptions, the relay channel from Transceiver p to Transceiver q, $(p, q \in \{1, 2\})$ can be viewed as a *multipath end-to-end channel* whose impulse response is given by

$$h_{pq}(t) = \sum_{l=1}^{L} b_{l_{pq}} \delta(t - \tau_{l_{pq}}) \,, \quad \text{for} \quad p, q \in \{1, 2\}$$

where

$$b_{l_{pq}} \triangleq w_l g_{lp} g_{lq} \tag{3.2.1}$$

is the total attenuation/amplification factor applied to the signal going through the lth relay, w_l is the complex beamforming weight of the lth relay, and g_{lq} is the frequency flat channel coefficient between Transceiver q and the lth relay. The signal $\check{s}_p(t)$ transmitted by Transceiver p to the relays is given by

$$\check{s}_p(t) = \sum_{k=-\infty}^{\infty} \check{s}_p[k]\varphi(t - kT_\mathrm{s}), \quad p \in \{1, 2\} \tag{3.2.2}$$

where $\varphi(t)$ is the response of the pulse shaping filter, $\check{s}_p[k]$ is the kth symbol transmitted[1] by Transceiver p, and T_s is the symbol period. The signals $\{\check{s}_p(t)\}_{p=1}^{2}$ produce, at Transceiver q, the following signal:

$$\begin{aligned} r_q(t) &= \sum_{p=1}^{2} \check{s}_p(t) \star_\mathrm{c} h_{pq}(t) \\ &= \sum_{p=1}^{2} \sum_{k=-\infty}^{\infty} \check{s}_p[k] \sum_{l=1}^{L} b_{l_{pq}} \varphi(t - kT_\mathrm{s} - \tau_{l_{pq}}) \end{aligned} \tag{3.2.3}$$

where $q \in \{1, 2\}$ and $\star_\mathrm{c}$ denotes the continuous-time convolution operation[2]. Note that we are not assuming that the two signals transmitted by the two transceivers arrive at a certain relay at the same time. The transceivers' transmitted symbols can arrive at different relays with different delays. Indeed, the only task that each relay performs is to amplify and forward its received signal regardless of the arrival time. Sampling $r_q(t)$ at the symbol rate $1/T_\mathrm{s}$, we express the discrete-time received

[1]Note that $\check{s}_p[k]$ is the kth symbol transmitted by Transceiver p and it is *not* the kth information symbol, denoted as $s_p[k]$, transmitted by this transceiver. We will shortly explain how $\check{s}_p[k]$ and $s_p[k]$ are related in our communication scheme.

[2]We consider noise later and add that to the received noise-free signal in (3.2.3).

sequence $r_q[nT_\mathrm{s}]$ as

$$\begin{aligned} r_q[nT_\mathrm{s}] &= r_q(t)\Big|_{t=nT_\mathrm{s}} \\ &= \sum_{p=1}^{2} \sum_{k=-\infty}^{\infty} \check{s}_p[k] \sum_{l=1}^{L} b_{l_{pq}} \varphi((n-k)T_\mathrm{s} - \tau_{l_{pq}}) \\ &= \sum_{p=1}^{2} \check{s}_p[n] \star_\mathrm{d} h_{pq}[n] \end{aligned} \tag{3.2.4}$$

where $\star_\mathrm{d}$ represents the discrete-time convolution and

$$h_{pq}[n] \triangleq \sum_{l=1}^{L} b_{l_{pq}} \varphi(nT_\mathrm{s} - \tau_{l_{pq}}) \tag{3.2.5}$$

is the equivalent discrete-time impulse response corresponding to the end-to-end channel between Transceivers p and q. The channel model in (3.2.5) shows that despite the fact that the transceiver-relay channels are frequency flat, the end-to-end channel is time-dispersive (or frequency selective), and thus, at sufficiently high data rates, it will produce ISI at the transceivers. Therefore, channel equalization becomes inevitable. Note also that the level of frequency selectivity of the end-to-end channel depends more on how spread the relays are distributed geographically, rather than, for example, on the number of relays. The network might have only two relays which are quite far apart from each other. In this case, the end-to-end channel impulse response, although highly sparse, could have a large maximum delay. On the other hand, a network with numerous relays which are located close to each other, may not exhibit any frequency selectivity.

We herein assume that the OFDM scheme is utilized at both transceivers as a means to eliminate the ISI as OFDM appears to be a natural approach to combat the frequency selectivity of our multipath end-to-end channel. Hence, it is herein assumed that both transceivers are equipped with OFDM-based transmission and

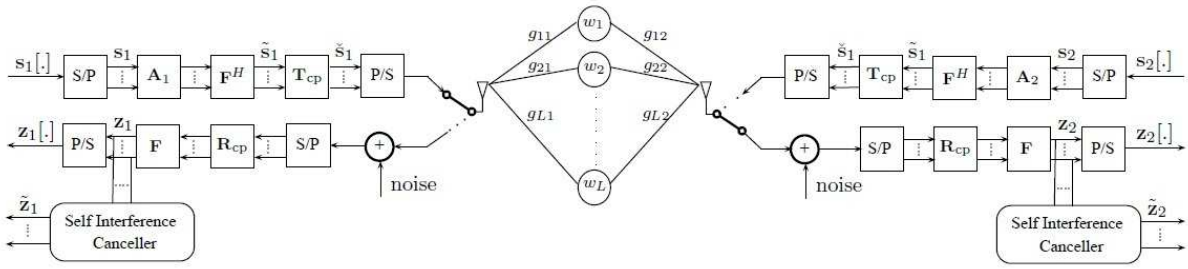

Figure 3.1: Block diagram of the OFDM-based two-way relay network.

reception schemes, as shown in Figure. 3.1. In this figure, "S/P" and "P/S" stand for serial-to-parallel and parallel-to-serial conversion operations, respectively, $\mathbf{F}$ and $\mathbf{F}^H$ are the $N \times N$ DFT and inverse DFT matrices, $\mathbf{T}_{\rm cp}$ and $\mathbf{R}_{\rm cp}$ are the matrices responsible, respectively, for the insertion and deletion of the cyclic prefix, and $(\cdot)^H$ denotes the Hermitian transpose.

Assuming that the duration of $\varphi(t)$ is equal to $T_{\rm s}$, the lth relay contributes to the nth tap of $h_{pq}[\cdot]$ only if $0 \leq nT_{\rm s} - \tau_{l_{pq}} \leq T_{\rm s}$ or, equivalently, if $(n-1)T_{\rm s} \leq \tau_{l_{pq}} \leq nT_{\rm s}$. Using the latter inequality and approximating $\varphi(t)$ with a rectangular pulse[3], the $N \times L$ matrix $\mathbf{B}_{pq}$ whose (n,l)th element is defined as

$$\mathbf{B}_{pq}(n,l) = \begin{cases} g_{lp}g_{lq}, & (n-1)T_{\rm s} \leq \tau_{l_{pq}} \leq nT_{\rm s} \\ 0, & \text{otherwise.} \end{cases}, \tag{3.2.6}$$

determines the contribution of different relaying paths to the end-to-end channel impulse response. Indeed, $\mathbf{B}_{pq}(n,l)w_l$ describes the contribution of the lth relay to the nth tap of $h_{pq}[\cdot]$ for $n = 0, 1, \ldots, N-1$ and $l = 1, 2, \ldots, L$. Here, N is the

[3]With respect to the assumption of rectangular pulses, note that in multi-carrier systems, non-rectangular pulses are not needed as a means to combat ISI. In fact, the OFDM transmission and reception schemes convert a frequency selective channel into parallel subchannels and this conversion eliminates the ISI regardless of the shape of the pulse.

maximum of the lengths of the discrete-time channel impulse responses $h_{pq}[\cdot]$, for $p, q \in \{1, 2\}$. Zero-padding can be used to ensure that the lengths of these channel impulse responses are all equal to N. Hence, without loss of generality, we assume that all the channel impulse responses $\{h_{pq}[\cdot]\}_{p,q=1}^{2}$ are all of the same length N. Also, the number of subcarriers is assumed to be equal to N. Using (3.2.6), we can express (3.2.5), in vector notation, as

$$\mathbf{h}_{pq} = \mathbf{B}_{pq}\mathbf{w} \tag{3.2.7}$$

where $\mathbf{h}_{pq} \triangleq \Big[h_{pq}[0] \;\; h_{pq}[1] \;\; \cdots \;\; h_{pq}[N-1]\Big]^T$ is the $N \times 1$ vector of the discrete-time end-to-end channel taps, $\mathbf{w} \triangleq [w_1 \;\; w_2 \;\; \cdots \;\; w_L]^T$ is the $L \times 1$ vector of the complex relay weights. Note that the reciprocity of the channel yields $\mathbf{B}_{12} = \mathbf{B}_{21} \triangleq \mathbf{B}$, and therefore, $\mathbf{h}_{12} = \mathbf{h}_{21} \triangleq \mathbf{h}$.

3.2.2 Noise Modeling

At the lth relay, we let $\gamma_l(t)$ represent the spatially and temporally white noise process with variance σ^2. This noise waveform is multiplied by w_l at the lth relay and arrives at Transceiver q with delay τ'_{lq}. That is, τ'_{lq} stands for the propagation delay between the lth relay and Transceiver q and $\tau'_{lq} < \tau_{l_{pq}}$, for $p, q \in \{1, 2\}$ and $l \in \{1, 2, \ldots, L\}$. Let us introduce matrices $\mathbf{G}_q$ and $\mathbf{\Gamma}_q$ as

$$\mathbf{G}_q \triangleq \text{diag}\{g_{1q}, g_{2q}, \cdots, g_{Lq}\}, \quad \text{for} \;\; q \in \{1, 2\} \tag{3.2.8}$$

$$\Gamma_q(m, l) \triangleq \gamma_l(mT_\text{s} - \tau'_{lq}), \;\; m = 1, 2, \ldots, M, \;\; l = 1, 2, \ldots, L \tag{3.2.9}$$

where diag$\{\cdot\}$ stands for a diagonal matrix, $M \triangleq N + N_\text{cp}$ is the total length of one OFDM block, N is the number of subcarriers, N_cp is the length of the cyclic prefix, and $\Gamma_q(m, l)$ is the (m, l)th element of the $M \times L$ matrix $\mathbf{\Gamma}_q$. Using (3.2.8) and (3.2.9),

the $M \times 1$ noise vector $\mathbf{n}_q$ at Transceiver q can be written as

$$\mathbf{n}_q \triangleq \mathbf{\Gamma}_q \mathbf{G}_q \mathbf{w} + \mathbf{n}'_q, \quad \text{for} \quad q \in \{1, 2\} \tag{3.2.10}$$

where $\mathbf{n}'_q$ is the $M \times 1$ vector of the corresponding measurement noise with variance σ^2, and the first term in (3.2.10) is the relay noises after being amplified and delayed and after they go through the channels $\{g_{lq}\}_{l=1}^{L}$ to arrive at Transceiver q.

3.2.3 OFDM Signal Modeling

The signal vectors of the Transceivers 1 and 2 are represented, respectively, as $\mathbf{s}_1 \triangleq \begin{bmatrix} s_1[1] & s_1[2] & \cdots & s_1[N] \end{bmatrix}^T$ and $\mathbf{s}_2 \triangleq \begin{bmatrix} s_2[1] & s_2[2] & \cdots & s_2[N] \end{bmatrix}^T$. At the output of the cyclic prefix deletion block, the vectors of the received signals over all subcarriers, denoted as $\mathbf{z}_1$ and $\mathbf{z}_2$, are given by

$$\mathbf{z}_1 \triangleq \mathbf{A}_1 \boldsymbol{\mathcal{D}}_{11} \mathbf{s}_1 + \mathbf{A}_2 \boldsymbol{\mathcal{D}}_{21} \mathbf{s}_2 + \mathbf{F} \mathbf{R}_{\text{cp}} \mathbf{n}_1 \tag{3.2.11}$$

$$\mathbf{z}_2 \triangleq \mathbf{A}_1 \boldsymbol{\mathcal{D}}_{12} \mathbf{s}_1 + \mathbf{A}_2 \boldsymbol{\mathcal{D}}_{22} \mathbf{s}_2 + \mathbf{F} \mathbf{R}_{\text{cp}} \mathbf{n}_2 \tag{3.2.12}$$

where $\boldsymbol{\mathcal{D}}_{pq} \triangleq \text{diag}\{\mathbf{F}\mathbf{h}_{pq}\}$ is a diagonal matrix whose diagonal entries are the frequency response of the channel impulse response $h_{pq}[\cdot]$ at the subcarrier frequencies, $\mathbf{A}_q \triangleq \text{diag}\{\sqrt{P_{1q}}, \sqrt{P_{2q}}, \ldots, \sqrt{P_{Nq}}\}$ is a diagonal matrix whose ith diagonal entry determines the power loading of the ith subcarrier at Transceiver q, P_{iq} is the power allocated to the ith subcarrier at Transceiver q, $\mathbf{R}_{\text{cp}} \triangleq [\mathbf{O} \;\; \mathbf{I}_N]$ is the matrix which removes the cyclic prefix, $\mathbf{I}_N$ is the $N \times N$ identity matrix, and $\mathbf{O}$ is the $N \times N_{\text{cp}}$ all-zero matrix. Let us define $\tilde{\mathbf{z}}_1$ and $\tilde{\mathbf{z}}_2$ as the received signals after self-interference cancelation is performed at Transceivers 1 and 2, respectively, i.e.,

$$\tilde{\mathbf{z}}_1 \triangleq \mathbf{z}_1 - \mathbf{A}_1 \boldsymbol{\mathcal{D}}_{11} \mathbf{s}_1 = \mathbf{A}_2 \boldsymbol{\mathcal{D}}_{21} \mathbf{s}_2 + \mathbf{F} \mathbf{R}_{\text{cp}} \mathbf{n}_1 \tag{3.2.13}$$

$$\tilde{\mathbf{z}}_2 \triangleq \mathbf{z}_2 - \mathbf{A}_2 \boldsymbol{\mathcal{D}}_{22} \mathbf{s}_2 = \mathbf{A}_1 \boldsymbol{\mathcal{D}}_{12} \mathbf{s}_1 + \mathbf{F} \mathbf{R}_{\text{cp}} \mathbf{n}_2 \,. \tag{3.2.14}$$

Indeed, in (3.2.11) and (3.2.12), the terms $\mathbf{A}_1\boldsymbol{\mathcal{D}}_{11}\mathbf{s}_1$ and $\mathbf{A}_2\boldsymbol{\mathcal{D}}_{22}\mathbf{s}_2$ are known to Transceivers 1 and 2, respectively. These terms can be subtracted form $\mathbf{z}_1$ and $\mathbf{z}_2$ to obtain $\tilde{\mathbf{z}}_1$ and $\tilde{\mathbf{z}}_2$, as in (3.2.13) and (3.2.14). Then the vectors $\tilde{\mathbf{z}}_1$ and $\tilde{\mathbf{z}}_2$ can be used for signal recovery at the corresponding transceiver.

3.2.4 Derivation of Subcarrier SNRs

Let P_{iq}^{s} denote the power of the signal component received by Transceiver q over the ith subcarrier. Then, using (3.2.7), (3.2.13), and (3.2.14), we can write

$$\begin{aligned} P_{iq}^{\mathrm{s}} &= \mathrm{E}\left\{\left|[\mathbf{A}_p\boldsymbol{\mathcal{D}}_{pq}\mathbf{s}_p]_i\right|^2\right\} \\ &= \mathrm{E}\left\{|\mathbf{A}_p(i,i)\boldsymbol{\mathcal{D}}_{pq}(i,i)[s_p]_i|^2\right\} \\ &= P_{ip}\mathrm{E}\left\{\left|\mathrm{s}_p[\,i\,]\right|^2\right\}\mathbf{h}_{pq}^H\mathbf{f}_i\mathbf{f}_i^H\mathbf{h}_{pq} \\ &= P_{ip}|\mathbf{h}_{pq}^H\mathbf{f}_i|^2 = P_{ip}|\mathbf{f}_i^H\mathbf{B}\mathbf{w}|^2, \quad \text{for } p,q\in\{1,2\}, \text{ and } p\neq q \end{aligned} \tag{3.2.15}$$

where $\mathrm{E}\{\cdot\}$ denotes the statistical expectation, $[\cdot]_i$ stands for the ith entry of a vector, $\mathbf{A}_p(i,i)=\sqrt{P_{ip}}$ is the ith diagonal entry of the diagonal matrix $\mathbf{A}_p$, $\boldsymbol{\mathcal{D}}_{pq}(i,i)=\mathbf{f}_i^H\mathbf{h}_{pq}$ is the ith diagonal entry of the diagonal matrix $\boldsymbol{\mathcal{D}}_{pq}$, and $\mathbf{f}_i$ is the ith Vandermonde column vector of $\mathbf{F}^H$ given by

$$\mathbf{f}_i = \frac{1}{\sqrt{N}}\left[\begin{array}{cccc} 1 & e^{\left(j\frac{2\pi(i-1)}{N}\right)} & \cdots & e^{\left(j\frac{2(N-1)(i-1)\pi}{N}\right)} \end{array}\right]^T. \tag{3.2.16}$$

In (3.2.15), we have used the fact that $\mathrm{E}\left\{\left|s_p[\,i\,]\right|^2\right\} = 1$, for $p\in\{1,2\}$ and for $i\in\{1,2,\ldots,N\}$. Using (3.2.10), the received noise power on the ith subcarrier of

Transceiver q can be written as

$$\begin{aligned} P_{iq}^{\mathrm{n}} &\triangleq \mathrm{E}\{|\mathbf{f}_i^H \mathbf{R}_{\mathrm{cp}} \mathbf{n}_q|^2\} \\ &= \mathrm{E}\left\{\mathbf{w}^H \mathbf{G}_q^H \mathbf{\Gamma}_q^H \mathbf{R}_{\mathrm{cp}}^T \mathbf{f}_i \mathbf{f}_i^H \mathbf{R}_{\mathrm{cp}} \mathbf{\Gamma}_q \mathbf{G}_q \mathbf{w}\right\} \\ &+ \mathrm{E}\left\{\mathbf{n'}_q^H \mathbf{R}_{\mathrm{cp}}^T \mathbf{f}_i \mathbf{f}_i^H \mathbf{R}_{\mathrm{cp}} \mathbf{n'}_q\right\} \\ &= \mathbf{w}^H \mathbf{D}_q \mathbf{w} + \sigma^2 \end{aligned} \tag{3.2.17}$$

where $\mathbf{D}_q \triangleq \mathrm{E}\left\{\mathbf{G}_q^H \mathbf{\Gamma}_q^H \mathbf{R}_{\mathrm{cp}}^T \mathbf{f}_i \mathbf{f}_i^H \mathbf{R}_{\mathrm{cp}} \mathbf{\Gamma}_q \mathbf{G}_q\right\}$ is an $L \times L$ diagonal matrix whose lth diagonal element, as shown in the appendix, is given by

$$\mathbf{D}_q(l,l) = \sigma^2 |g_{lq}|^2, \quad l = 1, 2, \ldots, L\,. \tag{3.2.18}$$

Using (3.2.15) and (3.2.17), the received SNR of Transceiver q on the ith subcarrier can be written as

$$\begin{aligned} \mathrm{SNR}_{iq}(\mathbf{w}) \triangleq \frac{P_{iq}^{\mathrm{s}}}{P_{iq}^{\mathrm{n}}} &= \frac{P_{ip} |\mathbf{f}_i^H \mathbf{B} \mathbf{w}|^2}{\mathbf{w}^H \mathbf{D}_q \mathbf{w} + \sigma^2} \\ &\text{for } p, q \in \{1, 2\}\,, p \neq q \quad , i = 1, 2, \ldots, N\,. \end{aligned} \tag{3.2.19}$$

3.2.5 Calculation of Relay Powers

We now express the transmit power of the lth relay in terms of the design parameters. To do so, as shown in Figure. 3.1, we note that the relays receive the time-domain signals transmitted by Transceivers 1 and 2. These time-domain signals are the elements of the vectors $\mathbf{T}_{\mathrm{cp}} \mathbf{F}^H \mathbf{A}_1 \mathbf{s}_1$ and $\mathbf{T}_{\mathrm{cp}} \mathbf{F}^H \mathbf{A}_2 \mathbf{s}_2$, respectively, These signals go through their corresponding channel vectors $\mathbf{g}_1 \triangleq [g_{11} \quad g_{21} \quad \cdots \quad g_{L1}]^T$ and $\mathbf{g}_2 \triangleq [g_{12} \quad g_{22} \quad \cdots \quad g_{L2}]^T$ and add up at the relays[4]. Thus, the time-domain signal relayed

[4]Here, we assume that the transmission length is much longer that the difference between times of arrivals of the transceiver's signals at relay.

by the lth relay is given by the elements of the $M \times 1$ vector $\mathbf{x}_l$, defined as

$$\mathbf{x}_l \triangleq w_l \left(g_{l1} \mathbf{T}_{\rm cp} \mathbf{F}^H \mathbf{A}_1 \mathbf{s}_1 + g_{l2} \mathbf{T}_{\rm cp} (\mathbf{f})^H \mathbf{A}_2 \mathbf{s}_2 + \boldsymbol{\gamma}_l \right) \tag{3.2.20}$$

where $\boldsymbol{\gamma}_l \triangleq [\gamma_l(T_{\rm s}) \quad \gamma_l(2T_{\rm s}) \quad \cdots \quad \gamma_l(MT_{\rm s})]^T$. Let us define $\tilde{\mathbf{s}}_q \triangleq \mathbf{F}^H \mathbf{A}_q \mathbf{s}_q$, for $q = 1, 2$. Then, denoting the ith entry of $\tilde{\mathbf{s}}_q$ as $\tilde{s}_{iq} = \mathbf{f}_i^T \mathbf{A}_q \mathbf{s}_q$, we can write

$$\mathrm{E}\{|\tilde{s}_{iq}|^2\} = \mathbf{f}_i^T \mathbf{A}_q E\{\mathbf{s}_q \mathbf{s}_q^H\} \mathbf{A}_q^H \mathbf{f}_i^* = \mathbf{f}_i^T \mathbf{A}_q^2 \mathbf{f}_i^* = \frac{1}{N} \mathrm{tr}(\mathbf{A}_q^2) = \frac{1}{N} \mathbf{1}^T \mathbf{p}_q \tag{3.2.21}$$

where $\mathbf{p}_q \triangleq [P_{1q} \quad P_{2q} \quad \cdots \quad P_{Nq}]^T$, for $q \in \{1, 2\}$, $\mathrm{tr}(\cdot)$ denotes the trace of a matrix, $\mathbf{1}$ is an all-one vector of size $N \times 1$, and $(\cdot)^*$ stands for complex conjugate. It follows from (3.2.21) that different elements of $\tilde{\mathbf{s}}_q$ have the same power. As the cyclic insertion does not change the average power of different entries of the resulting signal vector, the elements of the $M \times 1$ vector $\check{\mathbf{s}}_q \triangleq \mathbf{T}_{\rm cp} \mathbf{F}^H \mathbf{A}_q \mathbf{s}_q = [\check{s}_q[0] \quad \check{s}_q[1] \quad \cdots \quad \check{s}_q[M-1]]^T$ have the same average power equal to $\frac{1}{N} \mathbf{1}^T \mathbf{p}_q$, and hence, we can write

$$\mathrm{E}\{\check{\mathbf{s}}_q^H \check{\mathbf{s}}_q\} = \frac{M}{N} \mathbf{1}^T \mathbf{p}_q \,. \tag{3.2.22}$$

It follows from (3.2.20) and (3.2.22) that the average transmit power $\tilde{P}_l$ of the lth relay is given by

$$\begin{aligned}
\tilde{P}_l &= \frac{1}{M} \mathrm{E}\{\mathbf{x}_l^H \mathbf{x}_l\} \\
&= \frac{|w_l|^2}{M} \left(|g_{l1}|^2 \mathrm{E}\{\check{\mathbf{s}}_1^H \check{\mathbf{s}}_1\} + |g_{l2}|^2 \mathrm{E}\{\check{\mathbf{s}}_2^H \check{\mathbf{s}}_2\} + \mathrm{E}\{\boldsymbol{\gamma}_l^H \boldsymbol{\gamma}_l\} \right) \\
&= \frac{|w_l|^2}{M} \left(|g_{l1}|^2 \frac{M}{N} \mathbf{1}^T \mathbf{p}_1 + |g_{l2}|^2 \frac{M}{N} \mathbf{1}^T \mathbf{p}_2 + M\sigma^2 \right) \\
&= \frac{|w_l|^2}{N} \left(|g_{l1}|^2 \mathbf{1}^T \mathbf{p}_1 + |g_{l2}|^2 \mathbf{1}^T \mathbf{p}_2 + N\sigma^2 \right) \,.
\end{aligned} \tag{3.2.23}$$

In the next section, we use the data models in (3.2.13) and (3.2.14) along with (3.2.15), (3.2.17), (3.2.19), and (3.2.23) to obtain subcarrier power loading at the

transceivers and relay weights using two different optimality criteria. To do so, we herein assume that the relay-transceiver channel coefficients are perfectly available at both transceivers. Such an assumption is widely used in the literature on two-way relay networks [12–17, 19–35] and it is realistic provided that the channel training is accurate enough. Considering the imperfect channel state information is quite a relevant problem but it does not fit in this thesis.

We end up this section by mentioning that one advantage of our communication scheme is that it is not sensitive to carrier frequency offset *at the relays* as the relays do not utilize the OFDM technology. This is the strength of our approach as it relies on AF relaying and not on OFDM-based relaying. Note also that this work does *not* attempt to find a solution to the synchronization problem but it aims to communicate despite the lack of time synchronization.

3.3 Joint Power Loading and Distributed Beamforming

In this section, we present two different max-min design approaches to optimally calculate the subcarrier power loading at the two transceivers as well as beamforming weights at the relays. Each of these two methods uses an optimality criterion which is different from that used for the other algorithm.

3.3.1 Algorithm I: Max-Min-Max SNR

In what follows, $P_{\mathrm{Tx},1}$ and $P_{\mathrm{Tx},2}$ stand for the *symbol-wise* average transmitted powers of Transceivers 1 and 2, respectively, $P_{\mathrm{Tx1,max}}$ and $P_{\mathrm{Tx2,max}}$ are the corresponding

maximum available transmit powers per symbol, $\tilde{P}_l$ is the transmit power of the lth relay, $P_{l,\max}$ is the maximum power of the lth relay, and $\mathbf{p}_q = [P_{1q} \;\; P_{2q} \;\; \cdots \;\; P_{Nq}]^T$, for $q \in \{1, 2\}$. In this subsection, we aim to separate the problem of "channel design" (i.e., determining the relay beamforming weights) from the problem of subcarrier power allocation at the two transceivers. As such, we develop our first algorithm in two steps; Step 1: distributed beamforming at the relays and Step 2: power allocation at the two transceivers. We then summarize this algorithm in Step 3.

Step 1: Distributed Beamforming at the Relays

For any given pair of subcarrier power vectors $\mathbf{p}_1$ and $\mathbf{p}_2$ satisfying $\mathbf{1}^T\mathbf{p}_1 = NP_{\text{Tx1,max}}$ and $\mathbf{1}^T\mathbf{p}_2 = NP_{\text{Tx2,max}}$, let us consider the following optimization problem:

$$\max_{\mathbf{w}} \;\; \text{SNR}_{iq}(\mathbf{w}) \;\; \text{s.t.} \;\; \tilde{P}_l \leq P_{l,\max} \quad l = 1, 2, \ldots, L \tag{3.3.1}$$

where $\text{SNR}_{iq}(\mathbf{w})$ is the received SNR of Transceiver q on the ith subcarrier. The optimization problem (3.3.1) aims to find the weight vector $\mathbf{w}$ such that the received SNR of Transceiver q on the ith subcarrier is maximized under individual relay power constraints. Naturally, the solution to the optimization problem (3.3.1) may not result in a satisfactory performance for other values of q and i. Nevertheless, the solution to (3.3.1) (hereafter referred to as $\mathbf{w}_{iq}^{\text{o}}$) has certain properties which render this solution useful for a max-min fair design approach. The following lemmas express these properties of $\mathbf{w}_{iq}^{\text{o}}$.

Lemma 3.3.1. *For any subcarrier index i and any transceiver index q, (a) the phases of different entries of $\mathbf{w}_{iq}^{\text{o}}$ do not depend on q, (b) the amplitudes of different elements of $\mathbf{w}_{iq}^{\text{o}}$ do not depend on the subcarrier index i, and (c) the power-normalized SNR,*

Θ_{iq}, *defined as*

$$\Theta_{iq} \triangleq \max_{\mathbf{w}} \ \frac{|\mathbf{f}_i^H \mathbf{B}\mathbf{w}|^2}{\mathbf{w}^H \mathbf{D}_q \mathbf{w} + \sigma^2}$$
$$s.t. \quad |w_l|^2 \left(|g_{l1}|^2 \mathbf{1}^T \mathbf{p}_1 + |g_{l2}|^2 \mathbf{1}^T \mathbf{p}_2 + N\sigma^2\right) \leq N P_{l,max},$$
$$for\ l = 1, 2, \ldots, L \tag{3.3.2}$$

is the same for all subcarriers but it is different for different transceiver indices. Note that Θ_{iq} *defined in* (3.3.2) *is indeed equal to* $\frac{SNR_{iq}(\mathbf{w}_{iq}^{\circ})}{P_{ip}}$*, therefore it is referred to as power-normalized SNR.*

Proof : See the appendix.

It is also shown in the appendix that the optimization problem (3.3.2) can be efficiently solved using the results of [34].

Lemma 3.3.2. *Let* $\vartheta_{i'q'}^{iq}$ *be the SNR of Subcarrier* i' *at Transceiver* q' *when the transmit power of Transceiver* p *over subcarrier* i' *is equal to 1 and when* $\mathbf{w} = \mathbf{w}_{iq}^{\circ}$ *is chosen, that is*

$$\vartheta_{i'q'}^{iq} \triangleq \frac{SNR_{i'q'}(\mathbf{w}_{iq}^{\circ})}{P_{i'p'}} = \frac{|\mathbf{f}_{i'}^H \mathbf{B}\mathbf{w}_{iq}^{\circ}|^2}{(\mathbf{w}_{iq}^{\circ})^H \mathbf{D}_{q'} \mathbf{w}_{iq}^{\circ} + \sigma^2}\,. \tag{3.3.3}$$

Then, the set $\{\vartheta_{i'q'}^{i_1 q}\}_{i'=1}^{N}$ *is a permutation of the set* $\{\vartheta_{i'q'}^{i_2 q}\}_{i'=1}^{N}$*. In other words, the set of unit-power subcarrier SNRs are the same no matter which subcarrier is chosen to have a maximum SNR through optimally calculating* $\mathbf{w}$*.*

Proof : See the appendix.

As explained earlier, the solution to the inner maximization in (3.3.1) is given by $\mathbf{w}_{iq}^{\circ}$. As discussed above, $\mathbf{w}_{iq}^{\circ}$ is SNR-optimal only for the ith subcarrier of Transceiver q and it is not optimal for other subcarriers of this transceiver or for any of the subcarriers of the other transceiver. However, as proven in Lemma 3.3.2, the set of

transceiver SNRs, when normalized by the corresponding subcarrier powers, are the same for any i which is chosen to calculate $\mathbf{w}_{iq}^{o}$. Hence, no matter which subcarrier index i is used to obtain $\mathbf{w}_{iq}^{o}$, the same set of SNRs can be achieved by permuting each transceiver's subcarrier powers regardless of how such transmit powers are calculated. Therefore, as far as different subcarriers are concerned, no matter what subcarrier index i is chosen to determine $\mathbf{w}_{iq}^{o}$, the same set of SNRs is obtained. These subcarrier SNRs are not equal but we can assign different constellations (with different numbers of bits per symbol) to different subcarriers in a way that subcarriers with higher SNRs receive more valuable symbols compared to those subcarriers with lower SNRs which might receive less valuable or even no information symbols. That is, we can benefit from good subcarriers, thereby exploiting the channel dynamics over frequency. In other words, we can utilize adaptive modulation schemes to trade off low values of SNR on some of the subcarriers for more bits on the subcarriers with relatively high SNRs.

Note also from one transceiver to the other, we are concerned about the total bit error rate over all subcarriers and the symbol or bit error rate on a particular subcarrier is not of much significance as long as the overall probability of bit error rate is acceptable. Hence, the sub-optimality of $\mathbf{w}_{iq}^{o}$ for subcarriers other than the ith subcarrier of Transceiver q can be tackled by using adaptive modulation techniques[5]. As for the sub-optimality of $\mathbf{w}_{iq}^{o}$ for Transceiver $p \neq q$, one has to note that as proven in Lemma 3.3.1, the power-normalized SNR Θ_{iq}, defined in (3.3.2), is the same for all subcarriers but it is different for different transceiver indices. Indeed, Θ_{iq} depends on the diagonal matrix $\mathbf{D}_q$, which in turn depends on the channel coefficients

[5]Designing such adaptive modulation techniques does not fit in the scope of this thesis.

between Transceiver q and the relays. If these channel coefficients are drawn from the same distribution, Θ_{iq} will have the same distribution for $q = 1, 2$. Hence, in average, over different channel realizations, the subcarrier SNRs are the same for $q = 1, 2$. In other words, for any channel realization, the design problem in (3.3.1) aims to opportunistically exploit the "good" transceiver by maximizing its best power-normalized subcarrier SNRs. This will result in fair allocation of resources between the two transceivers over a sufficiently long period.

Step 2: Power Allocation at the Transceivers

To determine the subcarrier powers at each transceiver, let us consider the following optimization problem:

$$\begin{aligned} &\max_{\mathbf{p}_1, \mathbf{p}_2 \succeq \mathbf{0}} \quad \min_{i' \in \{1,2,\ldots,N\}} \quad \min_{q', q \in \{1,2\}} \quad \mathbf{SNR}_{i'q'}(\mathbf{w}_{iq}^{\mathrm{o}}) \\ &\text{subject to } \ \mathbf{1}^T \mathbf{p}_1 = NP_{\mathrm{Tx1,max}}\,, \ \ \mathbf{1}^T \mathbf{p}_2 = NP_{\mathrm{Tx2,max}}\,. \end{aligned} \tag{3.3.4}$$

The two objective functions and the corresponding optimizations in (3.3.2) and (3.3.4) are used to accomplish two different tasks. The optimization problem in (3.3.2) is used to design the multipath end-to-end channel by determining the beamforming relay weights. Given the beamforming relay weights obtained by solving (3.3.2), the optimization problem in (3.3.4) aims to find the transceivers' subcarrier power vectors such that the smallest SNR among all transceivers' subcarriers is maximized, when the weight vector is chosen to maximize the SNR of Subcarrier i of Transceiver q. In other words, solving (3.3.4) means that we are separating the optimal design of the distributed beamforming (or the optimal design of the *active multipath end-to-end channel*) at the relays from the optimal subcarrier power allocation at the transceivers. We first design the active multipath end-to-end channel by solving the optimization in (3.3.2), and then, assign power to different subcarriers using a max-min fair design

approach for the active channel obtained in the first step. The optimization problem in (3.3.4) is well justified as it aims to control the SNR of the weaker subchannels by controlling the powers allocated to them, thereby preventing those channels from strong attenuation. That is, this approach is a max-min fair power control scheme given that the multipath end-to-end channel is fixed.

It follows from Lemma 3.3.2 that the subcarrier powers obtained by solving (3.3.4) for $i = i_1$ are a permutation of those obtained by solving (3.3.4) for $i = i_2$, for any pair of i_1 and i_2. Therefore, the choice of i does not affect the set of the subcarrier SNRs or the corresponding set of the subcarrier powers.

We can write the optimization problem in (3.3.4) as

$$\begin{aligned} &\max_{\mathbf{p}_1,\, \mathbf{p}_2 \succeq \mathbf{0}} \quad \min_{i' \in \{1,2,\ldots,N\}} \quad \min_{q,q' \in \{1,2\}} P_{i'p'} \vartheta_{i'q'}^{iq}\,, \quad p' \neq q' \\ &\text{subject to } \; \mathbf{1}^T \mathbf{p}_1 = N P_{\text{Tx1,max}}\,, \quad \mathbf{1}^T \mathbf{p}_2 = N P_{\text{Tx2,max}} \end{aligned} \tag{3.3.5}$$

where $\vartheta_{i'q'}^{iq}$ is defined as the SNR of Subcarrier i' at Transceiver q' when the transmit power of Transceiver $p' \neq q'$ over subcarrier i' is equal to 1 and when $\mathbf{w} = \mathbf{w}_{iq}^{\text{o}}$ is chosen, that is

$$\vartheta_{i'q'}^{iq} \triangleq \frac{|\mathbf{f}_{i'}^H \mathbf{B} \mathbf{w}_{iq}^{\text{o}}|^2}{(\mathbf{w}_{iq}^{\text{o}})^H \mathbf{D}_{q'} \mathbf{w}_{iq}^{\text{o}} + \sigma^2}\,. \tag{3.3.6}$$

Note that given $\mathbf{w}_{iq}^{\text{o}}$, the values of $\vartheta_{i'q'}^{iq}$ can be calculated for all values of i', q, and q' and for a given i. As such, the optimization problem (3.3.5) can be turned into a linear programming (LP) problem. To show this, we define

$$t \triangleq \min_{i' \in \{1,2,\ldots,N\}} \quad \min_{q,q' \in \{1,2\}} \quad P_{i'p'} \vartheta_{i'q'}^{iq}$$

and rewrite the optimization problem (3.3.5) as

$$\begin{aligned} \max_{t,\mathbf{p}_1,\mathbf{p}_2\succeq\mathbf{0}} \quad & t \\ \text{subject to} \quad & \mathbf{1}^T\mathbf{p}_1 = NP_{\text{Tx1,max}} \quad \mathbf{1}^T\mathbf{p}_2 = NP_{\text{Tx2,max}} \\ & P_{i'p'}\vartheta_{i'q'}^{iq} \geq t, \qquad \text{for } i = 1, 2, \ldots, N \\ & \text{and } q, p', q' = 1, 2, \;\; p' \neq q' \end{aligned} \tag{3.3.7}$$

which is an LP problem, and thus, it can be solved efficiently using any LP solver software package.

A question that may arise is that how to choose the index i which is used to calculate $\mathbf{w}_{iq}^{\text{o}}$. That is, which subcarrier should be chosen to maximize its power-normalized SNR by choosing $\mathbf{w} = \mathbf{w}_{iq}^{\text{o}}$. Lemma 3.3.2 proves that while solving (3.3.5), the value of i is immaterial as long as the end-to-end total probability of error is concerned.

Step 3: Summarizing Algorithm I

We summarize our Max-Min-Max SNR approach as Algorithm 1.

Algorithm 1 : Max-Min-Max SNR

Step 1. For $i = 1, 2, \ldots N$, and $q \in \{1, 2\}$, use the method of [51] to solve the optimization (3.3.1) and obtain the corresponding weight vectors $\mathbf{w}_{iq}^{\text{o}}$. Let $\mathcal{A}$ represent the set of all such $\mathbf{w}_{iq}^{\text{o}}$'s.

Step 2. Calculate the values of $\vartheta_{i'q'}^{iq}$ as in (3.3.3), for $i', i = 1, 2, \ldots N$ and $q, q' \in \{1, 2\}$.

Step 3. Use linear programming to solve (3.3.7) and obtain the maximum value of t and the corresponding values of $P_{i'p'}$, for $i' = 1, 2, \ldots N$ and $p' \in \{1, 2\}$.

Step 4. Find the values of i and q such that for $p' \neq q'$, $P_{i'p'}\vartheta_{i'q'}^{iq}$ is equal to the maximum value of t for some i' and p'.

Step 5. Use those values of i and q obtained in the previous step to introduce $\mathbf{w}_{iq}^{\text{o}} \in \mathcal{A}$ as the relay beamforming vector.

3.3.2 Algorithm II: Max-Max-Min SNR

In this subsection, using the signal model developed earlier, *we aim to maximize the worst SNR among all transceiver subcarriers, subject to a total power constraint, by properly adjusting not only the transceivers' transmit powers but also the relay beamforming coefficients.* To do so, we take the following steps: Step 1: Introducing and justifying the corresponding optimization problem, Step 2: Simplifying and solving the optimization problem, and Step 3: Summarizing the algorithm.

Step 1: Introducing and justifying the corresponding optimization problem

We aim to solve the following optimization problem:

$$\begin{aligned} &\max_{\mathbf{p}_1,\mathbf{p}_2\succeq\mathbf{0}} \quad \max_{\mathbf{w}} \quad \min_{i\in\{1,2,\ldots,N\}} \quad \min_{q\in\{1,2\}} \quad \mathrm{SNR}_{iq}(\mathbf{w}) \\ &\text{subject to} \quad \frac{\mathbf{1}^T\mathbf{p}_1}{N}+\frac{\mathbf{1}^T\mathbf{p}_2}{N}+\sum_{l=1}^{L}\tilde{P}_l \le P_{\max}\,. \end{aligned} \tag{3.3.8}$$

Note that in the optimization problem (3.3.8), we have used a total transmit power constraint which is somehow looser as compared to individual power constraints. Replacing the total power constraint in (3.3.8) with $L+2$ individual power constraints (one constraint for each of the L relays and two constraints for the two transceivers) will result in an optimization problem which may not be amenable to a computationally efficient solution. In fact, it can be shown that such a problem can be solved using a combination of a $2N$ dimensional search over the space of $\mathbf{p}_1$ and $\mathbf{p}_2$ and a second order cone convex feasibility problem. That is, we can discretize the $(\mathbf{p}_1,\mathbf{p}_2)$ space to a sufficiently fine grid, and then, solve a second order cone convex feasibility problem at each vertex of this grid to obtain the maximum smallest SNR for that vertex. The vertex which results in the largest value for the maximum smallest SNR

yields the optimal values of $\mathbf{p}_1$ and $\mathbf{p}_2$. Naturally, the computational complexity of such an algorithm can be very high even when the number N of subcarriers is low. Thus, we hereafter focus on a total power constraint.

From a network design point of view, setting a total power constraint is valuable for network planning as it allows to control and/or optimize the total power consumed in the whole network. In addition, such a total transmit power constraint provides a guideline for how to set individual relay powers. As was shown in [25], when applying SNR balancing to the case of time-synchronous two-way relay networks with n_r nodes, the relays will collectively consume half of the available total transmit power. In such networks, it is reasonable to assume that each relay, on average,[6] consumes $1/n_r$ fraction of half of the total power budget. This argument is particularly correct when the relays are moving randomly in the environment. In such a scenario, different relay channels appear to be drawn from the same probability distribution. For all these reasons, a total power constraint has been adopted in the literature for performance analysis and optimal design [25, 55, 81, 82]. Moreover, the solution to the optimization problem (3.3.8) has a certain feature which allows us to develop a guideline (similar to that mentioned above for the case of synchronous relay networks) to determine individual relay power constraints. To show this, we obtain the solution to the optimization problem (3.3.8).

Step 2: Simplifying and solving the optimization problem

[6]The average relay power consumption, which we are herein referring to, is taken with respect to all channel realizations of a certain relay and not over different relays for a certain channel realization. The numerical simulations conducted in [25] have shown that when transceiver-relay channel coefficients have the same probability distribution, transceivers' powers are, on average (taken over all channel realizations) equal, while in a particular channel realization, the transceivers' powers may not be the same. The same is true for each relay's transmit power, if we average that over all possible channel realizations. In this case, the symmetry exists not in the exact location of the relays but in the probability distribution of the channel between the relays and the transceivers.

We prove in the appendix that the optimization problem (3.3.8) is equivalent to the following maximization:

$$\begin{aligned} \max_{\mathbf{w}} \quad & \frac{N\sigma^2\left(P_{\max}-\sigma^2\mathbf{w}^H\mathbf{w}\right)}{2\left[\left(\mathbf{w}^H\mathbf{D}_1\mathbf{w}+\sigma^2\right)\left(\mathbf{w}^H\mathbf{D}_2\mathbf{w}+\sigma^2\right)\right]\mathbf{1}^T\mathbf{u}(\mathbf{w})} \\ \text{subject to} \quad & \mathbf{w}^H\mathbf{w} \leq \frac{P_{\max}}{\sigma^2} \end{aligned} \tag{3.3.9}$$

where the $N \times 1$ vector $\mathbf{u}(\mathbf{w})$ is defined as

$$\mathbf{u}(\mathbf{w}) \triangleq \left[\frac{1}{|\mathbf{a}_1^H\mathbf{w}|^2} \quad \frac{1}{|\mathbf{a}_2^H\mathbf{w}|^2} \quad \cdots \quad \frac{1}{|\mathbf{a}_N^H\mathbf{w}|^2}\right]^T. \tag{3.3.10}$$

Here, $\mathbf{a}_i \triangleq \mathbf{B}^H\mathbf{f}_i$, for $i \in \{1,2,\ldots,N\}$ and $|\mathbf{a}_i^H\mathbf{w}| = |\mathbf{f}_i^H\mathbf{B}\mathbf{w}| = |\mathbf{f}_i^H\mathbf{h}|$ is the amplitude of the frequency response of the multipath end-to-end channel at Subcarrier i. Interestingly, the optimization problem (3.3.9) can be rewritten as

$$\begin{aligned} \max_{\mathbf{w}} \quad & \frac{N}{\displaystyle\sum_{i=1}^{N}\frac{1}{\phi_i(\mathbf{w})}} \\ \text{subject to} \quad & \|\mathbf{w}\|^2 \leq \frac{P_{\max}}{\sigma^2} \end{aligned} \tag{3.3.11}$$

where $\phi_i(\mathbf{w}) \triangleq \dfrac{\sigma^2\left(P_{\max}-\sigma^2\mathbf{w}^H\mathbf{w}\right)|\mathbf{w}^H\mathbf{a}_i|^2}{2\left(\mathbf{w}^H\mathbf{D}_1\mathbf{w}+\sigma^2\right)\left(\mathbf{w}^H\mathbf{D}_2\mathbf{w}+\sigma^2\right)}$ is, in light of the results of [28], *the maximum balanced SNRs that can be achieved with a given beamforming weight vector* $\mathbf{w}$ *over the ith subcarrier when the total power budget* P_{max} *is assigned to this subcarrier.* Thus, solving the optimization problem (3.3.11) means that we aim to maximize the harmonic mean of such maximum balanced SNRs.

The following lemma helps us to find the structure of the solution to the optimization problem (3.3.9).

Lemma 3.3.3. *The solution to the optimization problem* (3.3.9) *is such that only one of the entries of the vector of the channel impulse response* $\mathbf{h} = \mathbf{B}\mathbf{w}$ *is non-zero.*

Proof: See the appendix.

Lemma 3.3.3 states that in order to achieve the minimum of $\sum_{i=1}^{N} \frac{1}{\phi_i(\mathbf{w})}$ (i.e., if we want to ensure that $\sum_{i=1}^{N} \frac{1}{\phi_i(\mathbf{w})} = N^2(\sum_{i=1}^{N} \phi_i(\mathbf{w}))^{-1}$ holds true), all relays corresponding to the zero taps of $\mathbf{h}$ should be assigned a zero weight, i.e., they should be turned off, and only the relays corresponding to the only non-zero tap of $h_{pq}[\cdot]$ should be turned on.

The question is now which tap of $h_{pq}[\cdot]$ is non-zero? To answer this question, we need to find the set of the relays, all contributing to one of the taps $h_{pq}[\cdot]$, which result in the largest value for the balanced subcarrier SNRs, while all other relays are turned off. Note that when only the relays, which contribute to one tap of $h_{pq}[\cdot]$, are turned on, the equivalent end-to-end channel will become frequency flat, i.e., for the optimal value of $\mathbf{w}$ and for any i and j, $|\mathbf{a}_i^H \mathbf{w}| = |\mathbf{a}_j^H \mathbf{w}|$ holds true. Hence, we can solve an SNR balancing problem for each set of the relays, which correspond to one of the taps of $h_{pq}[\cdot]$, and obtain the corresponding maximum balanced subcarrier SNRs. We then compare the so-obtained balanced subcarrier SNRs for different taps. The highest balanced SNR will introduce the set of the relays which have to be selected to participate in the relaying and the remaining relays have to be turned off.

When the relays corresponding to only a certain tap are turned on, the end-to-end channel becomes frequency flat, and hence, OFDM technology is no longer needed to combat ISI at the transceivers and the network can be simplified to a synchronous two-way relay network[7]. In this case, the approach of [25] can be used to obtain the corresponding maximum balanced SNRs. This approach has a semi-closed-form

[7]Note that OFDM can still be useful to provide multiplexing gain at the price of reducing the diversity gain of the system.

solution as presented in [27, 28, 83]. Note that the non-zero rows of the matrix $\mathbf{B}$ determine the potentially non-zero taps of $\mathbf{h} = \mathbf{B}\mathbf{w}$. If the $(n+1)$th row of the matrix $\mathbf{B}$ is zero, then the nth tap of the end-to-end channel impulse response $h_{pq}[\cdot]$ is zero. Let $\mathbf{w}_n$ be the vector of those entries of $\mathbf{w}$ that contribute to the nth non-zero tap of the channel impulse response $h_{pq}[\cdot]$ (or, equivalently, to the $(n+1)$th non-zero entry for $\mathbf{h}$). Then, the max-min SNR optimal value of $\mathbf{w}_n$ has a semi-closed form and it is given by

$$\mathbf{w}_n^{\mathrm{o}} = \sigma^2 \kappa(\mu_n) \sqrt{2\nu_n} \Big(2\mu_n \mathbf{D}_1^{(n)} + 2\nu_n \mathbf{D}_2^{(n)} + \sigma^2 \mathbf{I} \Big)^{-1} \mathbf{b}_n \tag{3.3.12}$$

where $\nu_n \triangleq 0.5 P_{\max}/\sigma^2 - \mu_n$, the vector $\mathbf{b}_n^H$ captures the non-zero entries of the $(n+1)$th row of $\mathbf{B}$ that correspond to the entries of $\mathbf{w}_n$, $\mathbf{D}_q^{(n)}$ is a diagonal matrix whose diagonal entries are a subset of the diagonal entries of $\mathbf{D}_q$ which correspond to the relays that contribute to the nth tap of the end-to-end channel impulse response, $\kappa(\mu_n)$ is defined as

$$\kappa(\mu_n) \triangleq \sigma^{-1} \left(\mathbf{b}_n^H \left(\sigma^2 \mathbf{I} + 2\mu_n \mathbf{D}_1^{(n)} \right) \left(2\mu_n \mathbf{D}_1^{(n)} + 2\nu_n \mathbf{D}_2^{(n)} + \sigma^2 \mathbf{I} \right)^{-2} \mathbf{b}_n \right)^{-1/2} \tag{3.3.13}$$

and μ_n is the *unique* solution to the following equation:

$$\begin{aligned} 0 =& \sigma^2 \Big(\frac{P_{\max}}{\sigma^2} - 4\mu_n \Big) \mathbf{b}_n^H \left(2\mu_n \mathbf{D}_1^{(n)} + \Big(\frac{P_{\max}}{\sigma^2} - 2\mu_n \Big) \mathbf{D}_2^{(n)} + \sigma^2 \mathbf{I} \right)^{-1} \mathbf{b}_n - \\ & 2\sigma^2 \mu_n \Big(\frac{P_{\max}}{\sigma^2} - 2\mu_n \Big) \mathbf{b}_n^H \left[2\mu_n \mathbf{D}_1^{(n)} + \Big(\frac{P_{\max}}{\sigma^2} - 2\mu_n \Big) \mathbf{D}_2^{(n)} + \sigma^2 \mathbf{I} \right]^{-2} \Big(\mathbf{D}_1^{(n)} - \mathbf{D}_2^{(n)} \Big) \mathbf{b}_n \end{aligned} \tag{3.3.14}$$

which satisfies $0 \leq \mu_n \leq 0.5 P_{\max}/\sigma^2$. To solve (3.3.14), we can use a simple bisection method to find the value of μ_n in the interval $[0 \;\; 0.5 P_{\max}/\sigma^2]$ for which the left hand side (LHS) of (3.3.14) changes sign. Indeed, the LHS of (3.3.14) is positive/negative for those values of μ_n which are smaller/larger than the unique solution to (3.3.14).

We are now well-positioned to explain how a total power budget can be used to determine the individual relay power constraints: As was shown in [25], the solution in (3.3.12) requires those relays, which are participating in relaying, to collectively consume half of the available total transmit power. It is then reasonable to assume that each of these relays on average consumes $1/n_a$ fraction of half of the total power budget, where n_a is the number of active relays. This argument is particularly correct when the relays are moving randomly in the environment. In such a scenario, different relay channels appear to be drawn from the same distribution.

When the nth tap of $h_{pq}[\cdot]$ is nonzero, (i.e., when $\mathbf{w}_n$ is chosen as in (3.3.12) and when the remaining relays are turned off), the corresponding maximum balanced SNR is given by

$$\mathrm{SNR}_{\max}^{(n)} = \frac{\sigma^2}{N}\mu_n\left(\frac{P_{\max}}{\sigma^2} - 2\mu_n\right)\mathbf{b}_n^H\left(2\mu_n\mathbf{D}_1^{(n)} + 2\nu_n\mathbf{D}_2^{(n)} + \sigma^2\mathbf{I}\right)^{-1}\mathbf{b}_n\,. \tag{3.3.15}$$

The value of $\mathrm{SNR}_{\max}^{(n)}$ is calculated for all possible values of $n \in \{0, 1, \ldots, N-1\}$ and the value of n which results in the largest value for $\mathrm{SNR}_{\max}^{(n)}$ is introduced as the only non-zero tap of the impulse response of the multipath end-to-end channel.

Let $\mathbf{w}^{\mathrm{o}}$ denote the optimal relay weight vector. Note that if the lth relay is active, the lth entry of $\mathbf{w}^{\mathrm{o}}$ is equal to the element of $\mathbf{w}_n^{\mathrm{o}}$ which corresponds to the lth relay. If the lth relay is not active, then the lth entry of $\mathbf{w}^{\mathrm{o}}$ is zero. As shown in the appendix, the optimal value of P_{11} can be calculated as

$$P_{11}^{\mathrm{o}} = \left.\frac{N\sigma^2\left(P_{\max} - \sigma^2\mathbf{w}^H\mathbf{w}\right)}{2(\mathbf{w}^H\mathbf{D}_1\mathbf{w} + \sigma^2)|\mathbf{a}_1^H\mathbf{w}|^2\mathbf{1}^T\mathbf{u}(\mathbf{w})}\right|_{\mathbf{w}=\mathbf{w}^{\mathrm{o}}} = \frac{\sigma^2\left(P_{\max} - \sigma^2\|\mathbf{w}^{\mathrm{o}}\|^2\right)}{2(\mathbf{w}^{\mathrm{o},H}\,\mathbf{D}_1\mathbf{w}^{\mathrm{o}} + \sigma^2)} \tag{3.3.16}$$

where we have used the fact that $|\mathbf{a}_i^H\mathbf{w}^{\mathrm{o}}| = |\mathbf{a}_1^H\mathbf{w}^{\mathrm{o}}|$, for $i = 1, 2, \ldots, N-1$, and hence, $\mathbf{u}(\mathbf{w}^{\mathrm{o}}) = \frac{1}{|\mathbf{a}_1^H\mathbf{w}^{\mathrm{o}}|^2}\mathbf{1}$. Using (3.3.16) along with results from the appendix with relationship between subcarrier powers at the two transceivers, we can obtain the

remaining transceivers' subcarrier powers as

$$P_{12}^{\mathrm{o}} = \left.\frac{\mathbf{w}^H\mathbf{D}_1\mathbf{w}+\sigma^2}{\mathbf{w}^H\mathbf{D}_2\mathbf{w}+\sigma^2}\right|_{\mathbf{w}=\mathbf{w}^{\mathrm{o}}} \times P_{11}^{\mathrm{o}} = \frac{\sigma^2\left(P_{\max}-\sigma^2\|\mathbf{w}^{\mathrm{o}}\|^2\right)}{2(\mathbf{w}^{\mathrm{o},H}\,\mathbf{D}_2\mathbf{w}^{\mathrm{o}}+\sigma^2)}. \tag{3.3.17}$$

$$P_{iq}^{\mathrm{o}} = P_{1q}^{\mathrm{o}}\left.\frac{|\mathbf{a}_1^H\mathbf{w}|^2}{|\mathbf{a}_i^H\mathbf{w}|^2}\right|_{\mathbf{w}=\mathbf{w}^{\mathrm{o}}} = P_{1q}^{\mathrm{o}}\,, \quad \text{for } i=1,2,\ldots,N \text{ and } q\in\{1,2\}. \tag{3.3.18}$$

Interestingly, it follows from (3.3.18) that the subcarrier powers for each transceiver are all the same.

Step 3: Summarizing Algorithm II

We summarize Algorithm II as shown in the table below.

Algorithm 2 : Max-Min-Max SNR

Step 1. Set $n=0$.

Step 2. If no relay contributes to the nth tap of $h_{pq}[\cdot]$ (i.e., if the $(n+1)$th row of the matrix $\mathbf{B}$ is zero), let $\mathrm{SNR}_{\max}^{(n)}=0$ and go to Step 9. Otherwise, go to Step 3.

Step 3. Let $\mathbf{b}_n^H$ capture the non-zero entries of the $(n+1)$th row of $\mathbf{B}$.

Step 4. Use a bisection algorithm to obtain the solution to (3.3.14) for μ_n in the interval $[0 \;\; 0.5P_{\max}/\sigma^2]$ and calculate $\nu_n = 0.5P_{\max}/\sigma^2 - \mu_n$.

Step 5. Use (3.3.15) to calculate $\mathrm{SNR}_{\max}^{(n)}$.

Step 6. Let $n=n+1$. If $n\geq N$, go to Step 7. Otherwise, go to Step 2.

Step 7. Find n such that $\mathrm{SNR}_{\max}^{(n)} \geq \mathrm{SNR}_{\max}^{(n')}$, for $n'=0,1,\ldots N-1$.

Step 8. Use (3.3.12), (3.3.13), and (3.3.14) to calculate the optimal value of $\mathbf{w}_n$. where $\nu_n = 0.5P_{\max}/\sigma^2 - \mu_n$.

Step 9. Let $\mathbf{w}^{\mathrm{o}}$ denote the optimal relay weight vector. If the lth relay is active, the lth entry of $\mathbf{w}^{\mathrm{o}}$ is equal to the element of $\mathbf{w}_n^{\mathrm{o}}$ which corresponds to the lth relay. If the lth relay is not active, then the lth entry of $\mathbf{w}^{\mathrm{o}}$ is zero.

Step 10. Calculate the transceivers' subcarrier powers as in (3.3.16), (3.3.17), and (3.3.18).

We wrap up this section by mentioning that the two algorithms presented in this chapter lead to different solutions, each of which is optimal for its corresponding problem but suboptimal for the other problem. The first algorithm is concerned with achieving good (not necessarily minimal) bit error rate performance. This is done by separating relay beamforming design from subcarrier power allocation at the transceivers. The relay beamformer is then designed to maximize the SNR of one of the subcarriers at one of the transceivers. The choice of the subcarrier whose SNR is maximized, is immaterial as long as the end-to-end symbol or bit error rate is concerned. In this approach, the subcarrier transmit powers are obtained through a max-min SNR fair design approach to balance the SNRs as much as possible, thereby avoiding nulls in the frequency response of the multipath end-to-end channel. In the second algorithm, the goal is to balance all of the subcarrier SNRs between the two transceivers. This approach is suitable for cases where the information symbols are of the same value in terms of the number of bits they carry. Note that these two algorithms can be implemented in a distributed manner as they rely on the results of [25] and [51]. Indeed, Algorithm I uses the result of [25] and Algorithm II utilizes the solution provided in [51] for synchronous two-way relay networks. The methods presented in [25] and [51] are amenable to simple distributed realizations. We refer the reader to [25] and [51] for further details of such realizations.

3.4 Simulation Results

We consider an asynchronous two-way relay network with $N = 16$ subcarriers and $L = 8$ relays. The propagation delay $\tau_{l_{pq}}$ corresponding to the lth relay is modeled as a random variable uniformly distributed in the interval $[0, 8T_s]$. The channel

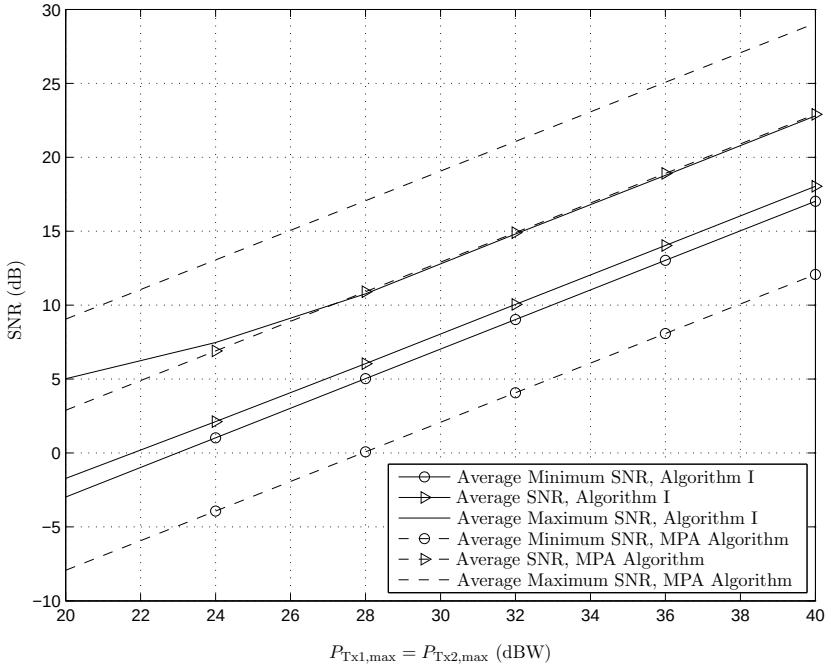

Figure 3.2: Average SNR across all subcarriers and simulation runs; the minimum subcarrier SNR, averaged across all simulation runs; and the maximum subcarrier SNR, averaged over all simulation runs; versus $P_{\mathrm{Tx1,max}} = P_{\mathrm{Tx2,max}}$, achieved by Algorithm I and the maximum power allocation technique, for $\eta = 0.1$.

coefficients are considered to be zero-mean independent and identically distributed complex Gaussian random variables with unit variance. The noise variance is chosen to be equal to one.

Algorithm I: To evaluate the performance of our Max-Min-Max approach, the maximum transmit power of the two transceivers are assumed to be equal, i.e., $P_{\mathrm{Tx1,max}} = P_{\mathrm{Tx2,max}}$. We also assume that all relays have the same maximum level of power. That is, $P_{l,\mathrm{max}}$ is the same for all l. We define η as the ratio of the maximum power of the relays to the maximum power of the transceivers, that is $\eta \triangleq \frac{P_{l,\mathrm{max}}}{P_{\mathrm{Tx1,max}}}$. Figure. 3.2, Figure. 3.3 and Figure. 3.4 illustrate the performance of Algorithm I versus $P_{\mathrm{Tx1,max}} = P_{\mathrm{Tx2,max}}$ presented in this chapter for $\eta = 0.1$, 1, and 10.

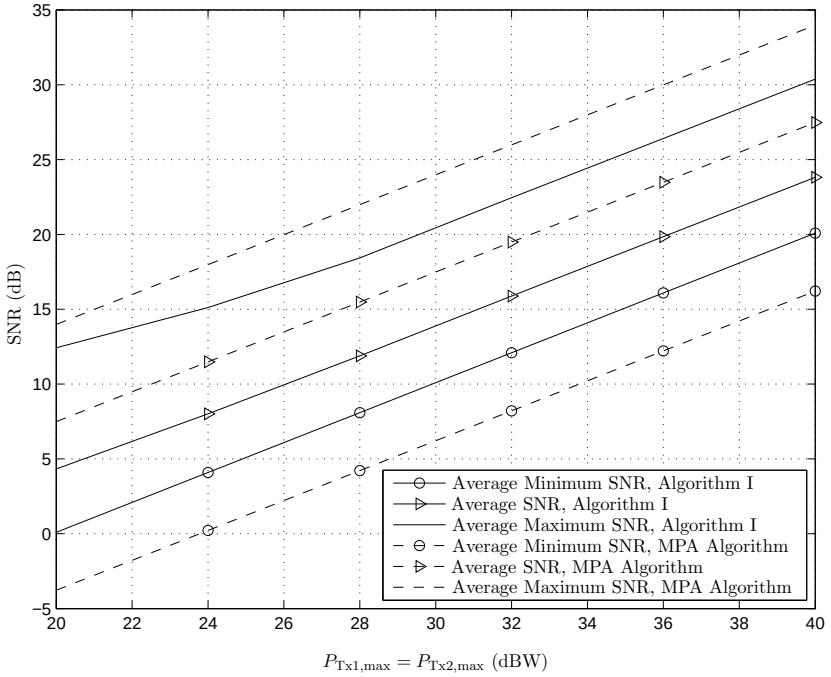

Figure 3.3: Average SNR across all subcarriers and simulation runs; the minimum subcarrier SNR, averaged across all simulation runs; and the maximum subcarrier SNR, averaged over all simulation runs; versus $P_{\mathrm{Tx1,max}} = P_{\mathrm{Tx2,max}}$, achieved by Algorithm I and the maximum power allocation technique, for $\eta = 1$.

In each figure, for Algorithm I, we have plotted the average SNR across all subcarriers and all simulation runs; the minimum subcarrier SNR, averaged across all simulation runs; and the maximum subcarrier SNR, averaged over all simulation runs. In these figures, we have also plotted the same average SNR quantities for a maximum power allocation (MPA) scheme where all nodes consume all their maximum power. We have chosen to compare the performance of our proposed Algorithm I only with this simple MPA scheme, as to the best of our knowledge, no other solution has been proposed in the literature that considers the model we described in this chapter, neither does any other method exist which considers asynchronous two-way relay networks. As can be seen from these figures, when η is increased, the average of

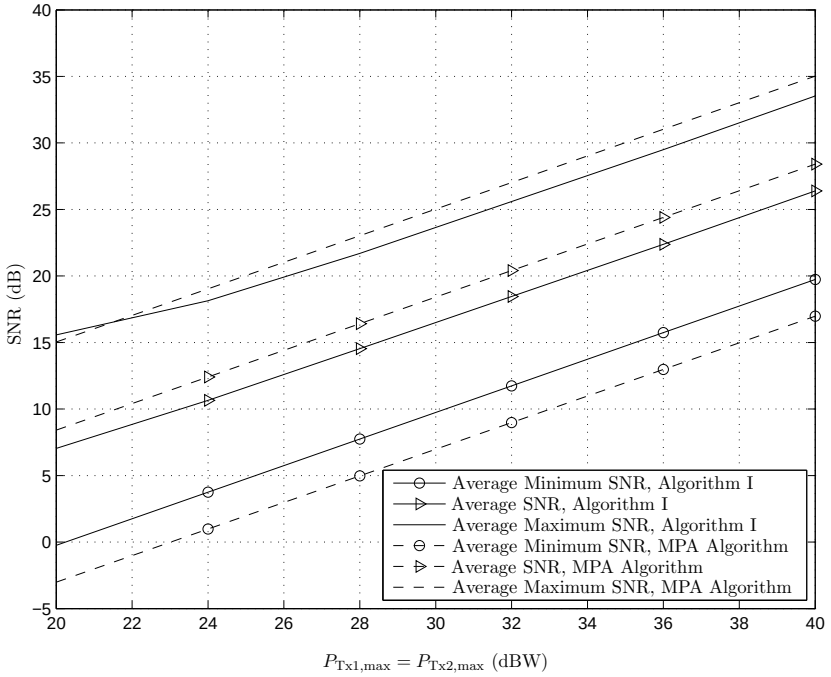

Figure 3.4: Average SNR across all subcarriers and simulation runs; the minimum subcarrier SNR, averaged across all simulation runs; and the maximum subcarrier SNR, averaged over all simulation runs; versus $P_{\mathrm{Tx1,max}} = P_{\mathrm{Tx2,max}}$, achieved by Algorithm I and the maximum power allocation technique, for $\eta = 10$.

the subcarrier SNRs moves towards the average maximum SNR. When η is too low, the average of the subcarrier SNRs is closer to the average minimum SNR indicating the subcarrier SNRs are in average close to the average minimum SNR. When $\eta = 10$, the average subcarrier SNR of Algorithm I moves away from the average minimum SNR. This phenomenon can be explained as follows: As η is increased, the relays will have more power to consume and this extra power will result in more spread values of subcarrier SNRs. Compared to the MPA scheme, Algorithm I has a higher smallest SNR. This phenomenon clearly shows that having all the relay nodes use their maximum power may not be optimal as far as the maximum smallest SNR is concerned. Indeed, by properly adjusting the relays' powers, each relay will amplify its received

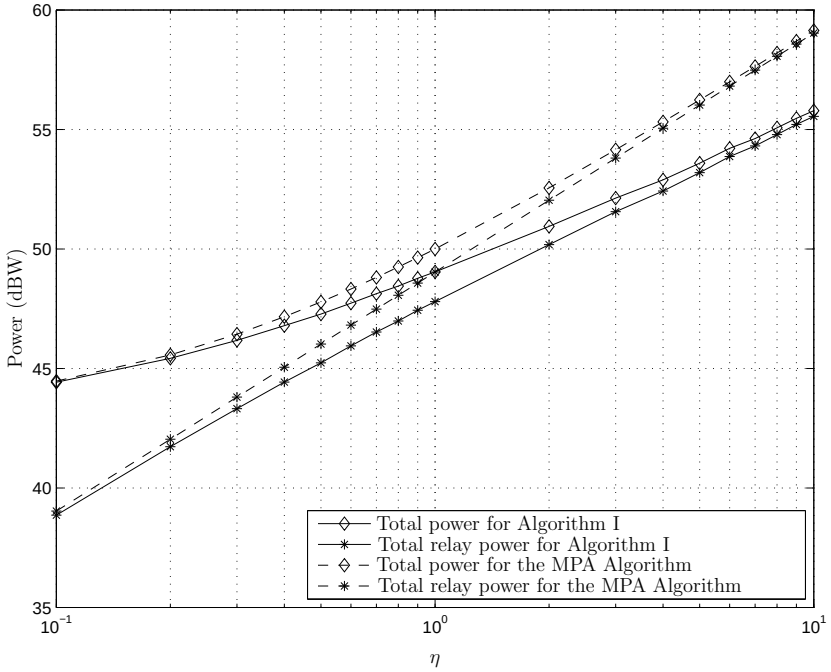

Figure 3.5: The average total transmit powers and average total relay transmit powers versus η for Algorithm I and the maximum power allocation scheme, $P_{\text{Tx1,max}} = P_{\text{Tx2,max}} = 40$ dBW.

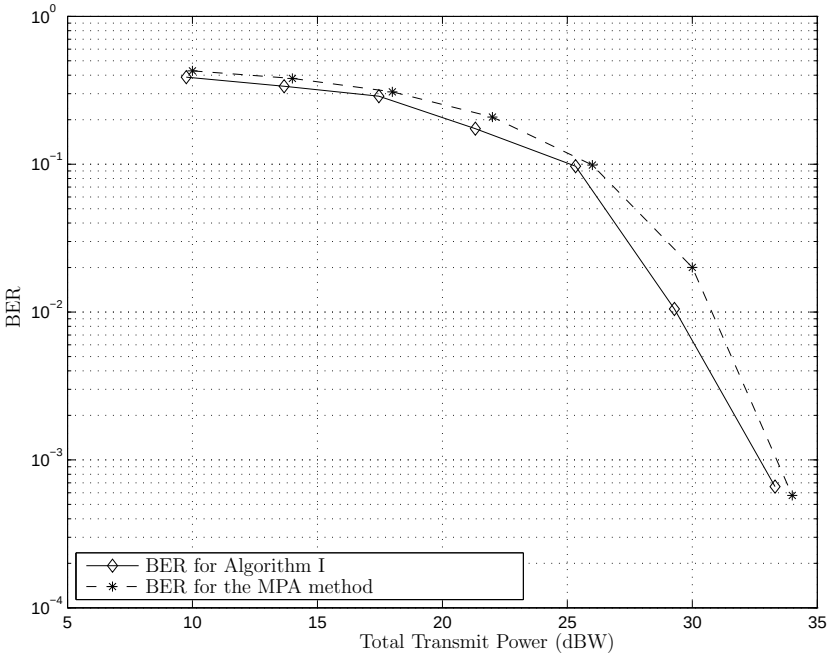

Figure 3.6: The bit error rates of the subcarrier with smallest subcarrier SNR for Algorithm I and for MPA method versus total transmit power; $\eta = 1$.

signal as much as needed and not more. If a certain relay amplifies its received signal more than what is optimal, it may contribute to the noise amplification more than that it contributes to the amplification of the desired signals, thereby resulting in a loss in the maximum smallest SNR.

Figure. 3.5 illustrates the average total transmit power as well as the total relay transmit power, consumed by Algorithm I and the MPA scheme, versus η, for $P_{\text{Tx1,max}} = P_{\text{Tx2,max}} = 40$ (dBW). As can be seen from this figure, as η is increased, the relays' contribution to the total power consumption increases. The reason is that as η is increased, the relays have a larger power margin and they can enjoy using a larger portion of the total available power when participating in relaying. Compared to the maximum power allocation, Algorithm I consumes less power as shown in Figure. 3.5. The reason is that in Algorithm I, the relays do not consume unnecessarily high level of powers, as otherwise, this could lead to the loss in the maximum smallest SNR.

Assuming a QPSK modulation, in Figure. 3.6, we show the bit error rate (BER) curves versus the total transmit power consumed in the whole network for Algorithm I and for the MPA method. As can be seen from this figure, Algorithm I outperforms the MPA technique as the former method optimizes the performance for the subcarrier with the smallest SNR, while the latter approach does not offer such optimality.[8]

Algorithm II: Figure. 3.7 shows the average values of the maximum smallest subcarrier SNR versus the maximum available transmit power for Algorithm II and for an equal power allocation (EPA) scheme. In the latter scheme, both transceivers

[8]Note that Algorithm I may not be optimal if the sum-rate or if the end-to-end BER is concerned.

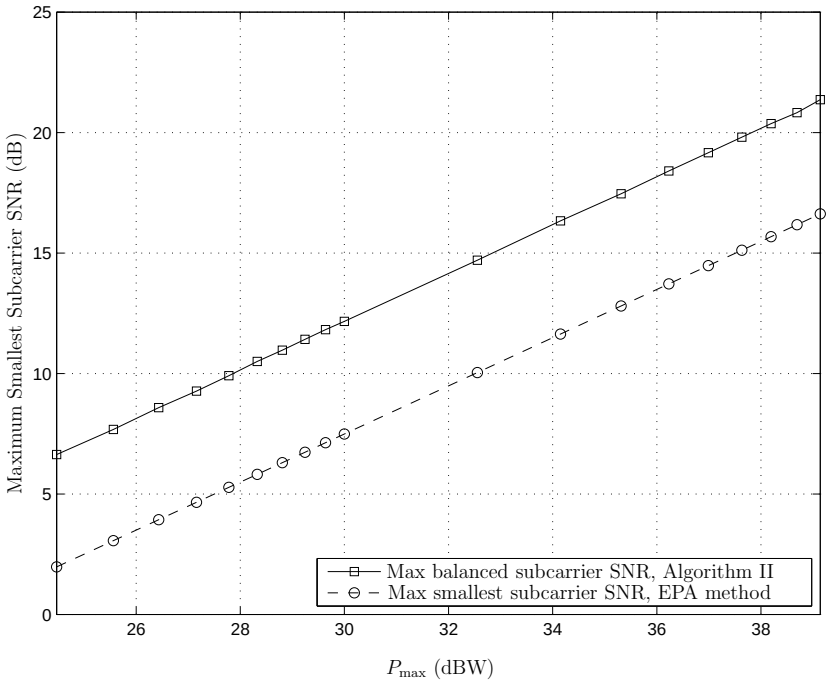

Figure 3.7: The average values of the maximum smallest subcarrier SNR versus the maximum available total transmit power for Algorithm II and equal power allocation technique.

and relay nodes consume the same amount of power. Compared to the EPA technique, Algorithm II performs around 4.5 dB better in terms of the maximum smallest subcarrier SNR or around 4.5 dBW better in terms of the total transmit power. Compared to the EPA technique, this superior performance of Algorithm II is well justified as Algorithm II maximizes the smallest subcarrier SNR for any given total transmit power, while the EPA method does not offer any optimality. Figure. 3.8 illustrates the average total transmit power and the average total relay transmit power for Algorithm II and the EPA technique. This figure shows that for Algorithm II, the total transmit power is always half of the available total transmit power. This is consistent with the results of [25]. However, in the EPA method, the total relay

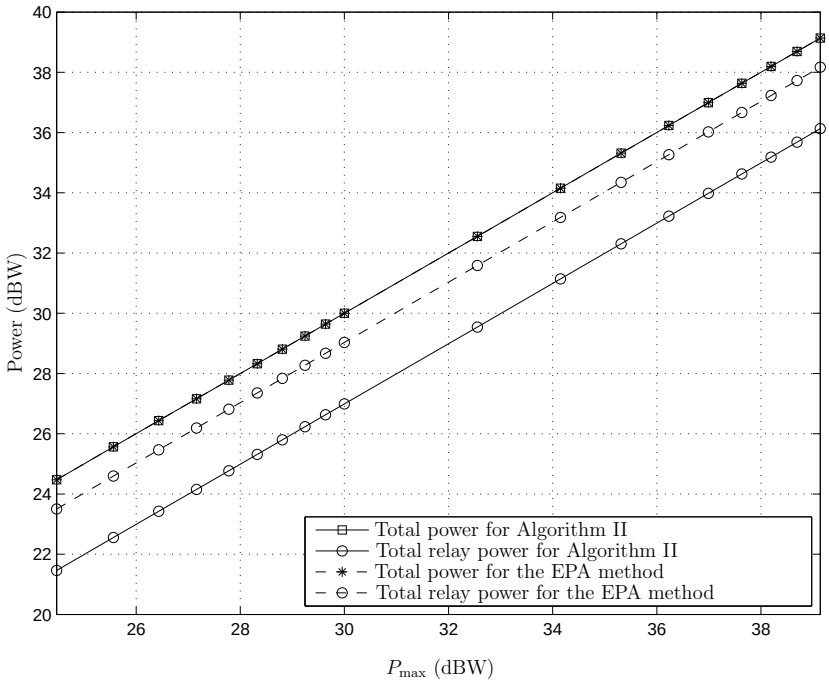

Figure 3.8: The average values of the total transmit power and the average values of the total relay transmit power versus the maximum available total transmit power for Algorithm II and for EPA technique.

power is a fraction ($\frac{L}{L+2}$) of the total available power as this method allocates the total available power equally among different nodes. As such, the EPA algorithm allocates too much power to the relays combined and too little power to the two transceivers. This sub-optimality of power allocation in the EPA approach results in around 4.5 dB loss in the maximum smallest subcarrier SNR as shown in Figure. 3.7.

In Figure. 3.9, we plot the end-to-end BER curves for Algorithm II and for the EPA scheme versus the total transmit power $P_{\max}$. As can be seen from this figure, Algorithm II outperforms the EPA method for moderate to high values of $P_{\max}$. This superior performance of Algorithm II shows that the SNR balancing nature of this algorithm can yield better BER as compared to the EPA approach.

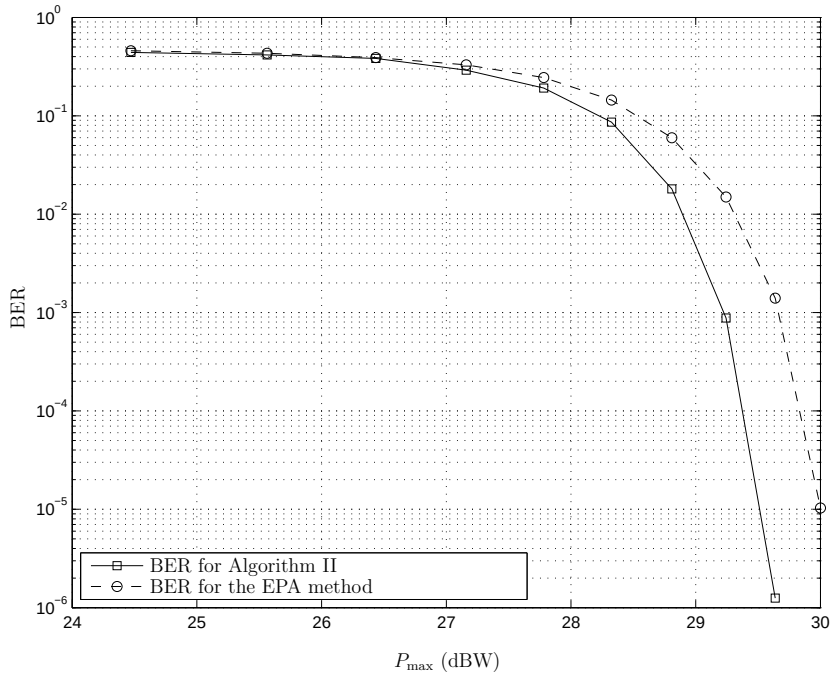

Figure 3.9: The bit error rate of Algorithm II and that of the EPA scheme versus the total transmit power.

Finally, in Figure. 3.10, we illustrate the sum-rate performance of Algorithm II and that of the EPA scheme. Interestingly, the sum-rate of Algorithm II is much better than that of the EPA method. This leads us to the conjecture that in our asynchronous two-way relay-assisted communication scheme, the SNR balancing is sum-rate optimal - a property that holds in synchronous two-way relay networks. Proving or disproving this conjecture does not fit in the scope of this thesis and we defer that to our future work in this area.

We wrap up this section by mentioning that as shown in Figs. 3.6 and 3.9, a relatively high transmit power is required by Algorithm II to achieve a satisfactory BER performance. This relatively high transmit power is the direct result of the fact that in our OFDM transmission scheme, we aim to maximize the multiplexing gain

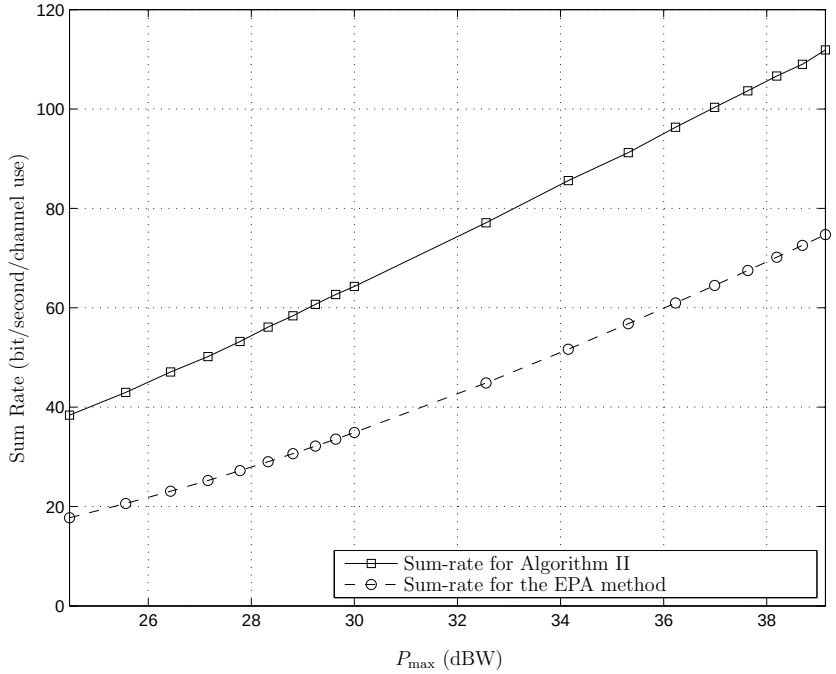

Figure 3.10: The sum-rate of Algorithm II and that of the EPA scheme versus the total transmit power.

of the communication scheme at the price of reducing its diversity gain.

3.5 Conclusion

In this chapter, we considered an asynchronous bi-directional relay network, where the relay paths are subject to different relaying and/or propagation delays. Such a network can be viewed as a multipath end-to-end channel which causes ISI at the two transceivers, when the data rates are sufficiently high. We deploy orthogonal frequency division multiplexing (OFDM) to diagonalize the end-to-end channel as seen by the two transceivers. For the sake of simplicity at the relays, we assumed simple amplify-and-forward (AF) relaying, thereby implementing a bi-directional network

beamformer in a distributed manner. For such a two-way collaborative scheme, we proposed two different max-min design approaches to optimally obtain the subcarrier power loading at the transceivers as well as the relay beamforming weights.

In the first approach, for any given pair of transceivers' transmit powers, we first obtain a set of relay beamforming weight vectors such that each member of this set maximizes the power-normalized signal-to-noise ratio (SNR) at one of the transceivers on one of the subcarriers, subject to per-relay power constraints. This set will have twice as many members as the number of subcarriers, each of which corresponds to one possible impulse response for the end-to-end multipath channel. To obtain the transceivers' subcarrier powers, we then maximize the smallest subcarrier SNR at both transceivers for all such possible choices of the end-to-end channel impulse response.

In the second approach, the worst SNR across all transceivers' subcarriers is maximized, subject to a total power constraint, by properly adjusting the transceiver's transmit powers as well as the relay beamforming coefficients. We rigorously proved that this approach leads to a relay selection solution where only the relays corresponding to one of the taps of the multipath end-to-end channel are turned on and the other relays do not participate in the communication scheme. A semi-closed-form solution is then presented that can be used to obtain the relay beamforming weights.

Chapter 4

Post-channel Equalization and Distributed Beamforming in Asynchronous Single-carrier Bi-directional Relay Networks

4.1 Introduction

As we discussed in the previous chapter, in order to mitigate the effect of ISI in frequency selective channels, essentially there appear to be two different competing approaches. In the first approach, which is based on multi-carrier equalization, the OFDM technology is employed at all nodes of the communication network to diagonalize the end-to-end channel. In other words, using OFDM, the frequency selective channel is transformed into multiple parallel frequency flat sub-channels [57, 78]. The goal in this approach is to optimize a certain performance metric through judiciously allocating power to different subcarriers at the two transceivers and at the relays. Note that the relays may use the OFDM signaling as in [44], or may utilize a simple AF relaying protocol as in Chapter 3, thereby avoiding the complexity involved in

OFDM reception and transmission. The second approach (often referred to as filter-and-forward method) is a single-carrier scheme, where the nodes of the network utilize FIR filters to equalize the channel in a distributed manner [36, 39, 40, 43, 55]. In such a single-carrier cooperative transmission/reception scheme, the goal is to optimally design the equalization filters at the relays, and possibly to determine the optimal transmit powers and/or the FIR filters of the transceivers. For example, assuming frequency-selective channels, the authors of [40], consider a one-way relay network which establishes a single-carrier communication between a source and a destination. They aim to maximize the signal-to-noise ratio (SNR) subject to the limited relay power and design the optimal filter-and-forward relay beamforming as well as the equalization filter at the destination.

Considering an MABC scheme, in this chapter, we consider an asynchronous bi-directional multi-relay network, which uses a single-carrier communication scheme to exchange information between two transceivers. For the sake of simplicity, channel equalization is assumed to be performed only at the transceivers and the relay nodes simply amplify and forward their received signals. Assuming block transmission, we develop and describe our channel, noise, and signal model in next section.

Then, for our developed system model, we aim to minimize the total mean squared error (MSE) of the total estimated received signal at both transceivers under a limited total power budget. We optimally obtain the block channel equalizers as well as the relay weight vector and the transceivers' transmit powers. We rigourously show that this approach leads to a relay selection scheme, where only the set of relays which all contribute to one tap of the end-to-end channel impulse response, are on and the rest are switched off. To determine which tap of the end-to-end channel impulse response

has to be non-zero, we present a simple search procedure. Assuming only a certain tap of the end-to-end channel impulse response is non-zero while all other taps are zero, we derive a semi-closed-form solution for the corresponding relay beamforming weight vector and the respective minimum total MSE of the symbol estimates. Such MSEs are calculated for all possible non-zero taps of the end-to-end channel impulse response. The non-zero tap which yields the smallest total MSE, introduces the relays which have to be turned on.

Comparing with the results of Chapter 3, we show that using block channel equalization in a single-carrier communication scheme leads to the same relay selection scheme as the OFDM-based transmission scheme of multi-carrier communication scheme introduced in the previous chapter does. The difference between the communication scheme studied in this chapter with the multi-carrier communication scheme is that the single-carrier communication considered herein trades off multiplexing gain to achieve a higher reliability, while the the multi-carrier communication scheme offers a higher multiplexing gain at the expense of lower reliability. As such, the communication scheme presented in this chapter and the one presented in Chapter 3 offer their own advantages and disadvantages and have their own potential application depending on the overall system design criteria.

In Section 4.5, we present our simulation results and show how the proposed method performs compared to an equal power allocation scheme, where all nodes receive the same level of transmit power. Finally, we conclude the chapter in Section 4.6.

4.2 Preliminaries

We consider a single-carrier bi-directional relay network, where two single-antenna transceivers exchange information with the help of L single-antenna relay nodes. Assuming no direct link between the two transceivers, the relays establish a bi-directional communication between the two transceivers by amplifying and forwarding the signals they receive from the transceivers. The propagation delay of each relaying path (originating from one transceiver, going through one of the relays, and ending at the other transceiver) differs from those of the other paths. Hence, the signals transmitted from different relays arrive at the two transceivers at different times. As a result, the end-to-end multi-path channel is frequency selective, and thus, it can cause ISI.

One way to combat such an ISI is to use block channel equalization, as shown in Figure. 4.1. In this figure, at each transceiver, the information symbols go through serial-to-parallel conversion block, denoted as "S/P", which converts the serial symbols into blocks of length N_s. We represent the ith block of the information symbols transmitted by Transceiver p, as $\mathbf{s}_p(i) = \left[\begin{array}{cccc} s_p[iN_s] & s_p[iN_s+1] & \cdots & s_p[iN_s+N_s-1] \end{array} \right]^T$, where $s_p[k]$ is the kth symbol transmitted by Transceiver p. The frequency selectivity of the end-to-end channel leads to inter-block-interference (IBI) between adjacent transmitted blocks, and hence, the signals received at Transceiver $q \neq p$, corresponding to the ith transmitted block, depend on the ith and the $(i-1)$th blocks transmitted by Transceiver p, i.e., $\mathbf{s}_p(i)$ and $\mathbf{s}_p(i-1)$. In order to eliminate the IBI, a cyclic prefix is added to $\mathbf{s}_p(i)$ by pre-multiplying it with the matrix $\mathbf{T}_{\text{cp}} \triangleq [\mathbf{I}_{\text{cp}}^T \ \ \mathbf{I}_{N_s}^T]^T$, where $\mathbf{I}_{\text{cp}}$ is the matrix of the last N rows of the identity matrix $\mathbf{I}_{N_s}$, and N is the length of the vector of the equivalent discrete-time end-to-end channel impulse response taps. After the cyclic insertion block, the corresponding ith transmitted block $\overline{\mathbf{s}}_p(i)$ is defined

as

$$\begin{aligned}\overline{\mathbf{s}}_p(i) &\triangleq \left[\begin{array}{cccc} \overline{s}_p[iN_t] & \overline{s}_p[iN_t+1] & \cdots & \overline{s}_p[iN_t+N_t-1] \end{array}\right]^T \\ &\triangleq \mathbf{T}_{\text{cp}}\mathbf{s}_p(i) \\ &= [s_p[(i+1)N_s-N] \ \cdots \ s_p[(i+1)N_s-1] \ s_p[iN_s] \ \cdots \ s_p[(i+1)N_s-1]]^T \end{aligned} \tag{4.2.1}$$

where $N_t \triangleq N + N_s$ is the length of the transmitted blocks. The data block $\overline{\mathbf{s}}_p(i)$ is passed through the parallel-to-serial conversion block, denoted as "P/S" and is turned into serial symbols, which are then transmitted over the multi-path relay channel.

At the other side of the channel, the noise-corrupted version of the signal received by Transceiver q, is passed through the "S/P" block and is turned into blocks (vectors) of received signals. After the self-interference cancelation, denoted as "SIC", the first N entries of any received block are simply discarded by pre-multiplying it with the cyclic removal matrix denoted, as $\mathbf{R}_{\text{cp}} \triangleq [\mathbf{0}_{N_s\times N} \quad \mathbf{I}_{N_s}]$. In order to mitigate the ISI which exists in the output vector of the cyclic prefix removal at both transceivers dueto the frequency selectivity of the end-to-end channel, two $N_s \times N_s$ block channel equalizers denoted as $\mathbf{F}_{r1}$ and $\mathbf{F}_{r2}$ are implemented at Transceivers 1 and 2, respectively. At Transceiver q, the estimates of the information symbol blocks, transmitted by Transceiver $p \neq q$, are obtained at the output of the corresponding block equalizer, $\mathbf{F}_{rq}$.

In the following subsections, we first develop our channel model. Then, we model the noises introduced at the relay nodes and the noises at transceivers and formulate the total noise received at each transceiver. Next, we model the signals received at each transceiver, and finally, derive an expression for the total power consumed in the whole network. Using the data model presented in the subsequent subsections, in

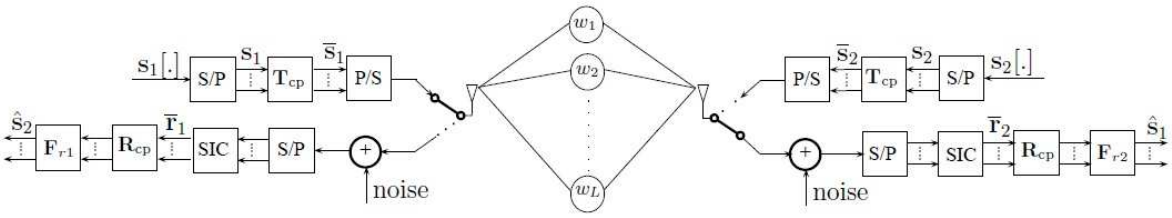

Figure 4.1: System block diagram for post-channel equalization using single-carrier communication scheme

the next section, we aim to minimize the total MSE of the symbol estimates under a total power constraint.

4.2.1 Channel Modeling

In this subsection, we present our channel model. This model is a discrete-time equivalent of the continuous-time channel model presented in Chapter 3. Let T_s be the symbol period and $\tau_{l_{pq}}$ denote the propagation delay of the lth signal path between Transceivers p and q, for $p, q \in \{1, 2\}$, corresponding to the lth relay. Assuming that the channel between each transceiver and each relay is reciprocal and frequency flat, the end-to-end channel between Transceiver p and Transceiver q, can be represented as a 2×2 matrix denoted as

$$\mathbf{H}[n] = \begin{bmatrix} h_{11}[n] & h_{12}[n] \\ h_{21}[n] & h_{22}[n] \end{bmatrix}.$$

Note that $h_{pq}[\cdot]$ represents the coefficients of the linear time-invariant (LTI) channel between Transceivers p and q. The impulse response $h_{pp}[\cdot]$ represents the channel which causes self-interference at Transceiver p. The end-to-end channel from

Transceiver p to Transceiver q, $(p, q \in \{1, 2\})$ can be viewed as a *multi-path channel* and it is represented by the following equivalent discrete-time finite impulse response:

$$h_{pq}[n] = \sum_{l=1}^{L} b_{l_{pq}} \delta[n - \breve{n}_{l_{pq}}], \quad \text{for} \quad p, q \in \{1, 2\} \quad \text{and} \quad 0 \leq n \leq N-1 \tag{4.2.2}$$

where $\breve{n}_{l_{pq}}$ is the discrete-time propagation delay of the lth relaying path, originating from Transceiver p and ending at Transceiver q, and it satisfies $(\breve{n}_{l_{pq}} - 1)T_s < \tau_{l_{pq}} \leq \breve{n}_{l_{pq}} T_s$. It is worth mentioning that N is the length of the equivalent discrete-time end-to-end channel impulse response $h_{pq}[\cdot]$, $p \neq q$, that is $N = 1 + \max_{l \leq L} \breve{n}_{l_{pq}}$. As we derived in the previous chapter, the vector of the taps of the end-to-end channel impulse response can be written as $\mathbf{h} = \mathbf{B}\mathbf{w}$.

4.2.2 Received Noise Modeling

Let τ'_{lq} represent the propagation delay between Transceiver q and the lth relay and n'_{lq} be an integer value which satisfies $\frac{\tau'_{lpq}}{T_s} \leq n'_{lq} < \frac{\tau'_{lpq}}{Ts} + 1$. We denote the spatially and temporally white noise at the lth relay as $\upsilon_l[n]$, which is assumed to be zero-mean with variance σ^2. This noise is amplified by w_l and arrives at Transceiver q with delay n'_{lq}. Hence, the superposition of the relay noises received at Transceiver q can be formulated as

$$\xi_q[n] = \sum_{l=1}^{L} w_l g_{lq} \upsilon_l[n - n'_{lq}] = \mathbf{v}_{n,q}^T \mathbf{G}_q \mathbf{w} \tag{4.2.3}$$

where

$$\mathbf{v}_{n,q} = \begin{bmatrix} \upsilon_1[n - n'_{1q}] & \upsilon_2[n - n'_{2q}] & \cdots & \upsilon_L[n - n'_{Lq}] \end{bmatrix}^T \tag{4.2.4}$$

$$\mathrm{G}_q = \mathrm{diag}\{g_{1q}, g_{2q}, \cdots, g_{Lq}\}. \tag{4.2.5}$$

Denoting the measurement noise at Transceiver q as $\gamma'_q[n]$, the total noise received at Transceiver q can be written as

$$\gamma_q[n] = \xi_q[n] + \gamma'_q[n]. \tag{4.2.6}$$

Using vector notation, we rewrite (4.2.6) as

$$\overline{\boldsymbol{\gamma}}_q(i) = \overline{\boldsymbol{\xi}}_q(i) + \overline{\boldsymbol{\gamma}}'_q(i) \tag{4.2.7}$$

where the following definitions are used:

$$\begin{aligned}
\overline{\boldsymbol{\gamma}}_q(i) &\triangleq \left[\begin{array}{cccc} \gamma_q[iN_t] & \gamma_q[iN_t+1] & \cdots & \gamma_q[iN_t+N_t-1] \end{array} \right]^T \\
\overline{\boldsymbol{\xi}}_q(i) &\triangleq \left[\begin{array}{cccc} \xi_q[iN_t] & \xi_q[iN_t+1] & \cdots & \xi_q[iN_t+N_t-1] \end{array} \right]^T \\
\overline{\boldsymbol{\gamma}}'_q(i) &\triangleq \left[\begin{array}{cccc} \gamma'_q[iN_t] & \gamma'_q[iN_t+1] & \cdots & \gamma'_q[iN_t+N_t-1] \end{array} \right]^T .
\end{aligned}$$

The total noise received at Transceiver q can be written as

$$\overline{\boldsymbol{\gamma}}_q(i) = \overline{\boldsymbol{\Upsilon}}_q(i)\mathbf{G}_q\mathbf{w} + \overline{\boldsymbol{\gamma}}'_q(i) \tag{4.2.8}$$

where $\overline{\boldsymbol{\Upsilon}}_q(i) \triangleq \left[\begin{array}{cccc} \mathbf{v}_{iN_t,q} & \mathbf{v}_{iN_t+1,q} & \cdots & \mathbf{v}_{(iN_t+N_t-1),q} \end{array} \right]^T$ is an $N_t \times L$ matrix whose lth column is the lth relay noise, after going through the delay between this relay and Transceiver q, corresponding to the ith received block.

4.2.3 Received Signal Modeling

Assuming $\mathrm{E}\{|s_p[k]|^2\} = 1$ and $\mathrm{E}\{s_p[k]\} = 0$, for $p \in \{1, 2\}$ and for any k, the ith signal block received at the output of the self-interference cancelation block of Transceiver q, can be written as [84]

$$\overline{\mathbf{r}}_q(i) = \sqrt{P_{\bar{q}}}\mathbf{H}_0(\mathbf{w})\overline{\mathbf{s}}_{\bar{q}}(i) + \sqrt{P_{\bar{q}}}\mathbf{H}_1(\mathbf{w})\overline{\mathbf{s}}_{\bar{q}}(i-1) + \overline{\boldsymbol{\gamma}}_q(i) \tag{4.2.9}$$

where $\bar{q} = 2$, for $q = 1$, and $\bar{q} = 1$, when $q = 2$, $P_{\bar{q}}$ is the transmit power of Transceiver $\bar{q}$ and we have used the following definitions:

$$\mathbf{H}_0(\mathbf{w}) \triangleq \begin{bmatrix} h[0] & 0 & 0 & \cdots & 0 \\ \vdots & h[0] & 0 & \cdots & 0 \\ h[N-1] & \cdots & \ddots & \cdots & \vdots \\ \vdots & \ddots & \cdots & \ddots & 0 \\ 0 & \cdots & h[N-1] & \cdots & h[0] \end{bmatrix}$$

$$\mathbf{H}_1(\mathbf{w}) \triangleq \begin{bmatrix} 0 & \cdots & h[N-1] & \cdots & h[1] \\ \vdots & \ddots & 0 & \ddots & \vdots \\ 0 & \cdots & \ddots & \cdots & h[N-1] \\ \vdots & \vdots & \vdots & \ddots & \vdots \\ 0 & \cdots & 0 & \cdots & 0 \end{bmatrix}. \tag{4.2.10}$$

The received signal vector $\overline{\mathbf{r}}_q(i)$ goes through the cyclic prefix removal matrix, and thus, its first N entries are discarded. One can easily verify that $\mathbf{R}_{\text{cp}}\mathbf{H}_1(\mathbf{w}) = \mathbf{0}$, and hence the IBI-inducing matrix $\mathbf{H}_1(\mathbf{w})$ is eliminated by cyclic prefix removal operation. Therefore, using (5.2.3), we can write

$$\begin{aligned} \mathbf{r}_q(i) \triangleq \mathbf{R}_{\text{cp}}\overline{\mathbf{r}}_q(i) &= \sqrt{P_{\bar{q}}}\mathbf{R}_{\text{cp}}\mathbf{H}_0(\mathbf{w})\mathbf{T}_{\text{cp}}\mathbf{s}_{\bar{q}}(i) + \mathbf{R}_{\text{cp}}\overline{\boldsymbol{\gamma}}_q(i) \\ &= \sqrt{P_{\bar{q}}}\widetilde{\mathbf{H}}(\mathbf{w})\mathbf{s}_{\bar{q}}(i) + \widetilde{\boldsymbol{\gamma}}_q(i) \end{aligned} \tag{4.2.11}$$

where $\widetilde{\boldsymbol{\gamma}}_q(i) \triangleq \mathbf{R}_{\text{cp}}\overline{\boldsymbol{\gamma}}_q(i)$ and $\widetilde{\mathbf{H}}(\mathbf{w}) \triangleq \mathbf{R}_{\text{cp}}\mathbf{H}_0(\mathbf{w})\mathbf{T}_{\text{cp}}$ is an $N_s \times N_s$ circulant matrix whose (k,l)th entry is given by $h[(k-l) \mod N_s]$. Considering the output of the block channel equalizer $\mathbf{F}_{rq}$, at Transceiver q, the linear estimate of the signal block transmitted by Transceiver $\bar{q}$, is represented as

$$\hat{\mathbf{s}}_{\bar{q}}(i) \triangleq \mathbf{F}_{rq}\mathbf{r}_q(i) = \sqrt{P_{\bar{q}}}\mathbf{F}_{rq}\widetilde{\mathbf{H}}(\mathbf{w})\mathbf{s}_{\bar{q}}(i) + \mathbf{F}_{rq}\widetilde{\boldsymbol{\gamma}}_q(i) \tag{4.2.12}$$

where $\hat{\mathbf{s}}_{\bar{q}}(i)$ is the $N_s \times 1$ vector of the linear estimates of the symbols transmitted by Transceiver $\bar{q}$.

4.2.4 Total Transmit Power Derivations

In this subsection, we derive the power consumed in the whole network in terms of relay weight vector $\mathbf{w}$ and transceivers' transmit powers. It follows from Figure. 4.1 that the $N_t \times 1$ vector $\overline{\mathbf{x}}_l(i)$ of the ith signal block relayed by the lth relay can be written as

$$\begin{aligned}\overline{\mathbf{x}}_l(i) &\triangleq \left[\begin{array}{cccc} \overline{x}_l[iN_t] & \overline{x}_l[iN_t+1] & \cdots & \overline{x}_l[iN_t+N_t-1] \end{array}\right]^T \\ &= w_l\left[\sqrt{P_1}g_{l1}\overline{\mathbf{s}}_1(i) + \sqrt{P_2}g_{l2}\overline{\mathbf{s}}_2(i) + \upsilon_l(i)\right] \end{aligned} \tag{4.2.13}$$

where the vector $\upsilon_l(i) \triangleq [\upsilon_l[iN_t] \;\; \upsilon_l[iN_t+1] \;\; \cdots \;\; \upsilon_l[iN_t+N_t-1]]^T$ is the ith block of measurement noise at the lth relay and $\overline{x}_l[t]$ is the signal transmitted by the lth relay at time t. We assume that $\upsilon_l(\cdot)$ is a stationary zero-mean random vector process whose entries are uncorrelated and have variances equal to σ^2. Using (4.2.13), the average transmit power of the lth relay is then obtained as

$$\begin{aligned}\widetilde{P}_l &\triangleq \frac{1}{N_t}\mathrm{E}\left\{\overline{\mathbf{x}}_l^H(i)\overline{\mathbf{x}}_l(i)\right\} \\ &= \frac{|w_l|^2}{N_t}\mathrm{E}\left\{\left[\sqrt{P_1}g_{l1}^*\overline{\mathbf{s}}_1^H(i) + \sqrt{P_2}g_{l2}^*\overline{\mathbf{s}}_2^H(i) + \upsilon_l^H(i)\right]\left[\sqrt{P_1}g_{l1}\overline{\mathbf{s}}_1(i) + \sqrt{P_2}g_{l2}\overline{\mathbf{s}}_2(i) + \upsilon_l(i)\right]\right\} \\ &= \frac{P_1|g_{l1}|^2|w_l|^2}{N_t}\mathrm{E}\left\{\overline{\mathbf{s}}_1^H(i)\overline{\mathbf{s}}_1(i)\right\} + \frac{P_2|g_{l2}|^2|w_l|^2}{N_t}\mathrm{E}\left\{\overline{\mathbf{s}}_2^H(i)\overline{\mathbf{s}}_2(i)\right\} + \frac{|w_l|^2}{N_t}\mathrm{E}\left\{\upsilon_l^H(i)\upsilon_l(i)\right\} \\ &= |w_l|^2\left(|g_{l1}|^2P_1 + |g_{l2}|^2P_2 + \sigma^2\right) \end{aligned} \tag{4.2.14}$$

where we have assumed that $\overline{\mathbf{s}}_1(\cdot)$, $\overline{\mathbf{s}}_2(\cdot)$, and $\upsilon_l(\cdot)$ are zero-mean mutually independent stationary random vector processes. Using (4.2.14), the total transmit power of the

network can be obtained as

$$\begin{aligned} P_{total} &\triangleq P_1 + P_2 + \sum_{l=1}^{L} \widetilde{P}_l \\ &= P_1 + P_2 + \sum_{l=1}^{L} |w_l|^2 \left(|g_{l1}|^2 P_1 + |g_{l2}|^2 P_2 + \sigma^2 \right) \\ &= P_1 \left(1 + \|\mathbf{G}_1 \mathbf{w}\|^2 \right) + P_2 \left(1 + \|\mathbf{G}_2 \mathbf{w}\|^2 \right) + \sigma^2 \mathbf{w}^H \mathbf{w}. \end{aligned} \tag{4.2.15}$$

In our design, the total power P_{total} is constrained to be less than, or equal to the maximum available power P_{max}.

4.3 Jointly Optimal Equalization, Relay Beamforming, and Power Loading

4.3.1 Problem Definition

In this section, our goal is to optimally obtain the block channel equalizers $\mathbf{F}_{r1}$ and $\mathbf{F}_{r2}$, the relay beamforming weight vector $\mathbf{w}$, and the transceivers' transmit powers P_1 and P_2, such that the total MSE of the symbol estimates (i.e., the equalizers' outputs) at the two transceivers is minimized under a total power budget constraint. To this end, we can write the $N_s \times 1$ vector of the symbol estimation errors at Transceiver q, i.e., $\mathbf{e}_q(i)$, corresponding to the ith block transmitted by Transceiver $\bar{q}$, as

$$\mathbf{e}_q(i) \triangleq \hat{\mathbf{s}}_{\bar{q}}(i) - \mathbf{s}_{\bar{q}}(i) = \mathbf{F}_{rq} \mathbf{r}_q(i) - \mathbf{s}_{\bar{q}}(i). \tag{4.3.1}$$

To obtain jointly optimal block channel equalizers and transmit powers at the two transceivers as well as the relay beamforming weight vector, the problem of minimizing the total MSE under the total available power constraint can be formulated as the

following optimization problem:

$$\begin{aligned} \min_{\substack{P_1\geq 0\\ P_2\geq 0}} \min_{\mathbf{w}} \min_{\mathbf{F}_{r1},\mathbf{F}_{r2}} \quad & \sum_{q=1}^{2} \mathrm{E}\left\{\|\mathbf{e}_q(i)\|^2\right\} \\ \text{subject to} \quad & P_{total} \leq P_{max} \end{aligned} \tag{4.3.2}$$

where P_{max} is the maximum available power of the network. In (4.3.2) the expectation is taken with respect to noise and random symbols. The solution to the optimization problem (4.3.2) has a certain feature which allows us to develop a guideline to determine individual relay power consumptions. This feature will be presented as we obtain the solution to the optimization problem (4.3.2) in the sequel.

4.3.2 Optimal Channel Equalizers

Let us consider the inner minimization problem in (4.3.2) and define

$$\lambda(\mathbf{w}, P_1, P_2) \triangleq \min_{\mathbf{F}_{r1},\mathbf{F}_{r2}} \sum_{q=1}^{2} \mathrm{E}\left\{\|\mathbf{e}_q(i)\|^2\right\} = \sum_{q=1}^{2} \min_{\mathbf{F}_{rq}} \mathrm{E}\left\{\mathbf{e}_q^H(i)\mathbf{e}_q(i)\right\}. \tag{4.3.3}$$

At Transceiver q, using (4.3.1) along with the assumption that $\mathrm{E}\{\mathbf{s}_{\bar{q}}(i)\} = \mathbf{0}$, the MSE at Transceiver q, $\mathrm{MSE}_q(\mathbf{w}, \mathbf{F}_{rq}, P_1, P_2)$ can be written as

$$\begin{aligned} \mathrm{MSE}_q(\mathbf{w}, \mathbf{F}_{rq}, P_1, P_2) &= \mathrm{E}\left\{\mathbf{e}_q^H(i)\mathbf{e}_q(i)\right\} \\ &= \mathrm{E}\left\{[\mathbf{r}_q^H(i)\mathbf{F}_{rq}^H - \mathbf{s}_{\bar{q}}^H(i)][\mathbf{F}_{rq}\mathbf{r}_q(i) - \mathbf{s}_{\bar{q}}(i)]\right\} \\ &= \mathrm{E}\left\{\mathbf{r}_q^H(i)\mathbf{F}_{rq}^H\mathbf{F}_{rq}\mathbf{r}_q(i) - \mathbf{s}_{\bar{q}}^H(i)\mathbf{F}_{rq}\mathbf{r}_q(i) - \mathbf{r}_q^H(i)\mathbf{F}_{rq}^H\mathbf{s}_{\bar{q}}(i) + \mathbf{s}_{\bar{q}}^H(i)\mathbf{s}_{\bar{q}}(i)\right\} \\ &= \mathrm{tr}\left\{\mathbf{F}_{rq}\mathbf{R}_q(\mathbf{w})\mathbf{F}_{rq}^H\right\} - \sqrt{P_{\bar{q}}}\,\mathrm{tr}\left\{\mathbf{F}_{rq}\widetilde{\mathbf{H}}(\mathbf{w}) + \widetilde{\mathbf{H}}^H(\mathbf{w})\mathbf{F}_{rq}^H\right\} + N_s \end{aligned} \tag{4.3.4}$$

where $\mathbf{R}_q(\mathbf{w}) \triangleq \mathrm{E}\left\{\mathbf{r}_q(i)\mathbf{r}_q^H(i)\right\}$ is the correlation matrix of the received block at Transceiver q. In (4.3.4), the last equality follows from the fact using (4.2.11), we can

write

$$\mathrm{E}\{\mathbf{r}_q(i)\mathbf{s}_{\bar{q}}^H(i)\} = \mathrm{E}\left\{\left(\sqrt{P_{\bar{q}}}\widetilde{\mathbf{H}}(\mathbf{w})\mathbf{s}_{\bar{q}}(i) + \widetilde{\boldsymbol{\gamma}}_q(i)\right)\mathbf{s}_{\bar{q}}^H(i)\right\}$$
$$= \sqrt{P_{\bar{q}}}\widetilde{\mathbf{H}}(\mathbf{w})\mathrm{E}\left\{\mathbf{s}_{\bar{q}}(i)\mathbf{s}_{\bar{q}}^H(i)\right\} = \sqrt{P_{\bar{q}}}\widetilde{\mathbf{H}}(\mathbf{w})\,. \tag{4.3.5}$$

Using (4.2.11) along with the assumption that the information symbols and the noises are uncorrelated, we can also write

$$\mathbf{R}_q(\mathbf{w}) \triangleq \mathrm{E}\left\{\mathbf{r}_q(i)\mathbf{r}_q^H(i)\right\} = P_{\bar{q}}\mathrm{E}\{\widetilde{\mathbf{H}}(\mathbf{w})\mathbf{s}_{\bar{q}}(i)\mathbf{s}_{\bar{q}}^H(i)\widetilde{\mathbf{H}}^H(\mathbf{w})\} + \mathrm{E}\{\widetilde{\boldsymbol{\gamma}}_q(i)\widetilde{\boldsymbol{\gamma}}_q^H(i)\}$$
$$= P_{\bar{q}}\widetilde{\mathbf{H}}(\mathbf{w})\widetilde{\mathbf{H}}^H(\mathbf{w}) + \mathbf{R}_{\mathrm{cp}}\mathrm{E}\{\overline{\boldsymbol{\gamma}}_q(i)\overline{\boldsymbol{\gamma}}_q^H(i)\}\mathbf{R}_{\mathrm{cp}}^H$$
$$= P_{\bar{q}}\widetilde{\mathbf{H}}(\mathbf{w})\widetilde{\mathbf{H}}^H(\mathbf{w}) + \sigma^2\left(\mathbf{w}^H\mathbf{G}_q^H\mathbf{G}_q\mathbf{w} + 1\right)\mathbf{I}_{N_s}$$
$$= P_{\bar{q}}\widetilde{\mathbf{H}}(\mathbf{w})\widetilde{\mathbf{H}}^H(\mathbf{w}) + \sigma^2\left(\|\mathbf{G}_q\mathbf{w}\|^2 + 1\right)\mathbf{I}_{N_s}\,. \tag{4.3.6}$$

The optimal value of $\mathbf{F}_{rq}$ can be obtained by differentiating (4.3.4) with respect to $\mathbf{F}_{rq}$ and equating the derivative to zero[1]. Using the fact that for any given relay beamforming weight $\mathbf{w}$, we can write $\mathbf{R}_q^H(\mathbf{w}) = \mathbf{R}_q(\mathbf{w})$, the optimal value of $\mathbf{F}_{rq}$ is obtained as

$$\mathbf{F}_{rq}^{\mathrm{opt}}(\mathbf{w}) = \sqrt{P_{\bar{q}}}\;\widetilde{\mathbf{H}}^H(\mathbf{w})\mathbf{R}_q^{-1}(\mathbf{w}). \tag{4.3.7}$$

In the next subsection, we use (4.3.7) to obtain the optimal value of the relay beamforming vector.

[1]Note that (4.3.4) is not differentiable with respect to $\mathbf{F}_{rq}$ in Cauchy-Riemann sense. Nevertheless, we can use the generalized complex derivative which is defined, for any function $f(\mathbf{F}_{rq})$, as

$$\frac{\partial f(\mathbf{F}_{rq})}{\partial \mathbf{F}_{rq}} = \frac{1}{2}\left(\frac{\partial f(\mathbf{F}_{rq})}{\partial \Re\{\mathbf{F}_{rq}\}} - j\frac{\partial f(\mathbf{F}_{rq})}{\partial \Im\{\mathbf{F}_{rq}\}}\right)$$

where $\Re\{\mathbf{F}_{rq}\}$ and $\Im\{\mathbf{F}_{rq}\}$ represent the real and imaginary parts of $\mathbf{F}_{rq}$, respectively.

4.3.3 Optimal Relay Beamforming Weights

Using (4.3.4) and (4.3.7), we can now write (4.3.3) as

$$\begin{aligned}\lambda(\mathbf{w}, P_1, P_2) &= \mathrm{MSE}_1(\mathbf{w}, \mathbf{F}_{r1}^{\mathrm{opt}}(\mathbf{w}), P_1, P_2) + \mathrm{MSE}_2(\mathbf{w}, \mathbf{F}_{r2}^{\mathrm{opt}}(\mathbf{w}), P_1, P_2) \\ &= \sum_{q=1}^{2} \left(N_s - P_{\bar{q}} \mathrm{tr} \left\{ \widetilde{\mathbf{H}}^H(\mathbf{w}) \mathbf{R}_q^{-1}(\mathbf{w}) \widetilde{\mathbf{H}}(\mathbf{w}) \right\} \right). \end{aligned} \tag{4.3.8}$$

where we have used the fact that $\mathbf{R}_q(\mathbf{w})$ is a Hermitian matrix. We note that the $N_s \times N_s$ circulant matrix $\widetilde{\mathbf{H}}(\mathbf{w})$ can be decomposed as

$$\widetilde{\mathbf{H}}(\mathbf{w}) = \mathbf{F}^H \mathbf{D}(\mathbf{w}) \mathbf{F} \tag{4.3.9}$$

where $\mathbf{D}(\mathbf{w}) \triangleq \mathrm{diag}\{H(e^{j0}) \ , \ H(e^{j\frac{2\pi}{N_s}}), \cdots, H(e^{j\frac{2\pi(N_s-1)}{N_s}})\}$ is an $N_s \times N_s$ diagonal matrix of the frequency response of the end-to-end channel at integer multiples of $\frac{1}{N_s}$, $H(e^{j2\pi f}) \triangleq \sum_{n=0}^{N-1} h[n] e^{-j2\pi f n}$ is the frequency response[2] of the end-to-end channel at the normalized frequency f, and $\mathbf{F}$ is the $N_s \times N_s$ DFT matrix whose (k,n)th element is defined as $F(k,n) = N_s^{-\frac{1}{2}} e^{-j2\pi kn/N_s}$. In the appendix, we use (4.3.9) to rewrite (4.3.8) as

$$\begin{aligned}\lambda(\mathbf{w}, P_1, P_2) &= \sum_{q=1}^{2} \left(N_s - P_{\bar{q}} \mathrm{tr} \left\{ \mathbf{F}^H \mathbf{D}^H(\mathbf{w}) \mathbf{F} \mathbf{R}_q^{-1}(\mathbf{w}) \mathbf{F}^H \mathbf{D}(\mathbf{w}) \mathbf{F} \right\} \right) \\ &= 2N_s - \sum_{q=1}^{2} P_{\bar{q}} \mathrm{tr} \left\{ \mathbf{D}^H(\mathbf{w}) \left(P_{\bar{q}} \mathbf{D}(\mathbf{w}) \mathbf{D}^H(\mathbf{w}) + \sigma^2 \left(\|\mathbf{G}_q \mathbf{w}\|^2 + 1 \right) \mathbf{I}_{N_s} \right)^{-1} \mathbf{D}(\mathbf{w}) \right\} . \end{aligned} \tag{4.3.10}$$

[2]Note that the same as the end-to-end channel impulse response $h[\cdot]$, the end-to-end channel frequency response $H(\cdot)$ depends on the relay beamforming weight vector $\mathbf{w}$. For the sake of notation simplicity, we do not show this dependency explicitly, rather we use $\mathbf{w}$ as the argument of $\widetilde{\mathbf{H}}(\mathbf{w})$ to emphasize this dependency.

Recall that $\mathbf{f}_k = \frac{1}{\sqrt{N_s}} \begin{bmatrix} 1 & e^{j\frac{2\pi(k-1)}{N_s}} & \dots & e^{j\frac{2(N-1)(k-1)\pi}{N_s}} \end{bmatrix}^T$, for $k = 1, 2, \dots, N_s$. Hence, we can write

$$\begin{aligned} \mathbf{D}(\mathbf{w}) &= \text{diag}\left\{ H(e^{j0}), H(e^{j\frac{2\pi}{N_s}}), \dots, H(e^{j\frac{2\pi(N_s-1)}{N_s}}) \right\} \\ &= \sqrt{N_s}\, \text{diag}\left\{ \mathbf{f}_1^H \mathbf{B}\mathbf{w}, \mathbf{f}_2^H \mathbf{B}\mathbf{w}, \dots, \mathbf{f}_{N_s}^H \mathbf{B}\mathbf{w} \right\}. \end{aligned} \tag{4.3.11}$$

Using (4.3.11), we can write (4.3.10) as

$$\begin{aligned} \lambda(\mathbf{w}, P_1, P_2) &= 2N_s - \sum_{q=1}^{2} \text{tr}\left\{ \text{diag}\left\{ \frac{N_s P_{\bar{q}} |\mathbf{f}_k^H \mathbf{B}\mathbf{w}|^2}{N_s P_{\bar{q}} |\mathbf{f}_k^H \mathbf{B}\mathbf{w}|^2 + \sigma^2 \left(\|\mathbf{G}_q \mathbf{w}\|^2 + 1 \right)} \right\}_{k=1}^{N_s} \right\} \\ &= 2N_s - \sum_{q=1}^{2} \sum_{k=1}^{N_s} \frac{N_s P_{\bar{q}} |\mathbf{f}_k^H \mathbf{B}\mathbf{w}|^2}{N_s P_{\bar{q}} |\mathbf{f}_k^H \mathbf{B}\mathbf{w}|^2 + \sigma^2 \left(\|\mathbf{G}_q \mathbf{w}\|^2 + 1 \right)} \\ &= \sum_{q=1}^{2} \sum_{k=1}^{N_s} \left(1 - \frac{N_s P_{\bar{q}} |\mathbf{f}_k^H \mathbf{B}\mathbf{w}|^2}{P_{\bar{q}} N_s |\mathbf{f}_k^H \mathbf{B}\mathbf{w}|^2 + \sigma^2 \left(\|\mathbf{G}_q \mathbf{w}\|^2 + 1 \right)} \right) \\ &= \sum_{q=1}^{2} \sum_{k=1}^{N_s} \left(\frac{\sigma^2 (\|\mathbf{G}_q \mathbf{w}\|^2 + 1)}{P_{\bar{q}} N_s |\mathbf{f}_k^H \mathbf{B}\mathbf{w}|^2 + \sigma^2 \left(\|\mathbf{G}_q \mathbf{w}\|^2 + 1 \right)} \right). \end{aligned} \tag{4.3.12}$$

Dividing the numerator and denominator by $\sigma^2 \left(\|\mathbf{G}_q \mathbf{w}\|^2 + 1 \right)$, we can write (4.3.12) as

$$\lambda(\mathbf{w}, P_1, P_2) = \sum_{q=1}^{2} \sum_{k=1}^{N_s} \frac{1}{\frac{P_{\bar{q}} N_s |\mathbf{f}_k^H \mathbf{B}\mathbf{w}|^2}{\sigma^2 \left(\|\mathbf{G}_q \mathbf{w}\|^2 + 1 \right)} + 1}. \tag{4.3.13}$$

Using (4.2.15) and (4.3.13), the optimization problem (4.3.2) can be rewritten as

$$\begin{aligned} \min_{\substack{P_1 \geq 0 \\ P_2 \geq}} \min_{\mathbf{w}} \quad & \sum_{k=1}^{N_s} \frac{1}{\phi_{k,1}(\mathbf{w})} + \sum_{k=1}^{N_s} \frac{1}{\phi_{k,2}(\mathbf{w})} \\ \text{subject to} \quad & P_1 \left(1 + \|\mathbf{G}_1 \mathbf{w}\|^2 \right) + P_2 \left(1 + \|\mathbf{G}_2 \mathbf{w}\|^2 \right) + \sigma^2 \mathbf{w}^H \mathbf{w} \leq P_{max} \end{aligned} \tag{4.3.14}$$

where we have used the following definition:

$$\phi_{k,q}(\mathbf{w}) \triangleq \left(\frac{P_{\bar{q}} N_s |\mathbf{f}_k^H \mathbf{B}\mathbf{w}|^2}{\sigma^2 \left(\|\mathbf{G}_q \mathbf{w}\|^2 + 1 \right)} + 1 \right), \text{ for } q = 1, 2. \tag{4.3.15}$$

In order to further simplify (4.3.14), we use the fact that the harmonic mean of any set of the positive numbers $\{\alpha_k\}_{k=1}^{N_s}$ is less than, or equal, to their arithmetic mean. i.e.,

$$\frac{1}{N_s}\sum_{k=1}^{N_s}\alpha_k \geq \frac{1}{\frac{1}{N_s}\sum_{i=1}^{N_s}\frac{1}{\alpha_k}}. \tag{4.3.16}$$

The equality holds in (4.3.16), iff α_k's are all equal. Using (4.3.16) along with the fact that $\phi_{k,q}(\mathbf{w})$ defined in (4.3.15) is positive, it is easy to prove that for $q = 1, 2$, the following inequality holds true:

$$\sum_{k=1}^{N_s}\frac{1}{\phi_{k,q}(\mathbf{w})} \geq \frac{N_s^2}{\sum_{k=1}^{N_s}\phi_{k,q}(\mathbf{w})} \tag{4.3.17}$$

where the equality holds iff, for a given q, we can find a set of $\mathbf{w}$'s for which $\{\phi_{k,q}(\mathbf{w})\}_{i=1}^{N_s}$ are all equal to each other. Using (4.3.17), we replace each summation in the objective function of (4.3.14) with its corresponding lower bound. To ensure that these lower bounds are both achieved simultaneously, we restrict $\mathbf{w}$ to be such that $\{\phi_{k,1}(\mathbf{w})\}_{i=1}^{N_s}$ are all equal to each other and at the same time $\{\phi_{k,2}(\mathbf{w})\}_{i=1}^{N_s}$ are all equal to each other. For any transceiver index q, let $\mathcal{W}_q$ represent the set of the values of $\mathbf{w}$ such that all $\{\phi_{k,q}(\mathbf{w})\}_{k=1}^{N_s}$ are equal. That is,

$$\mathcal{W}_q = \left\{\mathbf{w}\middle| |\mathbf{f}_k^H\mathbf{B}\mathbf{w}| = |\mathbf{f}_{k'}^H\mathbf{B}\mathbf{w}|, \forall k \neq k'\right\}. \tag{4.3.18}$$

From (4.3.18), it can be inferred that $\mathcal{W}_q$ does not depend on q, and hence, $\mathcal{W}_1 = \mathcal{W}_2 \triangleq \mathcal{W}$. However, it may not be inferred that $\phi_{k,1}(\mathbf{w})$ is equal to $\phi_{k,2}(\mathbf{w})$, for $k = 1, 2\cdots, N_s$. Nevertheless, we soon prove that $\phi_{k,1}(\mathbf{w})$ is indeed equal to $\phi_{k,2}(\mathbf{w})$, for $k = 1, 2\cdots, N_s$. Note that $\mathcal{W}$ can be written as $\mathcal{W} = \bigcup_{n=0}^{N-1}\mathcal{U}_n$, where $\mathcal{U}_n$ is the

set of the relay weight vectors such that only the nth tap of the end-to-end channel impulse response is non-zero and the remaining taps are zero. That is, $\mathcal{U}_n$ is the set of weight vectors $\mathbf{w}$ which have non-zero entries only for those relays which contribute to the nth tap and the other entries of $\mathbf{w}$ (which do not contribute to the nth tap of the end-to-end channel impulse response) are zero. Note that $\mathcal{U}_n \bigcap \mathcal{U}_{n'} = \emptyset$, for $n \neq n'$. Indeed, it can be seen from (4.2.2) and (3.2.1) that each relay contributes only to one of the taps of the end-to-end channel impulse response. Therefore, *without any loss of optimality*[3], we can write the optimization problem (4.3.14) as

$$\begin{aligned} \min_{\substack{P_1\geq 0\\ P_2\geq 0}} \min_{\mathbf{w}} \quad & \sum_{q=1}^{2} \frac{N_s^2}{\sum_{k=1}^{N_s} \phi_{k,q}(\mathbf{w})} \\ \text{subject to} \quad & P_1\left(1+\|\mathbf{G}_1\mathbf{w}\|^2\right) + P_2\left(1+\|\mathbf{G}_2\mathbf{w}\|^2\right) + \sigma^2\mathbf{w}^H\mathbf{w} \leq P_{max} \\ \text{and} \quad & \mathbf{w} \in \bigcup_{n=0}^{N-1} \mathcal{U}_n. \end{aligned} \tag{4.3.19}$$

Note that due to Parseval's theorem, we have that

$$\sum_{k=1}^{N_s} |\mathbf{f}_k^H\mathbf{B}\mathbf{w}|^2 = \|\mathbf{B}\mathbf{w}\|^2 = \mathbf{w}^H\mathbf{B}^H\mathbf{B}\mathbf{w}. \tag{4.3.20}$$

Using (4.3.20), we can write $\sum_{k=1}^{N_s} \phi_{k,q}(\mathbf{w}) = \frac{N_s P_{\bar{q}} \sum_{k=1}^{N_s} |\mathbf{f}_k^H\mathbf{B}\mathbf{w}|^2}{\sigma^2(\|\mathbf{G}_q\mathbf{w}\|^2+1)} + N_s = \frac{N_s P_{\bar{q}} \mathbf{w}^H\mathbf{B}^H\mathbf{B}\mathbf{w}}{\sigma^2(\|\mathbf{G}_q\mathbf{w}\|^2+1)} + N_s$, and hence, the optimization problem (4.3.19) can be rewritten as

$$\begin{aligned} \min_{\substack{P_1\geq 0\\ P_2\geq 0}} \min_{\mathbf{w}} \quad & \sum_{q=1}^{2} \frac{N_s^2}{\frac{N_s P_{\bar{q}} \mathbf{w}^H\mathbf{B}^H\mathbf{B}\mathbf{w}}{\sigma^2\left(\|\mathbf{G}_q\mathbf{w}\|^2+1\right)} + N_s} \\ \text{subject to} \quad & P_1\left(1+\|\mathbf{G}_1\mathbf{w}\|^2\right) + P_2\left(1+\|\mathbf{G}_2\mathbf{w}\|^2\right) + \sigma^2\mathbf{w}^H\mathbf{w} \leq P_{max} \\ \text{and} \quad & \mathbf{w} \in \bigcup_{n=0}^{N-1} \mathcal{U}_n. \end{aligned} \tag{4.3.21}$$

[3]There is no optimality loss when arriving from (4.3.14) to (4.3.19) because while minimizing the lower bound of the objective function, we restrict $\mathbf{w}$ such that it belongs to set $\mathcal{W}_1 = \mathcal{W}_2 \triangleq \mathcal{W}$. This restriction guarantees that the inequality in (4.3.17) holds with equality. Indeed, we minimize the lower bound under the constraint $\mathbf{w} \in \mathcal{W}$ to ensure that lower bound is tight.

To solve the optimization problem (4.3.21), we benefit from the fact that the sets $\{\mathcal{U}_n\}_{n=0}^{N-1}$ are mutually exclusive, and hence, the optimal $\mathbf{w}$ belongs only to one of these sets. To find the set $\mathcal{U}_n$ where the optimal $\mathbf{w}$ resides, we can decompose the optimization problem (4.3.21) into a set of maximum N subproblems[4], each of which assumes that $\mathbf{w}$ belongs to one of the sets $\{\mathcal{U}_n\}_{n=0}^{N-1}$. Each of these subproblems can then be solved separately and the corresponding minimum value of the objective function (i.e., the total MSE) can be obtained. This approach leads to N candidate values for optimal $\mathbf{w}$. The optimal value of $\mathbf{w}$ can then be easily found by determining which of these candidates results in the lowest possible value for the total MSE. Mathematically, this is equivalent to solving the following minimization problem:

$$\begin{aligned} \min_{0\le n\le N-1} \min_{\substack{P_1\ge 0\\ P_2\ge 0}} \min_{\mathbf{w}} \quad & \sum_{q=1}^{2} \frac{N_s}{\dfrac{P_{\bar{q}}\mathbf{w}^H\mathbf{B}^H\mathbf{B}\mathbf{w}}{\sigma^2\left(\|\mathbf{G}_q\mathbf{w}\|^2+1\right)}+1} \\ \text{subject to} \quad & P_1\left(1+\|\mathbf{G}_1\mathbf{w}\|^2\right)+P_2\left(1+\|\mathbf{G}_2\mathbf{w}\|^2\right)+\sigma^2\mathbf{w}^H\mathbf{w}\le P_{max} \\ \text{and} \quad & \mathbf{w}\in\mathcal{U}_n. \end{aligned} \tag{4.3.22}$$

Let $\mathbf{w}_n$ represent the vector of the weights of those relays which contribute to the nth tap of the end-to-end channel impulse response. If $\mathbf{w}\in\mathcal{U}_n$, then we can write

$$\mathbf{w}^H\mathbf{B}^H\mathbf{B}\mathbf{w}=\mathbf{w}_n^H\mathbf{b}_n\mathbf{b}_n^H\mathbf{w}_n \tag{4.3.23}$$

where $\mathbf{b}_n^H$ captures the non-zero entries of the $(n+1)$th row of the matrix $\mathbf{B}$. As mentioned above, in order to solve (4.3.21), we can solve N separate optimization problems (as in (4.3.22)), thereby choosing the value of n which leads to the minimum value for the objective function. Depending on which tap of the end-to-end

[4]We later show that the number of sub-problems is much smaller than the length N of the end-to-end channel. Indeed, we show that the maximum value for the number of sub-problems is equal to the number L of the relays.

channel impulse response is non-zero (by activating the corresponding relays), the total estimation error of the received signals can be different. Therefore, we need to turn on those relays which contribute to that tap of the end-to-end channel impulse response that leads to minimum total mean squared error of the estimated signals at both transceivers. In other words, the optimum n is obtained such that the total received signal error power is minimized at the two transceivers. Using (4.3.23), we can rewrite the optimization problem (4.3.22) as

$$\begin{aligned}
&\min_{0\le n\le N-1} \min_{\substack{P_1\ge 0\\ P_2\ge 0}} \min_{\mathbf{w}_n} \sum_{q=1}^{2} \frac{N_s}{\dfrac{P_{\bar{q}}\mathbf{w}_n^H\mathbf{b}_n\mathbf{b}_n^H\mathbf{w}_n}{\sigma^2\left(\|\mathbf{G}_q^{(n)}\mathbf{w}_n\|^2+1\right)}+1} \\
&\text{s.t. } P_1\left(1+\|\mathbf{G}_1^{(n)}\mathbf{w}_n\|^2\right)+P_2\left(1+\|\mathbf{G}_2^{(n)}\mathbf{w}_n\|^2\right)+\sigma^2\mathbf{w}_n^H\mathbf{w}_n\le P_{max} \qquad (4.3.24)
\end{aligned}$$

where $\mathbf{G}_q^{(n)}$, for $q=1,2$, is a diagonal matrix whose diagonal entries are a subset of those diagonal entries of $\mathbf{G}_q$ which correspond to the relays that contribute to the nth tap of the end-to-end channel impulse response. Let us define $\psi_q(\mathbf{w}_n) \triangleq \left(\dfrac{P_{\bar{q}}\mathbf{w}_n^H\mathbf{b}_n\mathbf{b}_n^H\mathbf{w}_n}{\sigma^2\left(\|\mathbf{G}_q^{(n)}\mathbf{w}_n\|^2+1\right)}+1\right)$. Without loss of optimality, we can assume that $\psi_1(\mathbf{w}_n)=\psi_2(\mathbf{w}_n)$. Otherwise, if for example at the optimum, $\psi_1(\mathbf{w}_n)>\psi_2(\mathbf{w}_n)$, then we can reduce the transmit power P_2 such that $\psi_1(\mathbf{w}_n)=\psi_2(\mathbf{w}_n)$, without violating the constraint in (4.3.24). Now, using the fact that $\psi_1(\mathbf{w}_n)=\psi_2(\mathbf{w}_n)$, we can rewrite the optimization problem (4.3.24) as

$$\begin{aligned}
\min_{0\le n\le N-1} \min_{\substack{P_1\ge 0\\ P_2\ge 0}} \min_{\mathbf{w}_n} \quad & \frac{2N_s}{\dfrac{P_1\mathbf{w}_n^H\mathbf{b}_n\mathbf{b}_n^H\mathbf{w}_n}{\sigma^2\left(\|\mathbf{G}_2^{(n)}\mathbf{w}_n\|^2+1\right)}+1} \\
\text{subject to} \quad & P_1\left(1+\|\mathbf{G}_1^{(n)}\mathbf{w}_n\|^2\right)+P_2\left(1+\|\mathbf{G}_2^{(n)}\mathbf{w}_n\|^2\right)+\sigma^2\mathbf{w}_n^H\mathbf{w}_n\le P_{max} \\
\text{and} \quad & P_1\left(1+\|\mathbf{G}_1^{(n)}\mathbf{w}_n\|^2\right)=P_2\left(1+\|\mathbf{G}_2^{(n)}\mathbf{w}_n\|^2\right) \qquad (4.3.25)
\end{aligned}$$

or, equivalently, as

$$\min_{0\le n\le N-1}\ \min_{P_1\ge 0}\ \min_{\mathbf{w}_n} \quad \frac{2N_s}{\dfrac{P_1\mathbf{w}_n^H\mathbf{b}_n\mathbf{b}_n^H\mathbf{w}_n}{\sigma^2\left(\|\mathbf{G}_2^{(n)}\mathbf{w}_n\|^2+1\right)}+1}$$
$$\text{subject to} \quad 2P_1\left(1+\|\mathbf{G}_1^{(n)}\mathbf{w}_n\|^2\right)+\sigma^2\mathbf{w}_n^H\mathbf{w}_n\le P_{max}\,. \tag{4.3.26}$$

We can show that the constraint in (4.3.26) can be satisfied with equality[5]. Therefore, the optimization problem (4.3.26) can be written as

$$\max_{0\le n\le N-1}\ \max_{P_1\ge 0}\ \max_{\mathbf{w}_n} \quad \frac{P_1\mathbf{w}_n^H\mathbf{b}_n\mathbf{b}_n^H\mathbf{w}_n}{\sigma^2\left(\|\mathbf{G}_2^{(n)}\mathbf{w}_n\|^2+1\right)}$$
$$\text{subject to} \quad P_1=\frac{P_{max}-\sigma^2\mathbf{w}_n^H\mathbf{w}_n}{2\left(1+\|\mathbf{G}_1^{(n)}\mathbf{w}_n\|^2\right)}. \tag{4.3.27}$$

We now can use the constraint in (4.3.27) to eliminate P_1, while noting $P_1\ge 0$ implies that $\mathbf{w}_n^H\mathbf{w}_n\le P_{max}/\sigma^2$. Hence, we can rewrite the optimization problem (4.3.27) as

$$\max_{0\le n\le N-1}\ \max_{\mathbf{w}_n} \quad \frac{(P_{max}-\sigma^2\mathbf{w}_n^H\mathbf{w}_n)\mathbf{w}_n^H\mathbf{b}_n\mathbf{b}_n^H\mathbf{w}_n}{2\sigma^2\left(\mathbf{w}_n^H\mathbf{Q}_1^{(n)}\mathbf{w}_n+1\right)\left(\mathbf{w}_n^H\mathbf{Q}_2^{(n)}\mathbf{w}_n+1\right)}$$
$$\text{subject to} \quad \mathbf{w}_n^H\mathbf{w}_n\le\frac{P_{max}}{\sigma^2} \tag{4.3.28}$$

where $\mathbf{Q}_q^{(n)}\triangleq(\mathbf{G}_q^{(n)})^H\mathbf{G}_q^{(n)}$, for $q=1,2$. According to the results of [83], the inner maximization aims to find $\mathbf{w}_n$ such that under a total power constraint of P_{max}, the smaller transceiver SNR is maximized for a synchronous relay sub-network where only those relays contributing to the nth tap of the impulse response of the end-to-end channel in the main network are deployed. This max-min SNR fair design approach has been shown to be equivalent to maximizing the sum-rate for the sub-network

[5]Otherwise, the optimal P_1 can be increased so that the total power consumed in the network is equal to P_{max}. Increasing the optimal P_1, furthermore reduces the objective function, thereby contradicting the optimality.

under the same total power constraint [44]. It is now well-known that the optimization problem (4.3.28) is amenable to a semi-closed-form solution for the optimal $\mathbf{w}_n$, denoted as $\mathbf{w}_n^o$, which is given by

$$\mathbf{w}_n^o = \sigma^2 \kappa_n \sqrt{2\nu_n} \Big(2\mu_n \mathbf{Q}_1^{(n)} + 2\nu_n \mathbf{Q}_2^{(n)} + \sigma^2 \mathbf{I} \Big)^{-1} \mathbf{b}_n \tag{4.3.29}$$

where $\nu_n \triangleq 0.5 P_{\max}/\sigma^2 - \mu_n$, κ_n is expressed as

$$\kappa_n \triangleq \sigma^{-1} \left(\mathbf{b}_n^H \left(\sigma^2 \mathbf{I} + 2\mu_n \mathbf{Q}_1^{(n)} \right) \left(\sigma^2 \mathbf{I} + 2\mu_n \mathbf{Q}_1^{(n)} + 2\nu_n \mathbf{Q}_2^{(n)} \right)^{-2} \mathbf{b}_n \right)^{-\frac{1}{2}} \tag{4.3.30}$$

and μ_n is the *unique* solution to the following equation

$$\begin{aligned} &\sigma^2 (P_{\max}/\sigma^2 - 4\mu_n) \mathbf{b}_n^H (2\mu_n \mathbf{Q}_1^{(n)} + (P_{\max}/\sigma^2 - 2\mu_n) \mathbf{Q}_2^{(n)} + \mathbf{I})^{-1} \mathbf{b}_n - \\ &\mu_n (P_{\max}/\sigma^2 - 2\mu_n) \mathbf{b}_n^H (2\mu_n \mathbf{Q}_1^{(n)} + (P_{\max}/\sigma^2 - 2\mu_n) \mathbf{Q}_2^{(n)} + \mathbf{I})^{-2} (2\mathbf{Q}_1^{(n)} - 2\mathbf{Q}_2^{(n)}) \mathbf{b}_n = 0 \end{aligned} \tag{4.3.31}$$

which satisfies $0 \leq \mu_n \leq 0.5 P_{\max}/\sigma^2$. Note that we can use a simple bisection algorithm to solve (4.3.31) and obtain the value of μ_n in the interval $[0 \;\; 0.5 P_{\max}/\sigma^2]$ for which the left hand side of (4.3.31) changes sign.

Once $\mathbf{w}_n$'s are obtained for $n = 0, 1, \cdots, N-1$, the optimal n is determined by evaluating the objective function in (4.3.28) for each $\mathbf{w}_n$ and choosing that value of n which leads to the largest value of this objective function. That is, the optimal value of n is obtained as

$$n^o = \arg \max_{0 \leq n \leq N-1} \frac{(P_{max} - \sigma^2 \|\mathbf{w}_n^o\|^2) |\mathbf{b}_n^H \mathbf{w}_n^o|^2}{2\sigma^2 \left(\mathbf{w}_n^{o,H} \mathbf{Q}_1^{(n)} \mathbf{w}_n^o + 1 \right) \left(\mathbf{w}_n^{o,H} \mathbf{Q}_2^{(n)} \mathbf{w}_n^o + 1 \right)}. \tag{4.3.32}$$

In other words, the set of the relays which contribute only to one tap of the end-to-end finite impulse response channel and which lead to the highest maximum balanced SNR (or, equivalently, to the minimum possible value for the MSE) among other relay

sets (each of which contribute to other taps) is selected and the remaining relays are turned off. Note that the search for optimal n is restricted only to the non-zero taps of $h[\cdot]$. If for a certain value of n, no relay contributes to $h[n]$, then $h[n] = 0$. In this case, the $(n+1)$th row of the matrix $\mathbf{B}$, i.e., the vector $\mathbf{b}_n$ is zero, and that value of n is skipped. Essentially, the maximum number of feasible values of n is exactly equal to the number of relays, L. Indeed, n belongs to the set $\{\breve{n}_{l_{pq}}, l = 1, 2, \ldots, L\}$ and we can restrict our search only to this set. If each relay contributes to a distinct tap of the end-to-end channel impulse response, then n can have exactly one of the L values $\{\breve{n}_{l_{pq}}\}_{l=1}^{L}$, if $\{\breve{n}_{l_{pq}}\}_{l=1}^{L}$ are distinct. Otherwise, the number of feasible values of n is smaller than L and it is equal to the number of distinct elements of the set $\{\breve{n}_{l_{pq}}\}_{l=1}^{L}$.

As we discussed in the previous chapter, in such a scenario, where only the relays contributing to one tap of the end-to-end channel impulse response are turned on, the end-to-end channel becomes frequency flat. Therefore, $\widetilde{\mathbf{H}}(\mathbf{w}_n)$ is a diagonal matrix with identical diagonal entries. Using (4.3.7), one can verify that $\mathbf{F}_{r1}^{\text{opt}}(\mathbf{w}_n^o)$ and $\mathbf{F}_{r2}^{\text{opt}}(\mathbf{w}_n^o)$ are also identity matrices.

We summarize our proposed method as Algorithm 3.

4.3.4 Remarks

Remark 1: Our mathematical derivations show that only the relays contributing to one tap of the end-to-end channel impulse response are chosen. This result is somehow unexpected and it is counter-intuitive as one expects that the relay resources should be fully used to have the best MMSE performance. Our derivations prove otherwise. One can interpret this result in the following way: The best channel, from

Algorithm 3 : Joint equalization, beamforming and power loading

Step 1. Set $n = 0$.

Step 2. If no relays contributes to the nth tap of $h_{pq}[\cdot]$ (i.e., if the $(n+1)$th row of the matrix $\mathbf{B}$ is zero), go to Step 9.

Step 3. Let $\mathbf{b}_n^H$ capture the non-zero entries of the $(n+1)$th row of $\mathbf{B}$.

Step 4. Use a bisection algorithm to obtain μ_n in the interval $[0 \;\; 0.5P_{\max}/\sigma^2]$ such that

$$\sigma^2(P_{\max}/\sigma^2 - 4\mu_n)\mathbf{b}_n^H \left(2\mu_n\mathbf{Q}_1^{(n)} + (P_{\max}/\sigma^2 - 2\mu_n)\mathbf{Q}_2^{(n)} + \mathbf{I}\right)^{-1}\mathbf{b}_n -$$
$$\mu_n(P_{\max}/\sigma^2 - 2\mu_n)\mathbf{b}_n^H \left(2\mu_n\mathbf{Q}_1^{(n)} + (P_{\max}/\sigma^2 - 2\mu_n)\mathbf{Q}_2^{(n)} + \mathbf{I}\right)^{-2}\left(2\mathbf{Q}_1^{(n)} - 2\mathbf{Q}_2^{(n)}\right)\mathbf{b}_n = 0$$

Step 5. Calculate $\nu_n = 0.5P_{\max}/\sigma^2 - \mu_n$.

Step 6. Calculate κ_n using

$$\kappa_n = \sigma^{-1}\left(\mathbf{b}_n^H\left(\sigma^2\mathbf{I} + 2\mu_n\mathbf{Q}_1^{(n)}\right)\left(\sigma^2\mathbf{I} + 2\mu_n\mathbf{Q}_1^{(n)} + 2\nu_n\mathbf{Q}_2^{(n)}\right)^{-2}\mathbf{b}_n\right)^{-\frac{1}{2}}.$$

Step 7. Having obtained values for κ_n, μ_n and ν_n, calculate $\mathbf{w}_n^o$ as

$$\mathbf{w}_n^o = \sigma^2\kappa_n\sqrt{2\nu_n}\left(2\mu_n\mathbf{Q}_1^{(n)} + 2\nu_n\mathbf{Q}_2^{(n)} + \sigma^2\mathbf{I}\right)^{-1}\mathbf{b}_n.$$

Step 8. Calculate the maximum balanced SNR as

$$\mathrm{SNR}_n(\mathbf{w}_n^o) = \frac{(P_{max} - \sigma^2\|\mathbf{w}_n^o\|^2)|\mathbf{b}_n^H\mathbf{w}_n^o|^2}{2\sigma^2\left(\mathbf{w}_n^{o,H}\mathbf{Q}_1^{(n)}\mathbf{w}_n^o + 1\right)\left(\mathbf{w}_n^{o,H}\mathbf{Q}_2^{(n)}\mathbf{w}_n^o + 1\right)}.$$

Step 9. Set $n = n+1$, if $n \geq N$ go to the next step, otherwise go to Step 2.

Step 10. Find the value of n which yields the maximum $\mathrm{SNR}_n(\mathbf{w}_n^o)$, i.e., $n = \arg\max_{0\leq k\leq N-1}\mathrm{SNR}_k(\mathbf{w}_k^o)$

Step 11. Let $\mathbf{w}_{opt}$ denote the optimal relay weight vector. If the lth relay is active, then the lth entry of $\mathbf{w}_{opt}$ is equal to the element of $\mathbf{w}_n^o$ which corresponds to the lth relay. If the lth relay is not active, then the lth entry of $\mathbf{w}_{opt}$ is zero.

Step 12. For $q \in \{1, 2\}$, calculate the transmit power of Transceiver q as

$$P_q = \frac{P_{max} - \sigma^2\|\mathbf{w}_{opt}\|^2}{2(1 + \|\mathbf{G}_q\mathbf{w}_{opt}\|^2)}.$$

an MMSE point of view, is a flat channel. Indeed, in our model, we are *designing* the channel. Unlike traditional models of wireless channels, a relay channel can be viewed as an *active* channel, implying that the channel characteristics can be adjusted, for optimal performance, somewhere between a source and a destination or between two transceivers (i.e., at the relays). We refer our reader to [85] for more on active channels.

Remark 2: Our study started off by assuming that the cyclic prefix is long enough. However, as we proved rigorously, the optimal design of the relay channel leads to a flat fading end-to-end relay channel, rendering the channel equalization trivial meaning that the length of the CP can be as small as zero! The parameters that the transceivers need to know, are the relaying delays and the channel coefficients. This is equivalent to saying that the transceivers need to know the end-to-end channel which is not a strong assumption, given that, in our scheme, similar to any other communication scheme, the channel training is implemented prior to exchanging information.

Remark 3: We would like to emphasize that our analysis in this chapter may not be applicable in a straightforward manner to the case where the relay-transceiver channels are frequency selective. Indeed, in such a case, the relays contribute to more than one tap of the end-to-end channel.

Remark 4: It is worth mentioning that at times, our solution may require a few relays to transmit at a very high power. Such a limitation exists in all the published results on relay-assisted communication schemes, where a total network or total relay power is used, see for example [25,55,81,82]. In such schemes, including our scheme, it is implicitly assumed that the transmit circuitry of each relay is capable

of transmitting this high level of power (in our case half of the maximum power available to the whole network) should the need arises and that the relay power source is designed for a worst case scenario when this relay is transmitting. In reality, however different relays will transmit at different times depending on their channel conditions as explained earlier.

Remark 5: It is worth mentioning that in terms of the computational complexity required to calculate the relay beamforming weight vector and the transceivers' transmit powers, the proposed single-carrier two-way relay-assisted communication scheme and the multi-carrier bi-directional relaying approach of Chapter 3 are identical. The difference relies in the fact that the scheme of Chapter 3 uses OFDM transmission and reception schemes at the transceivers, while the scheme proposed in this chapter is a single-carrier, and thus, it does not use the OFDM technology.

4.4 MSE Balancing, Min-Max MSE, and MSE Balancing

Earlier we observed that $\psi_1(\mathbf{w}_n) = \psi_2(\mathbf{w}_n)$ holds true. While this observation is useful to solve the optimization problem in (4.3.24), it is interesting on its own as explained in the sequel. One can easily see that the condition $\psi_1(\mathbf{w}_n) = \psi_2(\mathbf{w}_n)$ implies that at the optimum, where $\mathbf{w} \in \mathcal{W}$, the following property holds

$$\begin{aligned} N_s(\mathrm{MSE}_1(\mathbf{w}, \mathbf{F}_{r1}^{\mathrm{opt}}, P_1, P_2))^{-1} &= \frac{P_2 \mathbf{w}^H \mathbf{B}^H \mathbf{B} \mathbf{w}}{\sigma^2 \left(\|\mathbf{G}_1 \mathbf{w}\|^2 + 1 \right)} + 1 \\ &= \frac{P_1 \mathbf{w}^H \mathbf{B}^H \mathbf{B} \mathbf{w}}{\sigma^2 \left(\|\mathbf{G}_2 \mathbf{w}\|^2 + 1 \right)} + 1 = N_s(\mathrm{MSE}_2(\mathbf{w}, \mathbf{F}_{r2}^{\mathrm{opt}}, P_1, P_2))^{-1} . \end{aligned} \tag{4.4.1}$$

It follows from (4.4.1) that at the optimum, the MSE at the two transceivers will have to be balanced. Hence, the total MSE minimization problem in (4.3.2) results in MSE balancing at the two transceivers. Moreover, we can easily see that a min-max MSE fair design approach, formulated as the following optimization problem:

$$\begin{aligned} \min_{\substack{P_1\geq 0\\ P_2\geq 0}} \min_{\mathbf{w}} \max_{q\in\{1,2\}} \min_{\mathbf{F}_{rq}} \quad & \mathrm{MSE}_q(\mathbf{w},\mathbf{F}_{rq},P_1,P_2) \\ \text{subject to} \quad & P_{total}\leq P_{max} \end{aligned} \tag{4.4.2}$$

also leads to MSE balancing. Thus, we proved that *under a total power budget, the minimization of the total MSE and the min-max MSE fair design method are both equivalent to the MSE balancing*:

$$\begin{aligned} \min_{\substack{P_2\geq 0\\ P_2\geq 0}} \min_{\mathbf{w}} \min_{\mathbf{F}_{r1}} \quad & \mathrm{MSE}_1(\mathbf{w},\mathbf{F}_{r1},P_1,P_2) \\ \text{subject to} \quad & P_{total}\leq P_{max} \\ & \min_{\mathbf{F}_{r1}} \mathrm{MSE}_1(\mathbf{w},\mathbf{F}_{r1},P_1,P_2) = \min_{\mathbf{F}_{r2}} \mathrm{MSE}_2(\mathbf{w},\mathbf{F}_{r2},P_1,P_2)\,. \end{aligned}$$

Another interesting observation is that, for any $\mathbf{w}$, we can write

$$\begin{aligned} N_s(\mathrm{MSE}_q(\mathbf{w},\mathbf{F}_{rq}^{\mathrm{opt}},P_1,P_2))^{-1} &= \frac{P_{\bar{q}}\mathbf{w}^H\mathbf{B}^H\mathbf{B}\mathbf{w}}{\sigma^2\left(\|\mathbf{G}_q\mathbf{w}\|^2+1\right)}+1 \\ &= \frac{P_{\bar{q}}\sum_{n=0}^{N-1}\mathbf{w}_n^H\mathbf{b}_n\mathbf{b}_n^H\mathbf{w}_n}{\sigma^2\left(\|\mathbf{G}_q\mathbf{w}\|^2+1\right)}+1 \\ &= \frac{P_{\bar{q}}\sum_{n=0}^{N-1}\mathbf{w}_n^H\mathbf{b}_n\mathbf{b}_n^H\mathbf{w}_n}{\sigma^2\left(\|\mathbf{G}_q\mathbf{w}\|^2+1\right)}+1 \\ &= \frac{P_{\bar{q}}\sum_{n=0}^{N-1}\mathbf{w}_n^H\mathbf{b}_n\mathbf{b}_n^H\mathbf{w}_n}{\sigma^2\left(\|\mathbf{G}_q\mathbf{w}\|^2+1\right)}+1 \end{aligned} \tag{4.4.3}$$

As shown in the appendix, the first term in the right hand side of (4.4.3) can be viewed as the ratio of total signal power (defined as the sum of the powers of received signals corresponding to different symbols in a block) received by Transceiver q to the

noise power at this transceiver. We herein refer to this ratio as total SNR (T-SNR). It can be seen from (4.4.3) that the MSE at Transceiver q is an affine function of the inverse of the T-SNR. Hence, the sum-MSE minimization under a total power budget balances such T-SNRs. Equally interesting is the fact that $\psi_1(\mathbf{w}_n) = \psi_2(\mathbf{w}_n)$ implies that the total MSE minimization approach leads to balancing not only in the T-SNR but also in the SNR per entry of the received signal vector $\mathbf{r}_q(i)$, see appendix for further details.

A side result of our work in this chapter is that in application to the design problem of jointly optimal transceiver power control and relay beamforming for *synchronous* MABC type two-way relay networks under a total power constraint, the max-min SNR fair (i.e., SNR balancing) approach of [25], the sum-rate maximization of [44, 83], the total MSE minimization method and max-min MSE fair design technique presented in this chapter are all equivalent. Moreover, for the same design problem in *asynchronous* MABC type two-way relay networks, the max-min SNR fair (i.e., SNR balancing) approach of Chapter 3, where a multi-carrier communication scheme is used at the transceivers, and the total MSE minimization method, presented in this chapter for single-carrier communications, both lead to the same solution for the relay beamforming weight vector. For asynchronous MABC type two-way relay networks, the equivalence of the relay beamformer obtained via sum-rate maximization for multi-carrier schemes (through jointly optimal *subcarrier* power allocation at the transceivers and network beamforming at the relays under a total power constraint) to that obtained via the total MSE minimization method for single-carrier schemes (through jointly optimal power allocation to the two transceivers and network beamforming at the relays under a total power constraint) remains an open

problem. We conjecture that such an equivalency exists. Proving whether this conjecture is true or not, does not fit in the scope of this thesis and we will leave that to our future work. Note however that as proven in this chapter, the relay beamformer obtained via the total MSE minimization method or that obtained via max-min fair MSE design approach for single-carrier asynchronous two-way MABC type relaying schemes (through jointly optimal power allocation to the two transceivers and network beamforming at the relays under a total power constraint) is equivalent to the relay beamformer obtained via max-min SNR fair design approach for multi-carrier asynchronous two-way MABC type relaying schemes (through jointly optimal *sub-carrier* power allocation at the transceivers and network beamforming at the relays under a total power constraint).

4.5 Simulation Results

We consider two single-antenna transceivers communicating with each other with the help of $L = 60$ single-antenna relays in an asynchronous two-way relay network. We assume that the signals of the transceivers are transmitted in blocks with $N_s = 64$ symbols with a cyclic prefix length of $N = 8$. The frequency-flat channel coefficients between the relays and the transceivers are assumed to be independent complex Gaussian random variables with zero means and variances inversely proportional to the path loss. The path loss corresponding to the propagation from/to any transceiver to/from any relay is assumed to be proportional to the corresponding delay to the power of 3, i.e., path loss exponent is 3. The noises introduced at the relays and transceivers are zero-mean white Gaussian random processes with variance $\sigma^2 = 1$. In each simulation run, the delay of propagation from/to a transceiver to/from any

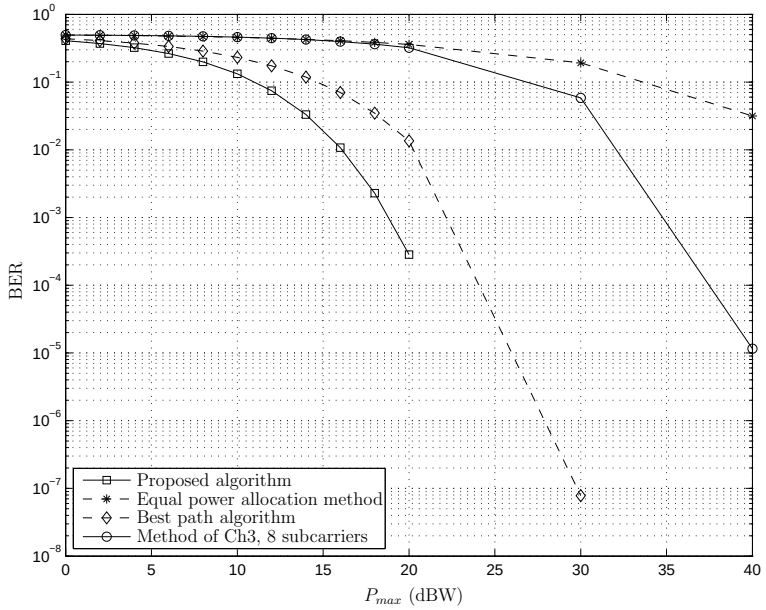

Figure 4.2: Bit error rate versus total available transmit power, P_{max}, for different methods.

relay is considered to be a random variable uniformly distributed in the interval $[T_s, 4T_s]$. As a result, the first two taps of the end-to-end discrete-time equivalent channel impulse response is always zero as no relay contributes to the first two taps. Indeed, the delay spread of the end-to-end channel is random variable which which has a triangular distribution in the interval $[2T_s \;\; 8T_s]$.

Figure. 4.2 depicts the total end-to-end bit error rate (BER) of our proposed algorithm versus the total transmit power P_{max}, assuming QPSK modulation. We compare the performance of our proposed method with three different methods: The first method is the so-called best path algorithm, where only one of the relays is selected. In this method, the mth relay is selected for communication, if the minimum of (g_{m1}, g_{m2}) is the maximum among minimum of (g_{l1}, g_{l2}), for all l. That is, $m =$

$\arg \max_{l} \min(g_{l1}, g_{l2})$.

The second method is an equal power allocation (EPA) scheme, where the total transmit power is equally distributed among all nodes of the network. The third method is the multi-carrier SNR-balancing scheme of Chapter 3 with 8 subcarriers. As it can be seen in this figure, for the same amount of total available transmit power, our proposed algorithm outperforms all the other three methods. Compared to the multi-carrier communication scheme of Chapter 3, for a given total available transmit power P_{max}, the single-carrier communication scheme studied in this chapter has a significantly lower BER. This is due to the fact that, in the multi-carrier transmission scheme of Chapter 3, the transceivers' powers are divided among different subcarriers, and hence, each subcarrier offers a comparably lower SNR at the receiver side. As a result the difference between the communication scheme studied in this chapter with that of Chapter 3 is that the single-carrier communication considered herein achieves a higher reliability (i.e., lower BERs) at the expense of multiplexing gain, while the scheme of Chapter 3 offers a higher multiplexing gain at the expense of lower reliability. In Figure. 4.3, we illustrate the sum-rate achieved by the single-carrier two-way relaying scheme presented in this chapter versus the total available transmit power P_{max} and compare that with the sum-rate achieved by the multi-carrier bi-directional relaying scheme of Chapter 3. As can be seen from this figure, compared to the single-carrier presented in this chapter, the multi-carrier scheme of Chapter 3 offers a significantly higher sum-rate for medium to high values of SNR. However, in low values of SNR, our proposed single-carrier scheme offers a higher sum-rate compared to the multi-carrier scheme of the previous chapter. As such, each of these two schemes offers its own advantages and disadvantages and each has

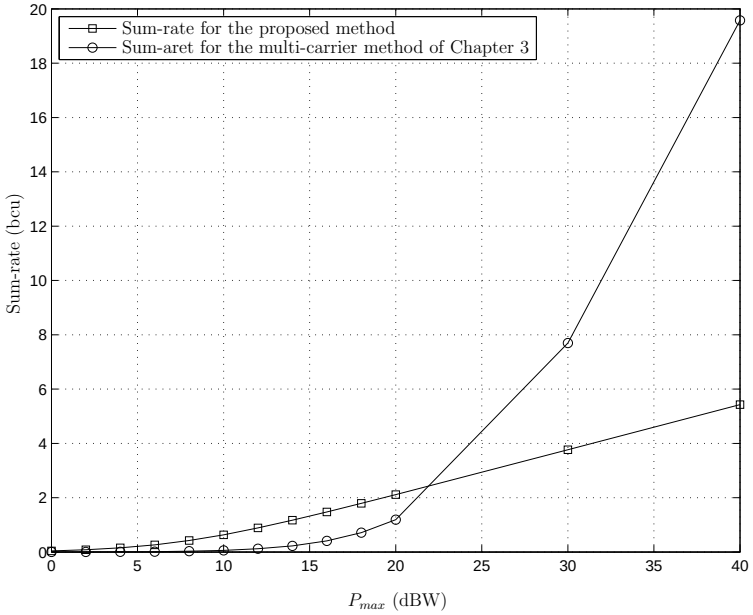

Figure 4.3: The sum-rate curves versus the total available transmit power, P_{max}; for the proposed single-carrier scheme and for the multi-carrier scheme of Chapter 3.

its own potential applications depending on the overall system design criterion.

In Figure. 4.4, we plot the total power consumed by all the relay nodes versus the total available transmit power budget of the communication network for our proposed algorithm, for the EPA method, and for the best path algorithm. The performance of the method of Chapter 3 is not plotted in this figure as for this method, the total relay power is also half of the total available power. As demonstrated in this figure, in our proposed method, the power consumed by all relay nodes is 3 dB lower than the total transmit power. In other words, half of the available power is allocated to both transceivers to transmit their signals and the other half is consumed by the relay nodes. In EPA scheme, the relay nodes collectively use an unnecessarily large fraction ($\frac{L}{L+2}$) of the total transmit power budget.

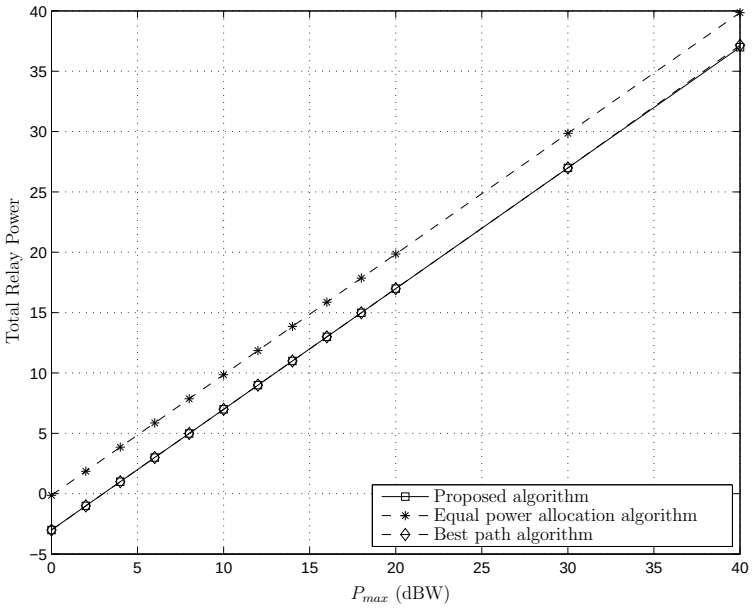

Figure 4.4: Total consumed relay power versus the total available transmit power, P_{max}; for different schemes.

Figure. 4.5 depicts the average maximum balanced SNRs[6] of the two transceivers for our proposed algorithm and for the other three methods. As shown in this figure, increasing the total transmit power increases the maximum balanced SNR at the transceivers. This figure also shows that our proposed method outperforms the EPA by around 3 dB in terms of maximum balanced SNR. Compared to the multi-carrier SNR-balancing scheme of Chapter 3, this figure shows that our scheme yields a higher balanced SNR. This is due to the fact that the method of Chapter 3 divides the transceivers' powers equally among different symbols (i.e., different subcarriers), while our approach in this chapter, assigns the total available power and all the bandwidth

[6]Note that as shown earlier, the total MSE is inversely proportional to the maximum balanced SNR.

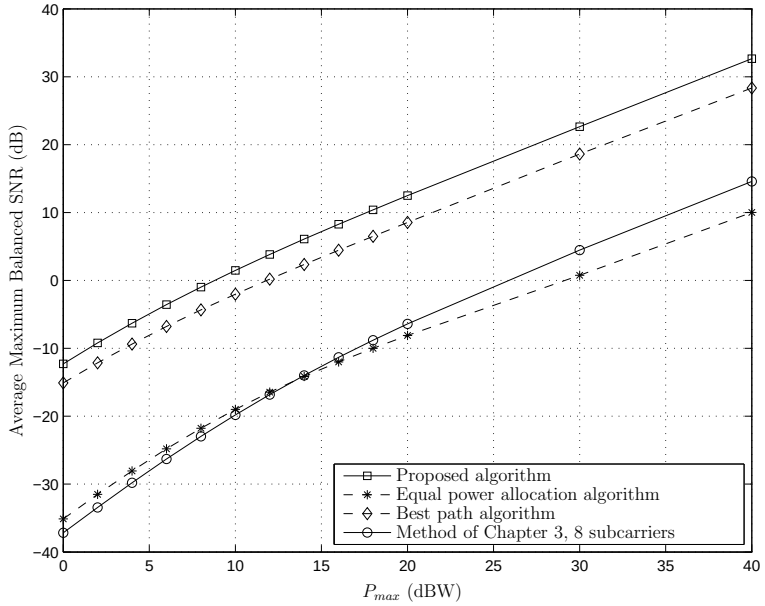

Figure 4.5: Average maximum balanced SNR versus total available transmit power, P_{max}; for different methods.

to one symbol.

Assuming $P_{max} = 20$ dBW, Figure. 4.6 shows the percentage of the cases in our scheme when the nth tap of the end-to-end channel is active, while the remaining taps are zero. This figure also shows the percentage of the cases in the best path approach, when the selected relay corresponds to the nth tap of the end-to-end channel impulse response. As can be seen from this figure, in the proposed scheme, the second tap has a higher chance to be active, while the chance of other taps (for example, the first, the third, and the fourth taps) being non-zero is not negligible. Compared to the best path approach, the proposed scheme relies, in average, on more than one relay. As can be seen in this figure, the optimal non-zero tap obtained by our method may not necessarily be the one introduced by the best path algorithm. Hence, this figure

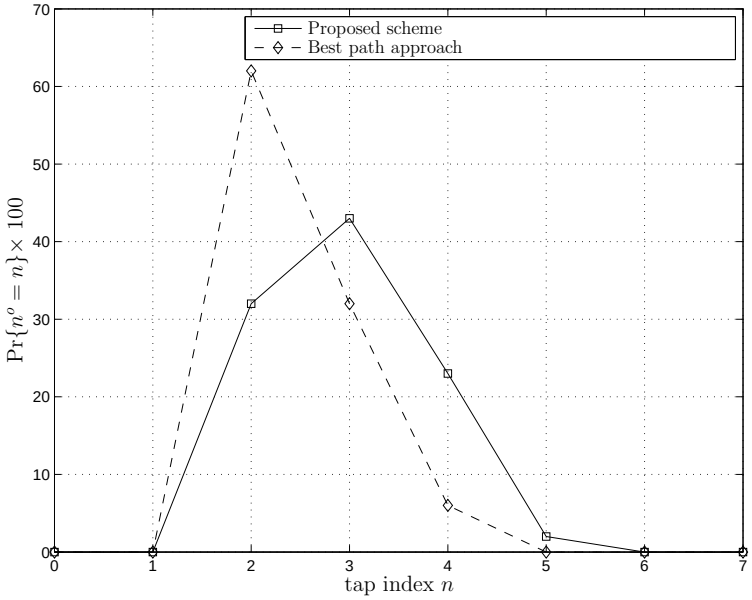

Figure 4.6: Percentage of the cases where the nth tap of the end-to-end channel impulse response is active, versus n, for the proposed method and for the best path algorithm.

confirms that one cannot assume in advance that the first tap (which corresponds to those relays that are the closest to the line connecting the two transceivers) is always active. The reason is that the number of the relays which contribute to the other taps (e.g., second tap) could be large enough to compensate the relatively high path loss for these relays. Note also that the number of the relays associated with each tap could be larger than one. Hence, the performance of the proposed scheme is guaranteed to outperform the best path method.

The reason why in this example the first tap is not the most active tap is explained in the sequel. As the delay of each transceiver-relay path is chosen as a random variable uniformly distributed in the interval $[T_s \;\; 4T_s]$, the end-to-end delay

corresponding to each relay is a random variable which has a triangular distribution in the interval $[2T_s \;\; 8T_s]$. Hence, the relays are most likely to produce an end-to-end delay around $5T_s$. Hence, in average more relays will contribute to the tap at $5T_s$, as compared to those which correspond to the first non-zero tap at $2T_s$. On the other hand, those relays which contribute to the tap at $2T_s$, have better channel quality compared to the other relays. The trade-off between the relatively better channel quality for the relays with minimal sum-distance from the two transceivers and larger number of relays with delays around $5T_s$ has resulted in the highest chance of selecting those relays which contribute to the tap at $3T_s$. .

4.6 Conclusion

In this chapter, we considered a single-carrier asynchronous two-way relay network, where two single-antenna transceivers exchange information symbols using several single-antenna relay nodes. The relays are assumed to simply amplify their received signals and forward them to the transceivers. The relaying paths are assumed to have different propagation delays. Although the relay paths are assumed to be frequency flat, the end-to-end channel is frequency selective, and therefore, inter-block-interference (IBI) is inevitable at both transceivers. To combat such an IBI, cyclic prefix is added to the transmitted signal blocks at the transceivers. Considering block channel equalization at the transceivers, we obtained the relay beamforming weights, the transmit power of the transceivers, and the transceiver block equalizers such that the total mean squared error (MSE) of the symbol estimates at the output of the block equalizers are minimized subject to a total power budget constraint. We rigorously proved that our proposed approach leads to a relay selection scheme, where only the

relays, which contribute to one tap of the end-to-end channel impulse response, are turned on and the remaining relays are all turned off. To determine which tap of the end-to-end channel impulse response has to be non-zero, we presented a simple search procedure. Assuming only a certain tap of the end-to-end channel impulse response is non-zero while all other taps are zero, we presented a semi-closed-form solution for the corresponding relay beamforming weight vector and the respective minimum total MSE of the symbol estimates. Such MSEs are calculated for all possible non-zero taps of the end-to-end channel impulse response. The only non-zero tap which yields the smallest total MSE, introduces the relays which have to be turned on.

Chapter 5

Pre-channel Equalization and Distributed Beamforming in Asynchronous Single-carrier Bi-directional Relay Networks

5.1 Introduction

In this chapter, assuming simple AF relaying, we consider an asynchronous two-way relay-assisted network similar to the one described in Chapter 4. This communication network consists of two single-antenna transceivers and multiple single-antenna relays. In order to mitigate the adverse effect of IBI, cyclic prefix insertion and removal blocks are provided at the transceivers and pre-channel block equalizers are taken into consideration. Nonetheless, in order to reduce the complexity, the relays simply amplify and forward their received signal by multiplying it with a complex beamforming weight. In this work, we consider pre-channel block equalization while in the previous chapter, the channel equalization is performed at the destination. After modeling the channel and considering the noise at the relays and transceivers, we aim to minimize the total mean squared error (MSE) of the estimated received

signals at both transceivers under the assumption that the total available transmit power is limited. This minization is performed by obtaining the optimal relay beamforming weight vector and the transceivers' powers as well as the pre-channel block equalizers. Such a design is proved to lead to a relay selection scheme, where only the relays contributing to one tap of the end-to-end channel impulse response are turned on and the remaining relays are switched off. We introduce two different optimization problems for sufficiently large and small amount of the available total transmit power of the network. Depending on the value of the total available transmit power, one of these optimization problems is solved to find the optimum relay beamforming vector and transceivers' powers. The simulation results show the performance of our proposed algorithm for various total power budgets and noise powers at the relays and transceivers. Our contribution in this chapter is summarized below.

- We model the transceivers' received signals, the end-to-end channel and the total received noise at each transceiver for an asynchronous two-way AF relay network, where the transceivers are equipped with pre-channel equalizers.

- We formulate and solve the problem of minimizing the total MSE at the two transceivers under a total transmit power budget.

- We analyze the performance of the proposed pre-channel block equalizer scheme and show its advantages over the post-channel equalizer approach of Chapter 4.

5.2 Preliminaries

5.2.1 System Setup

Similar to our system model developed in Chapter 4, we consider a two-way relay network, where two single-antenna transceivers exchange information, using a single-carrier transmission/reception scheme, with the help of L single-antenna relay nodes. In order to combat the IBI at the both transceivers, we use pre-channel block equalization as shown in Figure. 5.1. In this figure, the transmitted symbols go through serial-to-parallel conversion block, denoted as "S/P" which converts the serial symbols into blocks of length N_s.

We represent the ith block of information symbols transmitted by Transceiver p as $\mathbf{s}_p(i) = \begin{bmatrix} s_p[iN_s] & \cdots & s_p[iN_s + N_s - 1] \end{bmatrix}^T$, where $s_p[k]$ is the kth symbol transmitted by Transceiver p . In order to equalize the channel, two $N_s \times N_s$ block channel equalizers denoted as $\mathbf{F}_1$ and $\mathbf{F}_2$ are implemented at Transceivers 1 and 2, respectively. At the output of the *pre-channel* block equalizer at Transceiver p, the transmitted block can be represented as $\check{\mathbf{s}}_p(i) \triangleq \mathbf{F}_p\mathbf{s}_p(i)$, for $p = 1, 2$. The frequency selectivity of the end-to-end channel leads to IBI between adjacent transmitted blocks, and hence, the signals received at Transceiver $q \neq p$ corresponding to the ith transmitted block depend on both transmitted blocks i and $i-1$. In order to eliminate the IBI, a cyclic prefix is added to $\hat{\mathbf{s}}_p(i)$ by pre-multiplying $\hat{\mathbf{s}}_p(i)$ with the matrix $\mathbf{T}_{\text{cp}}$. After the cyclic insertion block, the corresponding ith transmitted block is defined as

$$\begin{aligned}\overline{\mathbf{s}}_p(i) \triangleq \mathbf{T}_{\text{cp}}\check{\mathbf{s}}_p(i) &= \begin{bmatrix} \overline{s}_p[iN_t] & \cdots & \overline{s}_p[iN_t + N_t - 1] \end{bmatrix}^T \\ &= \begin{bmatrix} \check{s}_p[(i+1)N_s - N] & \cdots & \check{s}_p[(i+1)N_s - 1] & \check{s}_p[iN_s] & \cdots & \check{s}_p[(i+1)N_s - 1] \end{bmatrix}^T \end{aligned} \tag{5.2.1}$$

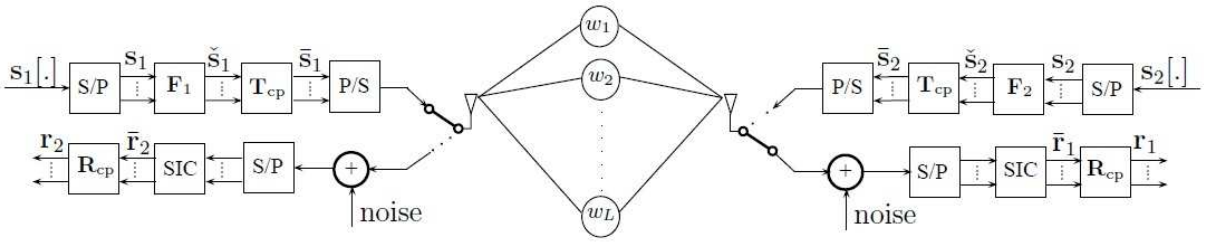

Figure 5.1: System block diagram for pre-channel equalization using single-carrier communication scheme

where $N_t \triangleq N + N_s$ is the length of the transmitted blocks. Then, vector $\bar{\mathbf{s}}_p(i)$ is turned into serial using the parallel-to-serial block, denoted as "P/S", and is passed through the multi-path channel.

At the other side of the channel, the noise-corrupted version of the transmitted block received by Transceiver q, goes through "S/P" block and becomes parallel. After the self-interference cancelation, denoted as "SIC", the first N entries of any received block are simply discarded by pre-multiplying it with the cyclic removal matrix, denoted as $\mathbf{R}_{\rm cp} = [\mathbf{0}_{N_s \times N} \;\; \mathbf{I}_{N_s}]$.

In the following subsections, we first develop our channel model. Then, the noises introduced at the relay nodes and at the transceivers are modeled and the total measured noise at each transceiver is formulated. For such a channel and considering block channel equalization at both transceivers, an expression is derived for the total mean squared error of the estimated received symbols at the two transceivers. Our goal is to minimize the total mean squared estimation error under a total power constraint. As such, in the last part of this section, we obtain the total power consumed in the whole network.

5.2.2 Modeling the Channel

In this subsection, we present our channel model which is a discrete-time equivalent of the continuous-time channel model presented in Chapter 3 and is the same as the signal model introduced in Chapter 4. For the sake of brevity, we avoid repeating the details of this data model. The end-to-end channel from Transceiver p to Transceiver q, $(p, q \in \{1, 2\})$ can be viewed as a *multipath channel* which is represented in (4.2.2). The vector of the taps of the channel impulse response is obtained in Chapter 3, and is given in (3.2.7).

5.2.3 Modeling the Noise

As it was earlier discussed in Chapter 4, for the system model described above, the relay noise received at Transceiver q is given in (4.2.3) and the total noise received at Transceiver q is expressed in (4.2.7). The total received noise at Transceiver q can be written as

$$\overline{\boldsymbol{\gamma}}_q(i) = \overline{\upsilon}_q(i)\mathbf{G}_q\mathbf{w} + \overline{\boldsymbol{\gamma}}'_q(i) \tag{5.2.2}$$

where $\overline{\upsilon}(iq) = \begin{bmatrix} \upsilon_{iN_t,q} & \upsilon_{iN_t+1,q} & \cdots & \upsilon_{(iN_t+N_t-1),q} \end{bmatrix}^T$ is an $N_t \times L$ matrix.

5.2.4 Modeling the Transmitted Signal

Assuming $\mathrm{E}\{|s_p[k]|^2\} = 1$ and $\mathrm{E}\{s_p[k]\} = 0$, for $p \in \{1, 2\}$, the ith transmitted block received at the output of self-interference cancelation block of Transceiver q can be written as [84]

$$\begin{aligned} \overline{\mathbf{r}}_q(i) &= \mathbf{H}_0(\mathbf{w})\overline{\mathbf{s}}_{\bar{q}}(i) + \mathbf{H}_1(\mathbf{w})\overline{\mathbf{s}}_{\bar{q}}(i-1) + \overline{\boldsymbol{\gamma}}_q(i) \\ &= \mathbf{H}_0(\mathbf{w})\mathbf{T}_{\mathrm{cp}}\mathbf{F}_{\bar{q}}\mathbf{s}_{\bar{q}}(i) + \mathbf{H}_1(\mathbf{w})\mathbf{T}_{\mathrm{cp}}\mathbf{F}_{\bar{q}}\mathbf{s}_{\bar{q}}(i-1) + \overline{\boldsymbol{\gamma}}_q(i) \end{aligned} \tag{5.2.3}$$

where $\mathbf{H}_0(\mathbf{w})$ and $\mathbf{H}_1(\mathbf{w})$ are defined in (4.2.10). The received signal vector $\overline{\mathbf{r}}_q(i)$ goes through the cyclic prefix removal matrix, and thus, its first N entries are discarded. As it was discussed in Chapter 4, $\mathbf{R}_{\rm cp}\mathbf{H}_1(\mathbf{w}) = \mathbf{0}$, and hence the IBI-inducing matrix $\mathbf{H}_1(\mathbf{w})$ is eliminated by cyclic prefix removal operation. Therefore, using (5.2.3), we can write

$$\begin{aligned}\mathbf{r}_q(i) \triangleq \mathbf{R}_{\rm cp}\overline{\mathbf{r}}_q(i) &= \mathbf{R}_{\rm cp}\mathbf{H}_0(\mathbf{w})\mathbf{T}_{\rm cp}\mathbf{F}_{\bar{q}}\mathbf{s}_{\bar{q}}(i) + \mathbf{R}_{\rm cp}\overline{\boldsymbol{\gamma}}_q(i) \\ &= \widetilde{\mathbf{H}}(\mathbf{w})\mathbf{F}_{\bar{q}}\mathbf{s}_{\bar{q}}(i) + \widetilde{\boldsymbol{\gamma}}_q(i) \end{aligned} \tag{5.2.4}$$

Note that $\widetilde{\boldsymbol{\gamma}}_q(i)$ and $\widetilde{\mathbf{H}}(\mathbf{w})$ are already defined in Chapter 4.

5.2.5 Calculating the Total Network Power

In this subsection, we derive the power consumed in the network in terms of the relay weight vector $\mathbf{w}$ and transceivers' transmit power. It follows from Figure. 5.1 that the $N_t \times 1$ vector of the ith signal block relayed by the lth relay can be written as

$$\overline{\mathbf{x}}_l(i) = w_l \left[g_{l1}\overline{\mathbf{s}}_1(i) + g_{l2}\overline{\mathbf{s}}_2(i) + \upsilon_l(i) \right] \tag{5.2.5}$$

where $\overline{\mathbf{x}}_l(i) \triangleq \begin{bmatrix} \overline{x}_l[iN_t] & \overline{x}_l[iN_t+1] & \cdots & \overline{x}_l[iN_t+N_t-1] \end{bmatrix}^T$, $\bar{\mathbf{s}}_1(i)$ and $\bar{\mathbf{s}}_2(i)$ are uncorrelated and zero mean random vectors, $\overline{x}_l[t]$ is the signal transmitted by the lth relay at time t. Using (5.2.5), the average transmit power of the lth relay is then obtained as

$$\begin{aligned}\widetilde{P}_l &\triangleq \frac{1}{N_t}\mathrm{E}\left\{\overline{\mathbf{x}}_l^H(i)\overline{\mathbf{x}}_l(i)\right\} \\ &= \frac{|w_l|^2}{N_t}\mathrm{E}\left\{\left[g_{l1}^*\overline{\mathbf{s}}_1^H(i) + g_{l2}^*\overline{\mathbf{s}}_2^H(i) + \upsilon_l^H(i)\right]\left[g_{l1}\overline{\mathbf{s}}_1(i) + g_{l2}\overline{\mathbf{s}}_2(i) + \upsilon_l(i)\right]\right\} \\ &= \frac{|g_{l1}|^2|w_l|^2}{N_t}\mathrm{E}\left\{\overline{\mathbf{s}}_1^H(i)\overline{\mathbf{s}}_1(i)\right\} + \frac{|g_{l2}|^2|w_l|^2}{N_t}\mathrm{E}\left\{\overline{\mathbf{s}}_2^H(i)\overline{\mathbf{s}}_2(i)\right\} + \frac{|w_l|^2}{N_t}\mathrm{E}\left\{\upsilon_l^H(i)\upsilon_l(i)\right\} \\ &= |w_l|^2\left(|g_{l1}|^2P_1 + |g_{l2}|^2P_2 + \sigma^2\right). \end{aligned} \tag{5.2.6}$$

Since the relay power calculated in (5.2.6) is the same as the one obtained in Chapter 4, the total transmit power of the network is the one given in (4.2.15).

5.3 Jointly Optimal Equalization, Relay Beamforming and Power Loading

5.3.1 Problem Formulation

In this section, our goal is to optimally obtain the block channel equalizers $\mathbf{F}_1$ and $\mathbf{F}_2$, the relay beamforming weight vector $\mathbf{w}$, and the transceivers' transmit powers P_1 and P_2, such that the total MSE of the received blocks at the two transceivers is minimized under a total power constraint. To this end, we can write the received signal error vector at Transceiver q as

$$\mathbf{e}_q(i) \triangleq \mathbf{r}_q(i) - \mathbf{s}_{\bar{q}}(i). \tag{5.3.1}$$

The transmit power of Transceiver q can be obtained as

$$\begin{aligned} P_q = \frac{1}{N_s}\mathrm{E}\{\check{\mathbf{s}}_q^H(i)\check{\mathbf{s}}_q(i)\} &= \frac{1}{N_s}\mathrm{E}\{(\mathbf{F}_q\mathbf{s}_q(i))^H(\mathbf{F}_q\mathbf{s}_q(i))\} = \frac{1}{N_s}\mathrm{E}\{\mathbf{s}_q^H(i)\mathbf{F}_q^H\mathbf{F}_{t\backslash q}\mathbf{s}_q(i)\} \\ &= \frac{1}{N_s}\mathrm{E}\{\mathrm{tr}\left[\mathbf{F}_q\mathbf{s}_q(i)\mathbf{s}_q^H(i)\mathbf{F}_q^H\right]\} = \frac{1}{N_s}\mathrm{tr}\left[\mathbf{F}_q\mathrm{E}\{\mathbf{s}_q(i)\mathbf{s}_q^H(i)\}\mathbf{F}_q^H\right] \\ &= \frac{1}{N_s}\mathrm{tr}\left[\mathbf{F}_q^H\mathbf{F}_q\right]. \end{aligned} \tag{5.3.2}$$

Hence, the squared Frobenius norm of $\mathbf{F}_q$ has to be equal to N_sP_q (i.e., $\|\mathbf{F}_q\|_F^2 = \mathrm{tr}[\mathbf{F}_q^H\mathbf{F}_q] = N_sP_q$). Seeking jointly optimal block equalization, relay beamforming, and power loading, the problem of minimizing the total MSE under the total available

power constraint can be formulated as the following optimization problem:

$$\min_{\substack{P_1\geq 0\\ P_2\geq 0}} \min_{\mathbf{w}} \min_{\mathbf{F}_1,\mathbf{F}_2} \sum_{q=1}^{2} \mathrm{E}\left\{\|\mathbf{e}_q(i)\|^2\right\}$$

$$\text{subject to } P_{total} \leq P_{max}$$

$$\|\mathbf{F}_q\|_F^2 = N_s P_q, \text{ for } q \in \{1,2\} \tag{5.3.3}$$

In (5.3.3), the expectation is taken with respect to the noise and the random symbols. Note that the total transmit power constraint which we use in this optimization problem is somehow looser as compared to individual power constraints on each node of the network.

5.3.2 Optimal Pre-Channel Block Equalization

Let us consider the inner minimization problem in (5.3.3) as

$$\lambda(\mathbf{w}, P_1, P_2) \triangleq \min_{\mathbf{F}_q} \sum_{q=1}^{2} \mathrm{E}\left\{\mathbf{e}_q^H(i)\mathbf{e}_q(i)\right\}$$

$$\text{subject to } \|\mathbf{F}_q\|_F^2 = P_q N_s, \text{ for } q \in \{1,2\}. \tag{5.3.4}$$

Using the fact that $\mathrm{E}\{\mathbf{s}_{\bar{q}}(i)\} = \mathbf{0}$, the MSE at Transceiver q can be written as

$$\begin{aligned}
\mathrm{E}\left\{\mathbf{e}_q^H(i)\mathbf{e}_q(i)\right\} &= \mathrm{E}\left\{[\mathbf{r}_q^H(i) - \mathbf{s}_{\bar{q}}^H(i)][\mathbf{r}_q(i) - \mathbf{s}_{\bar{q}}(i)]\right\} \\
&= \mathrm{E}\left\{\mathbf{r}_q^H(i)\mathbf{r}_q(i) - \mathbf{s}_{\bar{q}}^H(i)\mathbf{r}_q(i) - \mathbf{r}_q^H(i)\mathbf{s}_{\bar{q}}(i) + \mathbf{s}_{\bar{q}}^H(i)\mathbf{s}_{\bar{q}}(i)\right\} \\
&= \mathrm{tr}\left[\mathrm{E}\left\{\mathbf{r}_q(i)\mathbf{r}_q^H(i)\right\}\right] - \mathrm{tr}\left[\mathrm{E}\left\{\mathbf{r}_q(i)\mathbf{s}_{\bar{q}}^H(i)\right\}\right] \\
&\quad - \mathrm{tr}\left[\mathrm{E}\left\{\mathbf{s}_{\bar{q}}(i)\mathbf{r}_q^H(i)\right\}\right] + \mathrm{E}\left\{\mathbf{s}_{\bar{q}}^H(i)\mathbf{s}_{\bar{q}}(i)\right\} \\
&= \mathrm{tr}\left[\mathbf{R}_q(\mathbf{w})\right] - \mathrm{tr}\left[\widetilde{\mathbf{H}}(\mathbf{w})\mathbf{F}_{\bar{q}} - \mathbf{F}_{\bar{q}}^H\widetilde{\mathbf{H}}^H(\mathbf{w})\right] + N_s
\end{aligned} \tag{5.3.5}$$

where

$$\mathbf{R}_q(\mathbf{w}) \triangleq \mathrm{E}\left\{\mathbf{r}_q(i)\mathbf{r}_q^H(i)\right\} = \widetilde{\mathbf{H}}(\mathbf{w})\mathbf{F}_{\bar{q}}\mathbf{F}_{\bar{q}}^H\widetilde{\mathbf{H}}^H(\mathbf{w}) + \sigma^2\left(\mathbf{w}^H\mathbf{G}_q^H\mathbf{G}_q\mathbf{w} + 1\right)\mathbf{I}_{N_s} \tag{5.3.6}$$

is the correlation matrix of the received block at Transceiver q (see (5.2.4)). Hence, the optimization problem (5.3.4) can be written as

$$\lambda(\mathbf{w}, P_1, P_2) = \min_{\mathbf{F}_1, \mathbf{F}_2} \sum_{q=1}^{2} \left(\mathrm{tr}\left[\mathbf{R}_q(\mathbf{w}) - \widetilde{\mathbf{H}}(\mathbf{w}) \mathbf{F}_{\bar{q}} - \mathbf{F}_{\bar{q}}^H \widetilde{\mathbf{H}}^H(\mathbf{w}) \right] + N_s \right)$$
$$\text{subject to } \|\mathbf{F}_q\|_F^2 = P_q N_s, \text{ for } q \in \{1, 2\}. \tag{5.3.7}$$

or, equivalently, as

$$\lambda(\mathbf{w}, P_1, P_2) = \min_{\mathbf{F}_1, \mathbf{F}_2} \sum_{q=1}^{2} \Big(\mathrm{tr}\Big[\widetilde{\mathbf{H}}(\mathbf{w}) \mathbf{F}_{\bar{q}} \mathbf{F}_{\bar{q}}^H \widetilde{\mathbf{H}}^H(\mathbf{w}) + \sigma^2 \left(\mathbf{w}^H \mathbf{G}_q^H \mathbf{G}_q \mathbf{w} + 1 \right) \mathbf{I}_{N_s} - \widetilde{\mathbf{H}}(\mathbf{w}) \mathbf{F}_{\bar{q}} - \mathbf{F}_{\bar{q}}^H \widetilde{\mathbf{H}}^H(\mathbf{w}) \Big] + N_s \Big)$$
$$\text{subject to } \|\mathbf{F}_q\|_F^2 = P_q N_s, \text{ for } q \in \{1, 2\}. \tag{5.3.8}$$

Using (5.3.6), we can rewrite (5.3.8) as[1]

$$\lambda(\mathbf{w}, P_1, P_2) = \min_{\mathbf{F}_1, \mathbf{F}_2} \sum_{q=1}^{2} \Big(\mathrm{tr}\Big[\widetilde{\mathbf{H}}(\mathbf{w}) \mathbf{F}_q \mathbf{F}_q^H \widetilde{\mathbf{H}}^H(\mathbf{w}) - \widetilde{\mathbf{H}}(\mathbf{w}) \mathbf{F}_q - \mathbf{F}_q^H \widetilde{\mathbf{H}}^H(\mathbf{w}) \Big] + N_s \left(1 + \sigma^2 \left(\mathbf{w}^H \mathbf{G}_q^H \mathbf{G}_q \mathbf{w} + 1 \right) \right) \Big)$$
$$\text{subject to } \|\mathbf{F}_q\|_F^2 = P_q N_s, \text{ for } q \in \{1, 2\}. \tag{5.3.9}$$

The solution to the constrained optimization problem (5.3.9) can be found using the Lagrangian multiplier method. We define the Lagrangian as

$$\mathcal{L}(\mathbf{F}_1, \mathbf{F}_2, \mu_1, \mu_2) \triangleq \sum_{q=1}^{2} \Big(\mathrm{tr}\left[\mathbf{F}_q \mathbf{F}_q^H \widetilde{\mathbf{H}}^H(\mathbf{w}) \widetilde{\mathbf{H}}(\mathbf{w}) \right] - \mathrm{tr}\left[\widetilde{\mathbf{H}}(\mathbf{w}) \mathbf{F}_q + \mathbf{F}_q^H \widetilde{\mathbf{H}}^H(\mathbf{w}) \right] + N_s \left(1 + \sigma^2 \left(\|\mathbf{G}_{\bar{q}} \mathbf{w}\|^2 + 1 \right) \right) + \mu_q \left(\mathrm{tr}\left[\mathbf{F}_q^H \mathbf{F}_q \right] - N_s P_q \right) \Big) \tag{5.3.10}$$

[1]Note that

$$\sum_{q=1}^{2} \left(\mathrm{tr}\left[\widetilde{\mathbf{H}}(\mathbf{w}) \mathbf{F}_{\bar{q}} \mathbf{F}_{\bar{q}}^H \widetilde{\mathbf{H}}^H(\mathbf{w}) - \widetilde{\mathbf{H}}(\mathbf{w}) \mathbf{F}_{\bar{q}} - \mathbf{F}_{\bar{q}}^H \widetilde{\mathbf{H}}^H(\mathbf{w}) \right] \right) = \sum_{q=1}^{2} \left(\mathrm{tr}\left[\widetilde{\mathbf{H}}(\mathbf{w}) \mathbf{F}_q \mathbf{F}_q^H \widetilde{\mathbf{H}}^H(\mathbf{w}) - \widetilde{\mathbf{H}}(\mathbf{w}) \mathbf{F}_q - \mathbf{F}_q^H \widetilde{\mathbf{H}}^H(\mathbf{w}) \right] \right)$$

where μ_1 and μ_2 are the non-negative Lagrange multipliers. Taking the derivative of the Lagrangian function with respect to $\mathbf{F}_q^H$ leads us to

$$\frac{\partial}{\partial \mathbf{F}_q^H}\mathcal{L}(\mathbf{F}_1, \mathbf{F}_2, \mu_1, \mu_2) = \left(\widetilde{\mathbf{H}}^H(\mathbf{w})\widetilde{\mathbf{H}}(\mathbf{w})\mathbf{F}_q - \widetilde{\mathbf{H}}^H(\mathbf{w}) + \mu_q\mathbf{F}_q\right)^T, \quad \text{for } q \in \{1, 2\}. \tag{5.3.11}$$

Equating (5.3.11) to zero yields

$$\mathbf{F}_q = \left(\widetilde{\mathbf{H}}^H(\mathbf{w})\widetilde{\mathbf{H}}(\mathbf{w}) + \mu_q\mathbf{I}_{N_s}\right)^{-1}\widetilde{\mathbf{H}}^H(\mathbf{w}) \tag{5.3.12}$$

The constraints in (5.3.9) imply that

$$\text{tr}\left[\mathbf{F}_q^H\mathbf{F}_q\right] = \text{tr}\left[\widetilde{\mathbf{H}}(\mathbf{w})\left(\widetilde{\mathbf{H}}^H(\mathbf{w})\widetilde{\mathbf{H}}(\mathbf{w}) + \mu_q\mathbf{I}_{N_s}\right)^{-2}\widetilde{\mathbf{H}}^H(\mathbf{w})\right] = P_qN_s, \quad \text{for } q = 1, 2. \tag{5.3.13}$$

To further simplify the optimization problem, $\widetilde{\mathbf{H}}(\mathbf{w})$ can be decomposed as $\widetilde{\mathbf{H}}(\mathbf{w}) = \mathbf{F}^H\mathbf{D}(\mathbf{w})\mathbf{F}$. Hence, we can rewrite (5.3.13) as

$$\begin{aligned}
\text{tr}\left[\mathbf{F}_q\mathbf{F}_q^H\right] &= \text{tr}\left[\mathbf{F}^H\mathbf{D}(\mathbf{w})\mathbf{F}\left(\mathbf{F}^H\mathbf{D}^H(\mathbf{w})\mathbf{F}\mathbf{F}^H\mathbf{D}(\mathbf{w})\mathbf{F} + \mu_q\mathbf{I}_{N_s}\right)^{-2}\mathbf{F}^H\mathbf{D}^H(\mathbf{w})\mathbf{F}\right] \\
&= \text{tr}\left[\mathbf{F}\mathbf{F}^H\mathbf{D}(\mathbf{w})\mathbf{F}\left(\mathbf{F}^H\mathbf{D}^H(\mathbf{w})\mathbf{F}\mathbf{F}^H\mathbf{D}(\mathbf{w})\mathbf{F} + \mu_q\mathbf{I}_{N_s}\right)^{-2}\mathbf{F}^H\mathbf{D}^H(\mathbf{w})\right] \\
&= \text{tr}\left[\mathbf{D}(\mathbf{w})\mathbf{F}\left(\mathbf{F}^H\mathbf{D}^H(\mathbf{w})\mathbf{D}(\mathbf{w})\mathbf{F} + \mu_q\mathbf{I}_{N_s}\right)^{-2}\mathbf{F}^H\mathbf{D}^H(\mathbf{w})\right] \\
&= \text{tr}\left[\mathbf{D}(\mathbf{w})\mathbf{F}^H\left(\mathbf{D}^H(\mathbf{w})\mathbf{D}(\mathbf{w}) + \mu_q\mathbf{I}_{N_s}\right)^{-2}\mathbf{F}\mathbf{D}^H(\mathbf{w})\right] \\
&= \text{tr}\left[\left(\mathbf{D}^H(\mathbf{w})\mathbf{D}(\mathbf{w}) + \mu_q\mathbf{I}_{N_s}\right)^{-2}\mathbf{F}\mathbf{D}^H(\mathbf{w})\mathbf{D}(\mathbf{w})\mathbf{F}^H\right]
\end{aligned} \tag{5.3.14}$$

Using (5.3.12), (5.3.13) and (5.3.14), we can rewrite the optimization problem (5.3.9) as

$$\begin{aligned}\lambda(\mathbf{w},P_1,P_2)=\min_{\mu_1,\mu_2}\sum_{q=1}^{2}\mathrm{tr}\Bigg[&\left(\widetilde{\mathbf{H}}(\mathbf{w})\left(\widetilde{\mathbf{H}}^H(\mathbf{w})\widetilde{\mathbf{H}}(\mathbf{w})+\mu_q\mathbf{I}_{N_s}\right)^{-1}\widetilde{\mathbf{H}}^H(\mathbf{w})\right)^2\\&-2\widetilde{\mathbf{H}}(\mathbf{w})\left(\widetilde{\mathbf{H}}^H(\mathbf{w})\widetilde{\mathbf{H}}(\mathbf{w})+\mu_q\mathbf{I}_{N_s}\right)^{-1}\widetilde{\mathbf{H}}^H(\mathbf{w})\\&+N_s\left(1+\sigma^2\left(\mathbf{w}^H\mathbf{G}_{\bar{q}}^H\mathbf{G}_{\bar{q}}\mathbf{w}+1\right)\right)\Bigg]\\\text{subject to}\quad&\mathrm{tr}\left[\left(\mathbf{D}^H(\mathbf{w})\mathbf{D}(\mathbf{w})+\mu_q\mathbf{I}_{N_s}\right)^{-2}\mathbf{F}\mathbf{D}^H(\mathbf{w})\mathbf{D}(\mathbf{w})\mathbf{F}^H\right]=P_qN_s,\ \text{for } q=1,2.\end{aligned}\tag{5.3.15}$$

We can rewrite (5.3.15) as

$$\begin{aligned}\lambda(\mathbf{w},P_1,P_2)=\min_{\mu_1,\mu_2}\sum_{q=1}^{2}\Bigg(&\mathrm{tr}\Big[\left(\widetilde{\mathbf{H}}(\mathbf{w})\left(\widetilde{\mathbf{H}}^H(\mathbf{w})\widetilde{\mathbf{H}}(\mathbf{w})+\mu_q\mathbf{I}_{N_s}\right)^{-1}\widetilde{\mathbf{H}}^H(\mathbf{w})-\mathbf{I}_{N_s}\right)^2\Big]\\&+N_s\sigma^2\left(\mathbf{w}^H\mathbf{G}_{\bar{q}}^H\mathbf{G}_{\bar{q}}\mathbf{w}+1\right)\Big)\\\text{s.t.}\quad&\mathrm{tr}\left[\left(\mathbf{D}^H(\mathbf{w})\mathbf{D}(\mathbf{w})+\mu_q\mathbf{I}_{N_s}\right)^{-2}\mathbf{F}\mathbf{D}^H(\mathbf{w})\mathbf{D}(\mathbf{w})\mathbf{F}^H\right]=P_qN_s,\ \text{for } q=1,2\end{aligned}\tag{5.3.16}$$

or, equivalently, as

$$\begin{aligned}\lambda(\mathbf{w},P_1,P_2)=\sum_{q=1}^{2}\Bigg(&\mathrm{tr}\Big[\left(\mathbf{F}^H\mathbf{D}(\mathbf{w})\mathbf{F}\left(\mathbf{F}^H\mathbf{D}^H(\mathbf{w})\mathbf{D}(\mathbf{w})\mathbf{F}+\mu_q\mathbf{I}_{N_s}\right)^{-1}\mathbf{F}^H\mathbf{D}^H(\mathbf{w})\mathbf{F}-\mathbf{I}_{N_s}\right)^2\Big]\\&+N_s\sigma^2\delta_{\bar{q}}(\mathbf{w})\Big)\\\text{subject to}\quad&\mathrm{tr}\left[\left(\mathbf{D}^H(\mathbf{w})\mathbf{D}(\mathbf{w})+\mu_q\mathbf{I}_{N_s}\right)^{-2}\mathbf{F}\mathbf{D}^H(\mathbf{w})\mathbf{D}(\mathbf{w})\mathbf{F}^H\right]=P_qN_s,\ \text{for } q=1,2\end{aligned}\tag{5.3.17}$$

where $\delta_q(\mathbf{w}) = \left(\mathbf{w}^H \mathbf{G}_q^H \mathbf{G}_q \mathbf{w} + 1\right)$, for $q \in \{1, 2\}$. We can furthermore simplify (5.3.17) as

$$\lambda(\mathbf{w}, P_1, P_2) = \min_{\mu_1,\mu_2} \operatorname{tr} \sum_{q=1}^{2} \left(\left[\left(\left(\mathbf{D}^H(\mathbf{w})\mathbf{D}(\mathbf{w}) + \mu_q \mathbf{I}_{N_s} \right)^{-1} \mathbf{D}^H(\mathbf{w})\mathbf{D}(\mathbf{w}) - \mathbf{I}_{N_s} \right)^2 \right] + N_s \sigma^2 \delta_{\bar{q}}(\mathbf{w}) \right)$$
$$\text{subject to} \quad \operatorname{tr}\left[\left(\mathbf{D}^H(\mathbf{w})\mathbf{D}(\mathbf{w}) + \mu_q \mathbf{I}_{N_s} \right)^{-2} \mathbf{F}\mathbf{D}^H(\mathbf{w})\mathbf{D}(\mathbf{w})\mathbf{F}^H \right] = P_q N_s, \text{ for } q = 1, 2 \tag{5.3.18}$$

Recall that $\mathbf{D}(\mathbf{w}) = \operatorname{diag}\{\sqrt{N_s}\mathbf{f}_1^H \mathbf{B}\mathbf{w}, \cdots, \sqrt{N_s}\mathbf{f}_{N_s}^H \mathbf{B}\mathbf{w}\}$. Hence, we can represent (5.3.18) as

$$\lambda(\mathbf{w}, P_1, P_2) = \tag{5.3.19}$$
$$\min_{\mu_1,\mu_2} \sum_{q=1}^{2} \left(\operatorname{tr}\left[\left(\left(\operatorname{diag}\left\{ N_s |\mathbf{f}_k^H \mathbf{B}\mathbf{w}|^2 + \mu_q \right\}_{k=1}^{N_s} \right)^{-1} \left(\operatorname{diag}\left\{ N_s |\mathbf{f}_k^H \mathbf{B}\mathbf{w}|^2 \right\}_{k=1}^{N_s} \right) - \mathbf{I}_{N_s} \right)^2 \right] \right.$$
$$\left. + N_s \sigma^2 \delta_{\bar{q}}(\mathbf{w}) \right)$$
$$\text{s.t.} \quad \operatorname{tr}\left[\left(\operatorname{diag}\left\{ N_s |\mathbf{f}_k^H \mathbf{B}\mathbf{w}|^2 + \mu_q \right\}_{k=1}^{N_s} \right)^{-2} \mathbf{F}\mathbf{D}^H(\mathbf{w})\mathbf{D}(\mathbf{w})\mathbf{F}^H \right] = P_q N_s, \text{ for } q = 1, 2. \tag{5.3.20}$$

The optimization problem (5.3.19) can be rewritten as

$$\lambda(\mathbf{w}, P_1, P_2) = \min_{\mu_1,\mu_2} \sum_{q=1}^{2} \left(\operatorname{tr}\left[\operatorname{diag}\left\{ \left(\frac{\mu_q}{N_s |\mathbf{f}_k^H \mathbf{B}\mathbf{w}|^2 + \mu_q} \right)^2 \right\}_{k=1}^{N_s} \right] + N_s \sigma^2 \delta_{\bar{q}}(\mathbf{w}) \right)$$
$$\text{subject to} \quad \sum_{k=1}^{N_s} \frac{N_s |\mathbf{f}_k^H \mathbf{B}\mathbf{w}|^2}{\left(N_s |\mathbf{f}_k^H \mathbf{B}\mathbf{w}|^2 + \mu_q \right)^2} = P_q N_s, \text{ for } q = 1, 2 \tag{5.3.21}$$

or, equivalently, as

$$\lambda(\mathbf{w}, P_1, P_2) = \min_{\mu_1,\mu_2} \quad \sum_{q=1}^{2} \left(\left[\sum_{k=1}^{N_s} \left(\frac{\mu_q}{N_s |\mathbf{f}_k^H \mathbf{B}\mathbf{w}|^2 + \mu_q} \right)^2 \right] + N_s \sigma^2 \delta_{\bar{q}}(\mathbf{w}) \right)$$

$$\text{subject to} \quad \sum_{k=1}^{N_s} \frac{N_s |\mathbf{f}_k^H \mathbf{B}\mathbf{w}|^2}{\left(N_s |\mathbf{f}_k^H \mathbf{B}\mathbf{w}|^2 + \mu_q\right)^2} = P_q N_s, \text{ for } q = 1, 2. \tag{5.3.22}$$

5.3.3 Simplifying (5.3.3)

Let us define

$$\rho_k(\mathbf{w}) \triangleq N_s |\mathbf{f}_k^H \mathbf{B}\mathbf{w}|^2 \text{ for } k = 1, 2, \cdots, N_s. \tag{5.3.23}$$

Using (5.3.22), the optimization problem (5.3.3) can be written as

$$\min_{\substack{P_1 \geq 0 \\ P_2 \geq 0}} \min_{\mu_1,\mu_2} \min_{\mathbf{w}} \quad \sum_{q=1}^{2} \left(\left[\sum_{k=1}^{N_s} \left(\frac{\mu_q}{\rho_k(\mathbf{w}) + \mu_q} \right)^2 \right] + N_s \sigma^2 \delta_{\bar{q}}(\mathbf{w}) \right)$$

$$\text{subject to} \quad \sum_{k=1}^{N_s} \frac{\rho_k(\mathbf{w})}{\left(\rho_k(\mathbf{w}) + \mu_q\right)^2} = P_q N_s, \text{ for } q = 1, 2$$

$$P_1 \left(1 + \|\mathbf{G}_1 \mathbf{w}\|^2\right) + P_2 \left(1 + \|\mathbf{G}_2 \mathbf{w}\|^2\right) + \sigma^2 \mathbf{w}^H \mathbf{w} \leq P_{max} \tag{5.3.24}$$

or, equivalently, as

$$\min_{\substack{P_1 \geq 0 \\ P_2 \geq 0}} \min_{\mu_1,\mu_2} \min_{\mathbf{w}} \min_{\boldsymbol{\alpha}} \quad \sum_{q=1}^{2} \left(\left[\sum_{k=1}^{N_s} \left(\frac{\mu_q}{\alpha_k + \mu_q} \right)^2 \right] + N_s \sigma^2 \delta_{\bar{q}}(\mathbf{w}) \right)$$

$$\text{subject to} \quad \sum_{k=1}^{N_s} \frac{\alpha_k}{\left(\alpha_k + \mu_q\right)^2} = P_q N_s, \text{ for } q = 1, 2$$

$$P_1 \left(1 + \|\mathbf{G}_1 \mathbf{w}\|^2\right) + P_2 \left(1 + \|\mathbf{G}_2 \mathbf{w}\|^2\right) + \sigma^2 \mathbf{w}^H \mathbf{w} \leq P_{max}$$

$$\alpha_k = \rho_k(\mathbf{w}), \text{ for } k = 1, 2 \ldots, N_s. \tag{5.3.25}$$

where $\boldsymbol{\alpha} \triangleq [\alpha_1, \alpha_2, \cdots, \alpha_{N_s}]^T$.

Lemma 5.3.1. *Consider the following optimization problem:*

$$\zeta(\boldsymbol{\alpha}) = \min_{\boldsymbol{\alpha}} \quad \sum_{q=1}^{2} \sum_{k=1}^{N_s} \left(\frac{\mu_q}{\alpha_k + \mu_q} \right)^2$$

$$\textit{subject to} \quad \sum_{k=1}^{N_s} \frac{\alpha_k}{(\alpha_k + \mu_q)^2} = P_q N_s, \ \textit{for } q = 1, 2. \tag{5.3.26}$$

where α_k's are all positive values. At the optimum, all elements of α are the same (i.e., $\alpha_i = \alpha_j$ for $i, j \in \{1, 2, \cdots, N_s\}$).

Proof: See the Appendix.

Note that if α_k's have a certain structure (e.g., if they can be "parameterized" using a parameter vector), then the same minimum obtained by solving the optimization problem (5.3.26) is achieved if there exists such a parameter vector which makes α_k's all equal. More specifically, if α_k is constrained such that it can be written as $\alpha_k = \rho_k(\mathbf{w})$, then, for any fixed values of P_1, P_2, μ_1, and μ_2, the inner minimization in the optimization problem (5.3.25) will achieve the same minimum achieved by the optimization problem (5.3.26), if there exists a *feasible* $\mathbf{w}$ such that $\{\rho_k(\mathbf{w})\}_{k=1}^{N_s}$ are all equal. In other words, for any fixed values of P_1, P_2, μ_1, and μ_2 the minimum of the optimization problem (5.3.26) is a lower bound to the minimum of the objective function (5.3.25) and this lower bound is achieved if there is a value for the vector $\mathbf{w}$ such that all $\rho_k(\mathbf{w})$'s are equal. Requiring that $\{\rho_k(\mathbf{w})\}_{k=1}^{N_s}$ to be all equal at the optimum, means that the amplitude of the DFT representation of the discrete-time FIR channel impulse $\mathbf{h} = \mathbf{B}\mathbf{w}$ is constant (i.e., $|\mathbf{f}_i^H \mathbf{B}\mathbf{w}|^2 = |\mathbf{f}_j^H \mathbf{B}\mathbf{w}|^2$, for any i and j). This indeed implies that we need to find a set for $\mathbf{w}$ such that all diagonal entries of $\mathbf{D}(\mathbf{w})$ are equal to each other. Such a set of $\mathbf{w}$ is defined in Chapter 4 as $\mathcal{W}$. Again as it was shown in the previous chapters, for $\mathbf{w} \in \mathcal{W}$, only one of the taps of the channel impulse response is non-zero. As a result, the relays corresponding to that

tap has to be turned on and the other relays contributing to the other taps of the channel impulse response are switched off. Therefore, the global minimum is achieved when $\mathbf{w}$ belongs to the set $\mathcal{W}$, where only the relays corresponding to one tap of the end-to-end channel is non-zero. Later, we will discuss how to choose the tap of the end-to-end channel impulse response which needs to be turned on in order to achieve the minimum total MSE. Based on this discussion, the optimization problem (5.3.25) can be represented as

$$\lambda(\mathbf{w}, P_1, P_2) = \min_{\mu_1,\mu_2} \quad \sum_{q=1}^{2} \left(\left[N_s \left(\frac{\mu_q}{\rho_1(\mathbf{w}) + \mu_q} \right)^2 \right] + N_s \sigma^2 \delta_{\bar{q}}(\mathbf{w}) \right)$$
$$\text{subject to} \quad \frac{\rho_1(\mathbf{w})}{\left(\rho_1(\mathbf{w}) + \mu_q\right)^2} = P_q, \quad \text{for } q = 1, 2 \quad \text{and} \quad \mathbf{w} \in \mathcal{W} \quad (5.3.27)$$

where we have used the fact that based on the definition of the set $\mathcal{W}$ in (4.3.18), we can write $\rho_k(\mathbf{w}) = \rho_1(\mathbf{w})$, for $\mathbf{w} \in \mathcal{W}$. Using the first two constraints in (5.3.27) along with the fact that $\rho_1(\mathbf{w}) = N_s |\mathbf{f}_1^H \mathbf{B}\mathbf{w}|^2$ (see), we can obtain μ_q as[2]

$$\mu_q = \sqrt{\frac{N_s}{P_q}} |\mathbf{f}_1^H \mathbf{B}\mathbf{w}| - N_s |\mathbf{f}_1^H \mathbf{B}\mathbf{w}|^2 \quad (5.3.28)$$

Using Parseval's theorem $N_s |\mathbf{f}_1^H \mathbf{B}\mathbf{w}|^2 = \sum_{k=1}^{N_s} |\mathbf{f}_k^H \mathbf{B}\mathbf{w}|^2 = \mathbf{w}^H \mathbf{B}^H \mathbf{B}\mathbf{w} = \|\mathbf{B}\mathbf{w}\|^2$ in (5.3.28), we can write (5.3.27) as

$$\min_{\substack{P_1 \geq 0 \\ P_2 \geq 0}} \min_{\mathbf{w}} \quad N_s \sum_{q=1}^{2} \left(\left(1 - \sqrt{P_q} \|\mathbf{B}\mathbf{w}\| \right)^2 + \sigma^2 \delta_{\bar{q}}(\mathbf{w}) \right)$$
$$\text{subject to} \quad \left(\sum_{q=1}^{2} P_q \delta_q(\mathbf{w}) \right) + \sigma^2 \mathbf{w}^H \mathbf{w} \leq P_{max} \quad \text{and} \quad \mathbf{w} \in \mathcal{W}. \quad (5.3.29)$$

[2]It is worth mentioning that using the first two constraints in (5.3.28), we obtain that $\mu_q = \pm\sqrt{\frac{N_s}{P_q}} |\mathbf{f}_1^H \mathbf{B}\mathbf{w}| - N_s |\mathbf{f}_1^H \mathbf{B}\mathbf{w}|^2$. Note however that compared to the choice of μ_q in (5.3.28), the choice $\mu_q = -\sqrt{\frac{N_s}{P_q}} |\mathbf{f}_1^H \mathbf{B}\mathbf{w}| - N_s |\mathbf{f}_1^H \mathbf{B}\mathbf{w}|^2$ results in a larger value for the objective function in (5.3.27), and hence, this choice is not acceptable.

Defining $z_q \triangleq \sqrt{P_q}$, for $q = 1, 2$ and $\mathbf{z} \triangleq [z_1, z_2]^T$, the optimization problem (5.3.29) can be equivalently expressed as[3]

$$\begin{aligned} \min_{\mathbf{w}} \ \min_{\mathbf{z} \succeq \mathbf{0}} \ & N_s \sum_{q=1}^{2} \left((1 - z_1 \|\mathbf{B}\mathbf{w}\|)^2 + \sigma^2 \delta_q(\mathbf{w}) \right) \\ \text{subject to} \ & \left(\sum_{q=1}^{2} z_q^2 \delta_q(\mathbf{w}) \right) + \sigma^2 \mathbf{w}^H \mathbf{w} \leq P_{max} \quad \text{and} \quad \mathbf{w} \in \mathcal{W}. \end{aligned} \tag{5.3.30}$$

5.3.4 Solving the Inner Minimization in (5.3.30)

For any feasible $\mathbf{w}$, the inner minimization problem in (5.3.30) can be written as

$$\begin{aligned} \min_{\mathbf{z} \succeq \mathbf{0}} \ & \sum_{q=1}^{2} (1 - z_q \|\mathbf{B}\mathbf{w}\|)^2 \\ \text{subject to} \ & \left(\sum_{q=1}^{2} z_q^2 \delta_q(\mathbf{w}) \right) + \sigma^2 \mathbf{w}^H \mathbf{w} - P_{max} \leq 0. \end{aligned} \tag{5.3.31}$$

Note that for any fixed $\mathbf{w}$, the optimization problem (5.3.31) is convex in z_1 and z_2. Hence, for any given feasible value of $\mathbf{w}$, we can write the Lagrangian function, corresponding to the optimization problem (5.3.31), as[4]

$$\begin{aligned} \mathcal{L}_z(\mathbf{z}, \boldsymbol{\beta}, \zeta; \mathbf{w}) \triangleq & \sum_{q=1}^{2} (1 - z_q \|\mathbf{B}\mathbf{w}\|)^2 - \beta_1 z_1 - \beta_2 z_2 \\ & + \zeta \left[z_1^2 \delta_1(\mathbf{w}) + z_2^2 \delta_2(\mathbf{w}) + \sigma^2 \mathbf{w}^H \mathbf{w} - P_{max} \right] \end{aligned} \tag{5.3.32}$$

where $\boldsymbol{\beta} \triangleq [\beta_1, \beta_2]^T$, and β_1, β_2, and ζ are the Lagrange multipliers. The Lagrangian dual function can then be written as

$$g(\boldsymbol{\beta}, \zeta; \mathbf{w}) \triangleq \min_{\mathbf{z}} \ \mathcal{L}_z(\mathbf{z}, \boldsymbol{\beta}, \zeta; \mathbf{w}), \tag{5.3.33}$$

[3]Note that $\sum_{q=1}^{2} \delta_{\bar{q}}(\mathbf{w}) = \sum_{q=1}^{2} \delta_q(\mathbf{w})$.

[4]In what follows, we separate $\mathbf{w}$ from the other optimization variable with a semi-colon ';', to emphasize that when solving (5.3.31), $\mathbf{w}$ is fixed.

and hence, the dual optimization problem corresponding to the convex optimization (5.3.31) is written as

$$\begin{aligned} \max_{\boldsymbol{\beta},\zeta} \quad & g(\boldsymbol{\beta},\zeta;\mathbf{w}) \\ \text{subject to} \quad & \boldsymbol{\beta} \succeq 0 \\ & \zeta \geq 0. \end{aligned} \tag{5.3.34}$$

Since z_1 and z_2 are positive[5], due to complementary slackness conditions, at the optimum, $\beta_1 = \beta_2 = 0$ holds true. Hence, the derivative of the Lagrangian function in (5.3.32) with respect to z_q can be written as

$$\frac{\partial}{\partial z_q}\mathcal{L}_Z(\mathbf{z},\boldsymbol{\beta},\zeta;\mathbf{w}) = -2\|\mathbf{Bw}\|\left(1 - z_q\|\mathbf{Bw}\|\right) + 2\zeta z_q \delta_1(\mathbf{w}). \tag{5.3.35}$$

Equating (5.3.35) to zero, the optimum value of z_q is obtained, for any fixed value of $\mathbf{w}$, as

$$z_q = \sqrt{P_q} = \frac{\|\mathbf{Bw}\|}{\|\mathbf{Bw}\|^2 + \zeta\delta_q(\mathbf{w})}. \tag{5.3.36}$$

Substituting (5.3.36) in (5.3.33), the dual optimization problem can be written as

$$\max_{\zeta \geq 0} \quad \tilde{g}(\zeta;\mathbf{w}) \tag{5.3.37}$$

where

$$\tilde{g}(\zeta;\mathbf{w}) \triangleq \zeta\left[\sum_{q=1}^{2}\frac{\delta_q(\mathbf{w})}{\|\mathbf{Bw}\|^2 + \zeta\delta_q(\mathbf{w})} + \left(\sigma^2\mathbf{w}^H\mathbf{w} - P_{max}\right)\right] \tag{5.3.38}$$

The derivative of the objective function in (5.3.37) is given by

$$\frac{\partial\tilde{g}(\zeta;\mathbf{w})}{\partial\zeta} = \sum_{q=1}^{2}\frac{\|\mathbf{Bw}\|^2\delta_q(\mathbf{w})}{(\|\mathbf{Bw}\|^2 + \zeta\delta_q(\mathbf{w}))^2} + (\sigma^2\mathbf{w}^H\mathbf{w} - P_{max}) \tag{5.3.39}$$

$$= \sum_{q=1}^{2} z_q^2\delta_q(\mathbf{w}) + (\sigma^2\mathbf{w}^H\mathbf{w} - P_{max}) \leq 0. \tag{5.3.40}$$

[5]Otherwise, one or both transceivers will not transmit any data.

where we have used (5.3.36) in the second equality and the inequality follows from the fact that $\mathbf{w}$ is assumed to be feasible, i.e., $\mathbf{w}$ must satisfy the constraint in (5.3.30).

In the sequel, depending on whether $\frac{\partial \tilde{g}(\zeta;\mathbf{w})}{\partial \zeta}$ is negative or zero, we consider two cases.

5.3.5 Case I

For those values of $\mathbf{w}$ which result in a negative value for $\frac{\partial \tilde{g}(\zeta;\mathbf{w})}{\partial \zeta}$, for $\zeta \geq 0$, the function $\tilde{g}(\zeta;\mathbf{w})$ will be monotonically decreasing. Hence, the optimal value of ζ will be 0. In (5.3.36), replacing ζ with zero, we obtain the optimal values of the transceivers' transmit powers, in terms of the relay beamforming vector $\mathbf{w}$, as

$$P_1^{\text{opt}} = P_2^{\text{opt}} = \frac{1}{\|\mathbf{B}\mathbf{w}\|^2}. \tag{5.3.41}$$

Using (5.3.41), the optimization problem (5.3.29) can be written as

$$\begin{aligned} \min_{\mathbf{w}} \quad & N_s\sigma^2 \sum_{q=1}^{2} \delta_q(\mathbf{w}) \\ \text{subject to} \quad & \frac{\delta_1(\mathbf{w}) + \delta_2(\mathbf{w})}{\|\mathbf{B}\mathbf{w}\|^2} + \sigma^2 \mathbf{w}^H\mathbf{w} \leq P_{max} \\ & \mathbf{w} \in \mathcal{W}. \end{aligned} \tag{5.3.42}$$

Note that the inequality constraint in (5.3.42) can be satisfied with equality. Otherwise, if at the optimum, this constraint is satisfied with inequality, one can scale down the optimal $\mathbf{w}$ to satisfy the constraint with equality and furthermore reduce the objective function, thereby contradicting the optimality (see appendix). Hence, we can write

$$2 + \|\mathbf{G}_1\mathbf{w}\|^2 + \|\mathbf{G}_2\mathbf{w}\|^2 = \sum_{q=1}^{2} \delta_q(\mathbf{w}) = \left(P_{max} - \sigma^2\mathbf{w}^H\mathbf{w}\right)\|\mathbf{B}\mathbf{w}\|^2 \tag{5.3.43}$$

Using (5.3.44), the optimization problem (5.3.42) can be written as

$$\begin{aligned} \min_{\mathbf{w}} \quad & N_s\sigma^2 \left(P_{max} - \sigma^2 \mathbf{w}^H\mathbf{w}\right) \|\mathbf{B}\mathbf{w}\|^2 \\ \text{subject to} \quad & \frac{\left(P_{max} - \sigma^2 \mathbf{w}^H\mathbf{w}\right) \|\mathbf{B}\mathbf{w}\|^2}{2 + \|\mathbf{G}_1\mathbf{w}\|^2 + \|\mathbf{G}_2\mathbf{w}\|^2} = 1\,. \\ & \mathbf{w} \in \mathcal{W}. \end{aligned} \tag{5.3.44}$$

The same as the previous chapter, let $\mathbf{b}_n^H$ capture the non-zero entries of the $(n+1)$th row of $\mathbf{B}$. If only the relays corresponding to the nth tap of the end-to-end channel impulse response are active, we can write

$$\mathbf{w}^H\mathbf{B}^H\mathbf{B}\mathbf{w} = \mathbf{w}_n^H\mathbf{b}_n\mathbf{b}_n^H\mathbf{w}_n. \tag{5.3.45}$$

Using (5.3.45), the optimization problem (5.3.44) can be equivalently written as

$$\begin{aligned} \min_{n\in\mathcal{N}} \min_{\mathbf{w}_n} \quad & N_s\sigma^2 \left(P_{max} - \sigma^2 \mathbf{w}_n^H\mathbf{w}_n\right) \mathbf{w}_n^H\mathbf{b}_n\mathbf{b}_n^H\mathbf{w}_n \\ \text{subject to} \quad & \frac{\left(P_{max} - \sigma^2 \mathbf{w}_n^H\mathbf{w}_n\right) \mathbf{w}_n^H\mathbf{b}_n\mathbf{b}_n^H\mathbf{w}_n}{2 + \|\mathbf{G}_1^{(n)}\mathbf{w}_n\|^2 + \|\mathbf{G}_2^{(n)}\mathbf{w}_n\|^2} = 1 \end{aligned} \tag{5.3.46}$$

where $\mathcal{N} \triangleq \{1, 2, \ldots, N_s\}$ and as we explained in Chapter 4, $\mathbf{G}_q^{(n)}$, for $q = 1, 2$, is a diagonal matrix whose diagonal entries are a subset of those diagonal entries of $\mathbf{G}_q$ which correspond to the relays that contribute to the nth tap of the end-to-end channel impulse response. Note that the minimization over n aims to find the best tap of the channel which can be non-zero, while the other taps are all zero. Assuming that $\mathbf{w}_n = \sqrt{\eta}\tilde{\mathbf{w}}_n$, where $\|\tilde{\mathbf{w}}_n\| = 1$, we can rewrite the optimization problem (5.3.46)

as

$$\begin{aligned}\min_{n\in\mathcal{N}}\ \min_{\eta}\ \min_{\tilde{\mathbf{w}}_n}\quad & N_s\sigma^2\left(P_{max}-\sigma^2\eta\right)\eta\,\tilde{\mathbf{w}}_n^H\mathbf{b}_n\mathbf{b}_n^H\tilde{\mathbf{w}}_n \\ \text{subject to}\quad & \frac{\left(P_{max}-\sigma^2\eta\right)\eta\tilde{\mathbf{w}}_n^H\mathbf{b}_n\mathbf{b}_n^H\tilde{\mathbf{w}}_n}{\tilde{\mathbf{w}}_n^H\left(2\mathbf{I}+\eta\mathbf{G}_1^{(n)H}\mathbf{G}_1^{(n)}+\eta\mathbf{G}_2^{(n)H}\mathbf{G}_2^{(n)}\right)\tilde{\mathbf{w}}_n}=1 \\ & 0\le\eta\le\frac{P_{max}}{\sigma^2}\ \text{ and }\ \tilde{\mathbf{w}}_n^H\tilde{\mathbf{w}}_n=1. \end{aligned}\tag{5.3.47}$$

Note that in (5.3.47), we have added the constraint $0 \le \eta \le \frac{P_{max}}{\sigma^2}$ without any loss of optimality. Indeed, this constraint is implied by the first constraint in (5.3.47) , where the right hand side has to be non-negative. For a fixed η, let us first rewrite the inner minimization in (5.3.47) as

$$\begin{aligned}\min_{\tilde{\mathbf{w}}_n}\quad & \tilde{\mathbf{w}}_n^H\mathbf{b}_n\mathbf{b}_n^H\tilde{\mathbf{w}}_n \\ \text{subject to}\quad & \tilde{\mathbf{w}}_n^H\mathbf{Q}_n\tilde{\mathbf{w}}_n=2\ \text{ and }\ \tilde{\mathbf{w}}_n^H\tilde{\mathbf{w}}_n=1 \end{aligned}\tag{5.3.48}$$

where $\mathbf{Q}_n = \left[\left(P_{max}-\sigma^2\eta\right)\eta\mathbf{b}_n\mathbf{b}_n^H - \eta\mathbf{G}_1^{(n)H}\mathbf{G}_1^{(n)} - \eta\mathbf{G}_2^{(n)H}\mathbf{G}_2^{(n)}\right]$. The constraints in (5.3.48) imply that

$$\tilde{\mathbf{w}}_n^H\left(\kappa\mathbf{b}_n\mathbf{b}_n^H-\mathbf{U}_n(\eta)\right)\tilde{\mathbf{w}}_n=0 \tag{5.3.49}$$

where we have used the following definitions: $\mathbf{U}_n(\eta) \triangleq \left(\eta\mathbf{G}_1^{(n)H}\mathbf{G}_1^{(n)} + \eta\mathbf{G}_2^{(n)H}\mathbf{G}_2^{(n)} + 2\mathbf{I}\right)$ and $\kappa \triangleq \left(P_{max}-\sigma^2\eta\right)\eta$. We can write (5.3.49) equivalently as

$$\tilde{\mathbf{w}}_n^H\mathbf{U}_n^{\frac{1}{2}}(\eta)\left(k\mathbf{U}_n^{-\frac{1}{2}}(\eta)\mathbf{b}_n\mathbf{b}_n^H\mathbf{U}_n^{-\frac{1}{2}}(\eta)-\mathbf{I}\right)\mathbf{U}_n^{\frac{1}{2}}(\eta)\tilde{\mathbf{w}}_n=0. \tag{5.3.50}$$

There will be a non-zero value for $\tilde{\mathbf{w}}_n$ satisfying (5.3.50), if and only if $\det\left(\kappa\mathbf{c}\mathbf{c}^H-\mathbf{I}\right) = 0$, where $\mathbf{c} \triangleq \mathbf{U}_n^{-\frac{1}{2}}(\eta)\mathbf{b}_n$. In order for $\det\left(\kappa\mathbf{c}\mathbf{c}^H-\mathbf{I}\right) = 0$ to hold, we must ensure that at least one of the eigenvalues of $\kappa\mathbf{c}\mathbf{c}^H-\mathbf{I}$ is zero. Noting that the eigenvalues

of $\kappa\mathbf{c}\mathbf{c}^H - \mathbf{I}$ are either -1 or $\kappa\mathbf{c}^H\mathbf{c} - 1$, we conclude that in order to satisfy (5.3.50), the largest eigenvalue of $\kappa\mathbf{c}\mathbf{c}^H - \mathbf{I}$ has to be zero, that is

$$\kappa\mathbf{c}^H\mathbf{c} - 1 = \left(P_{max} - \sigma^2\eta\right)\eta\mathbf{b}_n^H\mathbf{U}_n^{-1}(\eta)\mathbf{b}_n - 1 = 0 \tag{5.3.51}$$

Moreover, (5.3.50) implies that $\mathbf{U}_n^{\frac{1}{2}}(\eta)\tilde{\mathbf{w}}_n$ has to be proportional to the principal eigenvector of the matrix $\kappa\mathbf{c}\mathbf{c}^H - \mathbf{I}$ which is the same as $\mathbf{c} = \mathbf{U}_n^{-\frac{1}{2}}(\eta)\mathbf{b}_n$. That is $\mathbf{U}_n^{\frac{1}{2}}(\eta)\tilde{\mathbf{w}}_n = \xi\mathbf{U}_n^{-\frac{1}{2}}(\eta)\mathbf{b}_n$, where ξ is a non-zero normalization constant ensuring that $\|\mathbf{w}_n^H\|^2 = 1$ holds true. Hence, we can write the optimal value of $\tilde{\mathbf{w}}_n$, in terms of ζ_n, as

$$\tilde{\mathbf{w}}_n = \frac{\mathbf{U}_n^{-1}(\eta)\mathbf{b}_n}{\sqrt{\mathbf{b}_n^H\mathbf{U}_n^{-2}(\eta)\mathbf{b}_n}}. \tag{5.3.52}$$

Using (5.3.51) and (5.3.52), the optimization problem (5.3.47) can be written as

$$\begin{aligned} \min_{n\in\mathcal{N}} \min_{\eta} \quad & N_s\sigma^2\left(P_{max} - \sigma^2\eta\right)\eta\frac{\left(\mathbf{b}_n^H\mathbf{U}_n^{-1}(\eta)\mathbf{b}_n\right)^2}{\mathbf{b}_n^H\mathbf{U}_n^{-2}(\eta)\mathbf{b}_n} \\ \text{subject to} \quad & \left(P_{max} - \sigma^2\eta\right)\eta\mathbf{b}_n^H\mathbf{U}_n^{-1}(\eta)\mathbf{b}_n = 1 \\ & 0 \le \eta \le \frac{P_{max}}{\sigma^2} \end{aligned} \tag{5.3.53}$$

or, equivalently, as

$$\begin{aligned} \min_{n\in\mathcal{N}} \min_{\eta} \quad & \frac{N_s\sigma^2}{\mathbf{b}_n^H\mathbf{U}_n^{-2}(\eta)\mathbf{b}_n\left(P_{max} - \sigma^2\eta\right)\eta} \\ \text{subject to} \quad & \left(P_{max} - \sigma^2\eta\right)\eta\mathbf{b}_n^H\mathbf{U}_n^{-1}(\eta)\mathbf{b}_n = 1 \\ & 0 \le \eta \le \frac{P_{max}}{\sigma^2}. \end{aligned} \tag{5.3.54}$$

The possible solutions to the equality constraint in (5.3.54) for η can be obtained by intersecting the concave parabolic function $\ell(\eta) = \left(P_{max} - \sigma^2\eta\right)\eta$ and the monotonically increasing and the concave[6] function $\hbar_n(\eta) = \left(\mathbf{b}_n^H\mathbf{U}_n^{-1}(\eta)\mathbf{b}_n\right)^{-1} > 0$. As shown

[6]Indeed, one can easily show that $\frac{\partial}{\partial\eta}(1/\hbar_n(\eta)) = -\mathbf{b}_n^H\mathbf{U}_n^{-2}(\eta)(\mathbf{G}_1^{(n)H}\mathbf{G}_1^{(n)} + \mathbf{G}_2^{(n)H}\mathbf{G}_2^{(n)})\mathbf{b}_n < 0$

in Figure. 5.2, the maximum number of the solutions to the equality constraint in (5.3.54) is 2. We can categorize these solutions as it follows.

Case I-a : If P_{max} is too small, there may not exist a value for η to satisfy the equality constraint in (5.3.54), and hence, the optimization problem (5.3.54) is not feasible. In this case, $\hbar_n(\eta) > \ell(\eta)$ holds true for $0 \leq \eta \leq \frac{P_{max}}{\sigma^2}$.

Case I-b : In this case, the functions $\ell(\eta)$ and $\hbar_n(\eta)$ intersect at two points. In this case, the feasible values for the optimization problem are limited to the corresponding values of η

Case I-c : This case corresponds to a scenario, where $\hbar_n(\eta)$ intersects $\ell(\eta)$ at only one point which is located left to the peak of $\ell(\eta)$. However, this case does not happen because, due to the fact that the matrix $\mathbf{U}_n(\eta)$ is positive-definite, the function $\hbar_n(\eta)$ is always positive.

Case I-d : In this case, the functions $\ell(\eta)$ and $\hbar_n(\eta)$ intersect at one point, which is located left to the peak of $\ell(\eta)$. This case does not happen either, as the function $\hbar_n(\eta)$ is always positive.

Based on the above categorization, one can easily find the feasible values of η as explained in the sequel: One can start from $\eta = 0$ and using a sufficiently fine search algorithm find a value for η, say $\eta^{(1)}$, where $\hbar_n(\eta) - \ell(\eta)$ is smaller than an arbitrarily small positive number. If such a value for η cannot be found, then the problem is infeasible for the chosen n. Otherwise, $\eta^{(1)}$ is introduced as one of the two feasible values for η. Then a bisection algorithm is used to obtain the other feasible value for η, say $\eta^{(2)}$, in the interval $[\eta^{(1)} \ \ \frac{P_{max}}{\sigma^2}]$. Then the optimal value of η, denoted as η_n, is

holds true. Hence the function $(1/\hbar_n(\eta))$ is monotonically decreasing. As a result, the function $\hbar_n(\eta)$ is monotonically increasing. Moreover, it can be easily shown that $\frac{\partial^2}{\partial \eta^2}(1/\hbar_n(\eta)) = 2\mathbf{b}_n^H \mathbf{U}_n^{-3}(\eta)(\mathbf{G}_1^{(n)H}\mathbf{G}_1^{(n)} + \mathbf{G}_2^{(n)H}\mathbf{G}_2^{(n)})\mathbf{b}_n > 0$ holds true, and hence the function $1/\hbar_n(\eta)$ is convex, and consequently, $\hbar_n(\eta)$ is concave.

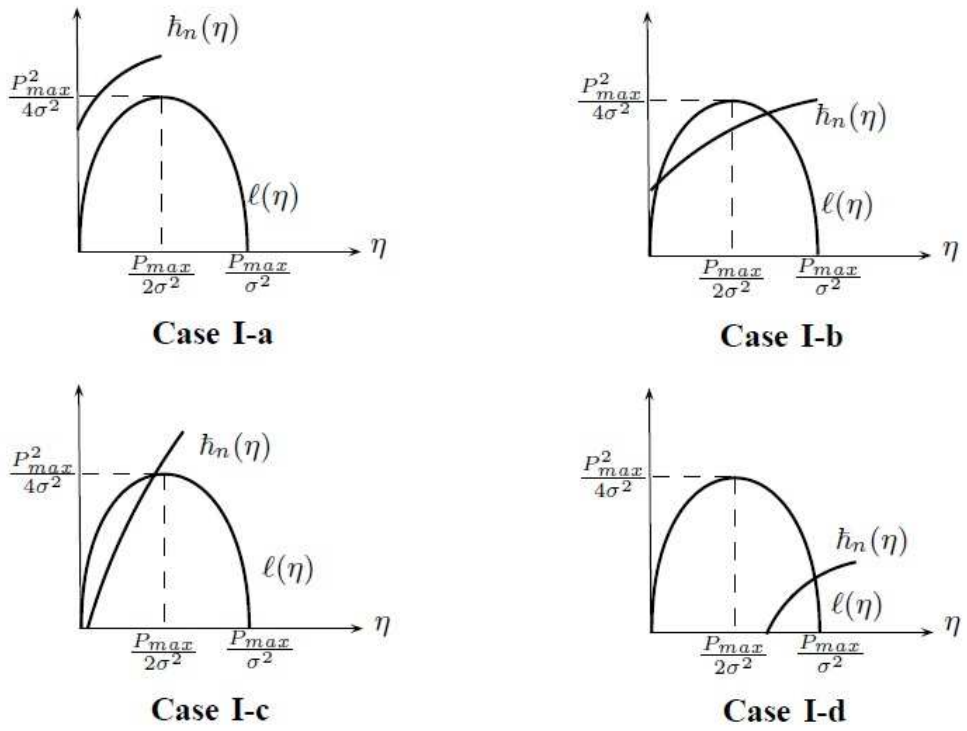

Figure 5.2: Different possible scenarios for intersection point(s) of $\ell(\eta)$ and $\hbar_n(\eta)$.

the one which results in the minimum value for the objective function, that is.

$$\eta_n = \arg \min_{\eta \in \{\eta^{(1)}, \eta^{(2)}\}} \quad \frac{N_s \sigma^2}{\mathbf{b}_n^H \mathbf{U}_n^{-2}(\eta) \mathbf{b}_n \left(P_{max} - \sigma^2 \eta\right) \eta} \,. \tag{5.3.55}$$

The optimal value of n is then obtained as the one which results in the smallest value for the MSE, that is, we use (5.3.54) to obtain the optimal value of n, denoted by n^{o}, as

$$n^{\mathrm{o}} = \arg \min_{n \in \mathcal{N}} \quad \frac{N_s \sigma^2}{\mathbf{b}_n^H \mathbf{U}_n^{-2}(\eta_n) \mathbf{b}_n \left(P_{max} - \sigma^2 \eta_n\right) \eta_n} \,. \tag{5.3.56}$$

If the equality constraint in (5.3.53) is not feasible for any value of n, then Case I does not occur. Whether Case I is feasible or not, Case II needs to be taken into

account.

5.3.6 Case II

Now let us consider those values of $\mathbf{w}$ which result in a zero value for $\frac{d\tilde{g}(\zeta)}{d\zeta}$, for some $\zeta > 0$. In this case, the nonlinear equation

$$\frac{\partial \tilde{g}(\zeta;\mathbf{w})}{\partial \zeta} = \sum_{q=1}^{2} \frac{\|\mathbf{Bw}\|^2 \delta_q(\mathbf{w})}{(\|\mathbf{Bw}\|^2 + \zeta\delta_q(\mathbf{w}))^2} + (\sigma^2 \mathbf{w}^H\mathbf{w} - P_{max}) = 0 \tag{5.3.57}$$

has a positive solution for ζ. This means that in this case, the optimal values of P_1 and P_2 are smaller than the corresponding values in case I as they are given in (5.3.41). Indeed, the optimal values of P_1 and P_2 are given by (5.3.36), when ζ is replaced with the solution to the nonlinear equation (5.3.57). We now show that for any feasible value of $\mathbf{w}$, the non-linear equation in (5.3.57) has only one positive solution. To do so, note that for any fixed $\mathbf{w}$, $\frac{\partial \tilde{g}(\zeta;\mathbf{w})}{\partial \zeta}$ in (5.3.57) is a monotonically decreasing function of ζ and $\frac{\partial g(\zeta;\mathbf{w})}{\partial \zeta}|_{\zeta=0} > 0$, while $\frac{\partial g(\zeta;\mathbf{w})}{\partial \zeta}|_{\zeta\to+\infty} = (\sigma^2\mathbf{w}^H\mathbf{w} - P_{max}) < 0$. The latter inequality holds, because, otherwise (5.3.40) would not hold. In fact, as we are considering only feasible values of $\mathbf{w}$, it is required that (5.3.40) holds true. Therefore, for any feasible value of $\mathbf{w}$, using the fact that $\frac{\partial \tilde{g}(\zeta;\mathbf{w})}{\partial \zeta}$ is a monotonically decreasing function of ζ and $\frac{\partial g(\zeta;\mathbf{w})}{\partial \zeta}|_{\zeta=0} > 0$, while $\frac{\partial g(\zeta;\mathbf{w})}{\partial \zeta}|_{\zeta\to+\infty} < 0$, there exists only one positive value for ζ which makes $\frac{\partial g(\zeta;\mathbf{w})}{\partial \zeta}$ in (5.3.39) equal to zero (i.e., it satisfies the non-linear equation (5.3.57)), thereby maximizing $g(\zeta;\mathbf{w})$. For any given feasible value for $\mathbf{w}$, let $\zeta^{\text{opt}}(\mathbf{w})$ be the solution to the non-linear equation (5.3.57). Hence, using (5.3.36), we rewrite the optimization problem (5.3.30) as

$$\begin{aligned} \min_{\mathbf{w}} \quad & \sum_{q=1}^{2} N_s \left(\left(\frac{\zeta^{\text{opt}}(\mathbf{w})\delta_q(\mathbf{w})}{\|\mathbf{Bw}\|^2 + \zeta^{\text{opt}}(\mathbf{w})\delta_q(\mathbf{w})} \right)^2 + \sigma^2 \delta_{\bar{q}}(\mathbf{w}) \right) \\ \text{subject to} \quad & \mathbf{w}^H\mathbf{w} \le \frac{P_{max}}{\sigma^2} \ \text{ and } \ \mathbf{w} \in \mathcal{W} \end{aligned} \tag{5.3.58}$$

where the first constraint in (5.3.30) is no longer needed because due to the fact that $\zeta^{\text{opt}}(\mathbf{w})$ is obtained by solving (5.3.57), this constraint is already satisfied with equality. The first constraint in (5.3.58) is required to ensure that $\mathbf{w}$ satisfies (5.3.40) and that $\zeta^{\text{opt}}(\mathbf{w}) > 0$ holds true. The optimization problem (5.3.58) can be equivalently rewritten as

$$\min_{n\in\mathcal{N}} \min_{\mathbf{w}_n} \sum_{q=1}^{2} N_s \left(\left(\frac{\zeta_n^{\text{opt}}(\mathbf{w}_n)\delta_q^{(n)}(\mathbf{w}_n)}{\mathbf{w}_n^H \mathbf{b}_n \mathbf{b}_n^H \mathbf{w}_n + \zeta_n^{\text{opt}}(\mathbf{w}_n)\delta_q^{(n)}(\mathbf{w}_n)} \right)^2 + \sigma^2 \delta_q^{(n)}(\mathbf{w}_n) \right)$$
$$\text{subject to} \quad \mathbf{w}_n^H \mathbf{w}_n \leq \frac{P_{max}}{\sigma^2} \tag{5.3.59}$$

where $\delta_q^{(n)}(\mathbf{w}_n) = \left(1 + \|\mathbf{G}_q^{(n)}\mathbf{w}_n\|^2\right)$ and $\zeta_n^{\text{opt}}(\mathbf{w}_n)$ is the solution to (5.3.57) for any feasible value of $\mathbf{w}_n$, when we choose $\mathbf{w} \in \mathcal{U}_n$, i.e., when only the nth tap of the end-to-end channel is non-zero[7]. For any fixed value of n, the inner minimization does not appear convex, and thus, may not be amenable to a computationally efficient solution. To tackle this inner minimization, we propose to use a sequential quadratic programming (SQP) algorithm. It is worth mentioning that the SQP method converges a minimum, however the global convergence cannot be guaranteed. We comment on the performance of this method in the next section.

Below, we summarize our proposed method.

Step 1. Set $n = 0$ and choose MSE to have a very large number.

Step 2. If no relay contributes to the nth tap of $h_{pq}[\cdot]$ (i.e., if the $(n+1)$th row of the matrix $\mathbf{B}$ is zero), go to Step 10.

Step 3. Define $\mathbf{U}_n(\eta) \triangleq \left(\eta \mathbf{G}_1^{(n)H}\mathbf{G}_1^{(n)} + \eta \mathbf{G}_2^{(n)H}\mathbf{G}_2^{(n)} + 2\mathbf{I}\right)$, $\ell(\eta) \triangleq (P_{max} - \sigma^2\eta)\,\eta$, and $\hbar_n(\eta) \triangleq (\mathbf{b}_n^H \mathbf{U}_n^{-1}(\eta)\mathbf{b}_n)^{-1}$, where $\mathbf{G}_q^{(n)}$, for $q = 1, 2$, is a diagonal matrix whose

[7]Recall that for any $\mathbf{w} \in \mathcal{U}_n$, all the non-zero entries of $\mathbf{w}$ are stacked in the vector $\mathbf{w}_n$.

diagonal entries are a subset of those diagonal entries of $\mathbf{G}_q$ which correspond to the relays that contribute to the nth tap of the end-to-end channel impulse response.

Step 4. Let $\mathbf{b}_n^H$ capture the non-zero entries of the $(n+1)$th row of $\mathbf{B}$.

Step 5. If the two functions $\hbar_n(\eta)$ and $\ell(\eta)$ intersect, then using a combination of a one-dimensional search and the bisection method, find $\eta^{(1)}$ and $\eta^{(2)}$ where these two functions intersect. Otherwise go Step 8.

Step 6. Calculate η_n as

$$\eta_n = \arg \min_{\eta \in \{\eta^{(1)}, \eta^{(2)}\}} \quad \frac{N_s \sigma^2}{\mathbf{b}_n^H \mathbf{U}_n^{-2}(\eta) \mathbf{b}_n \left(P_{max} - \sigma^2 \eta\right) \eta} .$$

Step 7. If MSE $> \dfrac{N_s \sigma^2}{\mathbf{b}_n^H \mathbf{U}_n^{-2}(\eta_n) \mathbf{b}_n \left(P_{max} - \sigma^2 \eta_n\right) \eta_n}$, then set the value of MSE as MSE $= \dfrac{N_s \sigma^2}{\mathbf{b}_n^H \mathbf{U}_n^{-2}(\eta^{\text{opt}}) \mathbf{b}_n \left(P_{max} - \sigma^2 \eta^{\text{opt}}\right) \eta^{\text{opt}}}$, choose $n^{\text{o}} = n$, and set Case $= 1$.

Step 8. Use an SQP technique to solve the following minimization, thereby obtaining ρ_n as

$$\rho_n \triangleq \min_{\mathbf{w}_n} \sum_{q=1}^{2} N_s \left(\left(\frac{\zeta_n^{\text{opt}}(\mathbf{w}_n) \delta_q^{(n)}(\mathbf{w}_n)}{\mathbf{w}_n^H \mathbf{b}_n \mathbf{b}_n^H \mathbf{w}_n + \zeta_n^{\text{opt}}(\mathbf{w}_n) \delta_q^{(n)}(\mathbf{w}_n)} \right)^2 + \sigma^2 \delta_q^{(n)}(\mathbf{w}_n) \right)$$

$$\text{subject to} \quad \mathbf{w}_n^H \mathbf{w}_n \leq \frac{P_{max}}{\sigma^2}$$

where $\delta_q^{(n)}(\mathbf{w}_n) \triangleq \left(1 + \|\mathbf{G}_q^{(n)} \mathbf{w}_n\|^2\right)$ and $\zeta_n^{\text{opt}}(\mathbf{w}_n)$ is the solution to the following nonlinear equation:

$$\sum_{q=1}^{2} \frac{\mathbf{b}_n^H \mathbf{w}_n \mathbf{w}_n^H \mathbf{b}_n \delta_q^{(n)}(\mathbf{w}_n)}{(\mathbf{b}_n^H \mathbf{w}_n \mathbf{w}_n^H \mathbf{b}_n + \zeta \delta_q^{(n)}(\mathbf{w}_n))^2} + (\sigma^2 \mathbf{w}_n^H \mathbf{w}_n - P_{max}) = 0$$

for any feasible value of $\mathbf{w}_n$, i.e., when we choose $\mathbf{w} \in \mathcal{U}_n$, or equivalently, when only the nth tap of the end-to-end channel is non-zero[8].

[8]Note that for any $\mathbf{w} \in \mathcal{U}_n$, all the non-zero entries of $\mathbf{w}$ are stacked in the vector $\mathbf{w}_n$.

Step 9. If MSE $> \rho_n$, then MSE $= \rho_n$, choose $n^{\text{o}} = n$, and set Case $= 2$.

Step 10. $n := n + 1$. If $n = N$, then go to Step 11, otherwise go to Step 2.

Step 11. If Case $= 1$, then calculate the relay beamforming vector and the transceivers' transmit powers, respectively, as

$$\mathbf{w}_{n^{\text{o}}} = \frac{\mathbf{U}_{n^{\text{o}}}^{-1}(\eta_{n^{\text{o}}})\mathbf{b}_{n^{\text{o}}}}{\sqrt{\mathbf{b}_{n^{\text{o}}}^H \mathbf{U}_{n^{\text{o}}}^{-2}(\eta_{n^{\text{o}}})\mathbf{b}_{n^{\text{o}}}}}$$
$$P_1^{\text{opt}} = P_2^{\text{opt}} = \frac{1}{\|\mathbf{w}_{n^{\text{o}}}^H \mathbf{b}_{n^{\text{o}}} \mathbf{b}_{n^{\text{o}}}^H \mathbf{w}_{n^{\text{o}}}\|^2}. \tag{5.3.60}$$

Otherwise, set $n = n^{\text{o}}$ and obtain $\mathbf{w}_{n^{\text{o}}}$ by solving the following optimization problem as

$$\mathbf{w}_{n^{\text{o}}} = \arg\min_{\mathbf{w}_n} \sum_{q=1}^{2} N_s \left(\left(\frac{\zeta_{n^{\text{o}}}^{\text{opt}}(\mathbf{w}_n)\delta_q^{(n^{\text{o}})}(\mathbf{w}_n)}{\mathbf{w}_n^H \mathbf{b}_{n^{\text{o}}} \mathbf{b}_{n^{\text{o}}}^H \mathbf{w}_n + \zeta_{n^{\text{o}}}^{\text{opt}}(\mathbf{w}_{n^{\text{o}}})\delta_q^{(n^{\text{o}})}(\mathbf{w}_n)} \right)^2 + \sigma^2 \delta_q^{(n^{\text{o}})}(\mathbf{w}_n) \right)$$
$$\text{subject to} \quad \mathbf{w}_n^H \mathbf{w}_n \leq \frac{P_{max}}{\sigma^2}$$

where $\zeta_{n^{\text{o}}}^{\text{opt}}(\mathbf{w}_n)$ is the solution to the following non-linear equation:

$$\sum_{q=1}^{2} \frac{\mathbf{w}_n^H \mathbf{b}_{n^{\text{o}}} \mathbf{b}_{n^{\text{o}}}^H \mathbf{w}_n \delta_q^{(n^{\text{o}})}(\mathbf{w}_n)}{(\mathbf{w}_n^H \mathbf{b}_{n^{\text{o}}} \mathbf{b}_{n^{\text{o}}}^H \mathbf{w}_n + \zeta \delta_q^{(n^{\text{o}})}(\mathbf{w}_n))^2} + (\sigma^2 \mathbf{w}_n^H \mathbf{w}_n - P_{max}) = 0.$$

Calculate the Transceivers' transmit powers as

$$P_q = \frac{\mathbf{w}_{n^{\text{o}}}^H \mathbf{b}_{n^{\text{o}}} \mathbf{b}_{n^{\text{o}}}^H \mathbf{w}_{n^{\text{o}}}}{(\mathbf{w}_{n^{\text{o}}}^H \mathbf{b}_{n^{\text{o}}} \mathbf{b}_{n^{\text{o}}}^H \mathbf{w}_{n^{\text{o}}} + \zeta_{n^{\text{o}}}^{\text{opt}}(\mathbf{w}_{n^{\text{o}}})\delta_q^{(n^{\text{o}})}(\mathbf{w}_{n^{\text{o}}}))^2}.$$

5.4 Simulation Results

Similar to our simulation model is Chapter 4, we consider an asynchronous relay network where two single-antenna transceivers exchange information with the help of $L = 60$ single-antenna relays. The signals of the transceivers are transmitted in

blocks of $N_s = 64$ symbols. In each simulation run, the propagation delay between a transceiver and any relay is chosen as a random variable uniformly distributed in the interval $[T_s, 4T_s]$. In this case, the delay spread of the end-to-end channel is a random variable which has a triangular distribution in the interval $[2T_s \;\; 8T_s]$. As a results, no relay contributes to the first two taps, these taps of the end-to-end discrete-time equivalent channel impulse response are always zero. We assume that the flat fading channel coefficients between the relays and the transceivers are independent and identically distributed (i.i.d.) complex Gaussian random variables with zero mean and have a variance inversely proportional to the path delay to the power of 3, i.e., the path loss is 3. The noises introduced at the transceivers and relays are white Gaussian random variables with zero mean.

Figure. 5.3 depicts the total MSE obtained by our proposed algorithm and compares that with the MSE calculated for the post-channel equalizer presented in Chapter 4, for the case when $\sigma^2 = -10$ dB is chosen. As can be seen from this figure, when the transmit power is low, the communication scheme with a pre-channel equalizer has a lower total MSE compared to the scheme with post-channel equalizer. This better performance of the pre-channel equalizer at low values of total transmit power can be explained by the fact that this equalizer can control and improve the signal quality without affecting the receiver noise (i.e., $\gamma'_q[n]$ in (4.2.6)) at the two transceivers. The post-channel equalizer method is however somehow limited as it has to process the received signal in the presence of noise. As a result, when the signal quality is low, the post-channel equalizers are not capable of improving the quality of the received signal at their output without amplifying the receiver noise. When P_{max} is increased, the total MSE of our proposed method saturates at $2N_s\sigma^2$, which is equal to the total

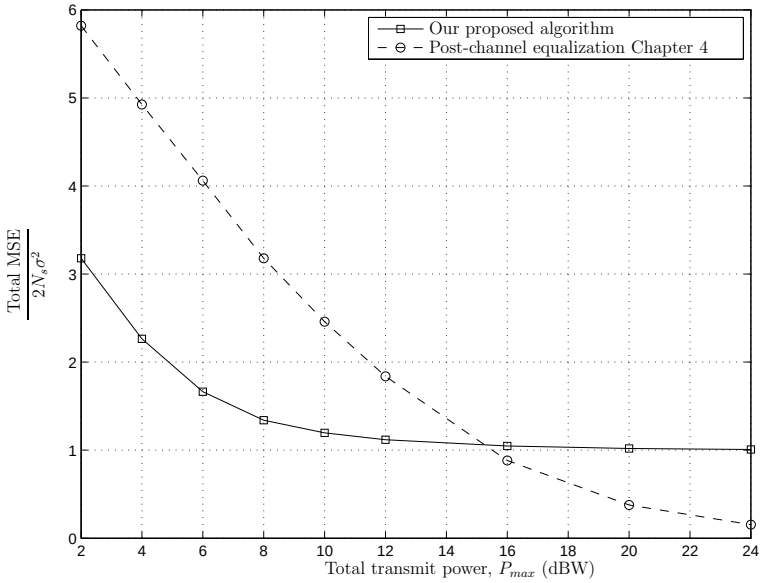

Figure 5.3: Total MSE versus the total available transmit power, P_{max} for $\sigma^2 = -10$ dBW.

receiver noise power for all symbols and for both transceivers. Indeed, the disadvantage of the pre-channel equalizer is that it cannot control the receiver noise power of the two transceivers. On the other hand, the post-channel equalizer can consistently result in better performance, when P_{max} is increased. The reason is that as P_{max} is increased, the post-channel equalizer will have more freedom to suppress the receiver noise at the two transceivers.

Assuming QPSK modulation and for a noise power equal to -10 dB, Figure. 5.4 depicts the end-to-end bit error rates (BERs) versus the total transmit power P_{max} for our proposed scheme in this chapter and for the post-channel equalizer of Chapter 4. As shown in this figure, for a fixed relay/transceiver noise power, increasing the total transmit power leads to a more reliable communication network. As we also

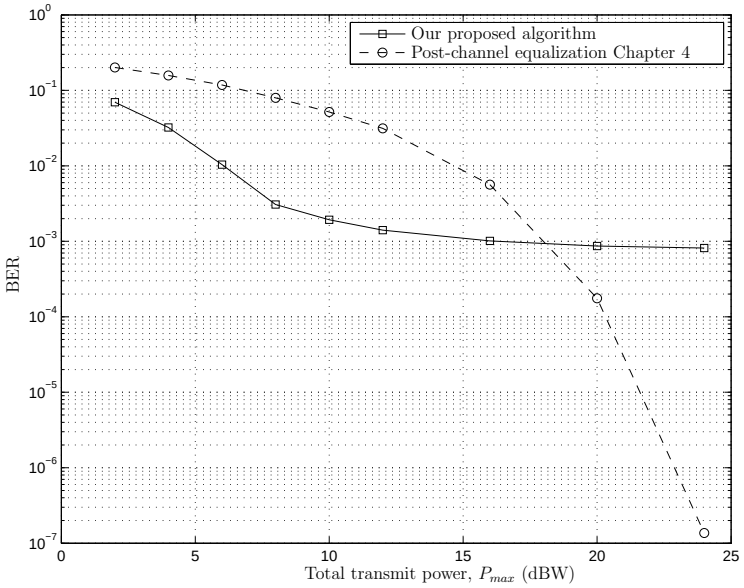

Figure 5.4: BER versus the total available transmit power, P_{max} for $\sigma^2 = -10$ dB.

explained from the MSE point of view, for low values of P_{max}, our proposed method in this chapter outperforms the post-channel equalizer in terms of BER. However, for relatively high values of transmit powers, since the minimum total MSE for our method approaches $2N_s\sigma^2$, the BER of this method cannot be less than some certain limit and it saturates.

Figure. 5.5 shows the performance of the proposed algorithm as well as that of the post-channel equalizer scheme in terms of the end-to-end BER versus the relay and transceiver noise power for a fixed total power $P_{max} = 10$ dBW. As shown in this figure, increasing the noise power increases the BER for both methods. Again, this figure shows that for low noise powers, our proposed method is more reliable compared to the method proposed in Chapter 4. As the noise power is increased, the BER

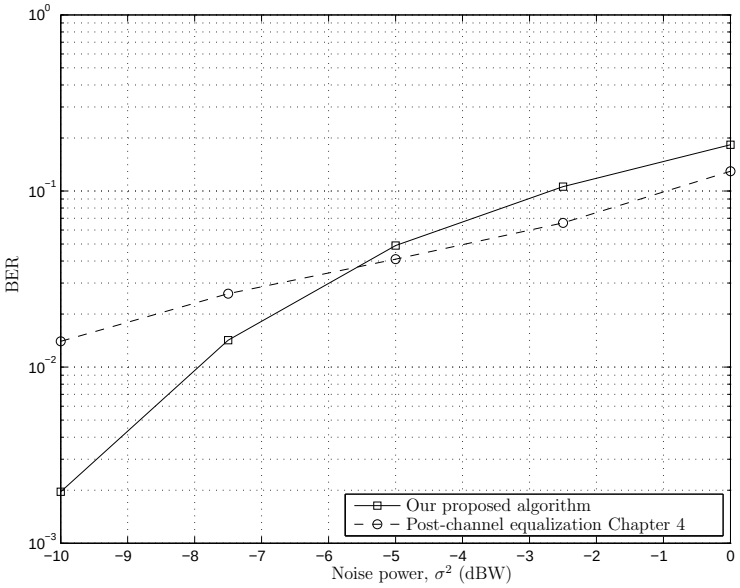

Figure 5.5: BER versus the the relay/transceiver noise power, σ^2, for $P_{max} = 10$ dBW.

advantage of the pre-channel equalizer over the post-channel equalizer diminishes. As explained earlier, this advantage is due to the fact that the pre-channel equalizer can control the signal quality without affecting the receiver noise at the two transceivers. Note however that the pre-channel equalizer method does not have any control on the receiver noise as long as the total available power is fixed, while the post-channel equalizer method can control the contribution of the receiver noise to total noise at the equalizers' outputs. Hence, as the noise power is increased, the performance of the pre-channel equalizer degrades faster than the post-channel equalizer.

In Figure. 5.6, for a fixed total transmit power $P_{max} = 10$ dBW, we depict the total MSEs for both methods versus the noise power. This figure demonstrates that for a fixed amount of transmit power, increasing the noise power at the relays and

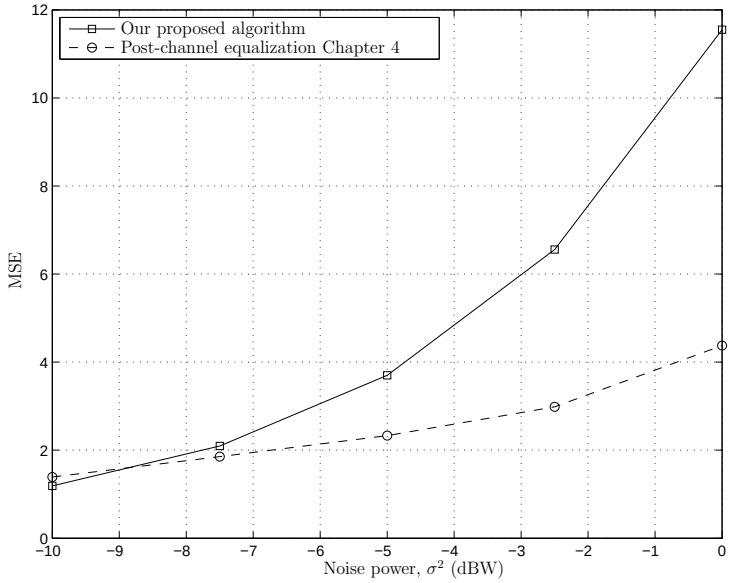

Figure 5.6: Total MSE versus the noise of the relays and transceivers for $P_{max} = 10$ dB.

transceivers increases the total MSE for both pre- and post-channel equalization schemes. Figs. 5.5 and 5.6 show that increasing MSE in the communication system for both pre- and post-channel equalization schemes, reduces the received symbol SNRs, and therefore leads, to a higher rate of error in the received bits. Here a question comes to mind: why the total MSE curves in Figure. 5.6 intersect at a certain value of σ^2, while the BER curves intersect in Figure. 5.5 at a different value of σ^2? To answer this question, we need to explore the relationship between the transceiver MSE and the BER, or equivalently, the relationship between the transceiver MSE and the symbol SNR. To do so, it has been shown in Chapter 4 that for the post-channel equalizer, the relationship between the total MSE and the symbol SNR for

Transceiver q is expressed as

$$\mathrm{MSE}_q^{\mathrm{post}} = \frac{N_s}{\mathrm{SNR}_q^{\mathrm{post}} + 1} \tag{5.4.1}$$

where the superscript "post" signifies the post-channel equalizer method. For the pre-channel equalizer presented in this chapter, we can derive the relationship between MSE and SNR for Transceiver q as (see appendix)

$$\mathrm{MSE}_q = \| \widetilde{\mathbf{H}}(\mathbf{w}^{\mathrm{o}})\mathbf{F}_{\bar{q}} - \mathbf{I} \|_F^2 + \frac{\| \widetilde{\mathbf{H}}(\mathbf{w}^{\mathrm{o}})\mathbf{F}_{\bar{q}} \|_F^2}{\mathrm{SNR}_q} \tag{5.4.2}$$

where $\mathbf{w}^{\mathrm{o}}$ is the optimal value of the relay weight vector $\mathbf{w}$. Note that in Case I, where $\widetilde{\mathbf{H}}(\mathbf{w}^{\mathrm{o}})\mathbf{F}_{\bar{q}} = \mathbf{I}$ holds true, we can simplify (5.4.2) as

$$\mathrm{MSE}_q = \frac{N_s}{\mathrm{SNR}_q} \tag{5.4.3}$$

Comparing (5.4.1) and (5.4.2), explains why the equality of the total MSEs of pre- and post-channel equalizer schemes does not necessarily results in the same SNR, and consequently, the same BER performance of these two competing methods.

5.5 Conclusion

In this chapter, an *asynchronous* two-way relay communication network is considered with two single-antenna transceivers exchanging data with the help of multiple relay nodes in a single-carrier communication scheme. Under the assumption that the propagation delay of each certain path from one transceiver going to different relays and ending at the other transceiver is different than the other paths, the end-to-end channel is turned to a frequency selective channel. Therefore, inter-symbol-interference (ISI) is unavoidable at the two transceivers. Since the information symbols are assumed to be transmitted in blocks, such an ISI causes IBI between consecutive transmitted blocks. To mitigate the adverse effect of IBI, both transceivers are equipped

with cyclic prefix insertion/removal blocks and block channel equalization is utilized before sending the data into the channel in each transceiver to compensate the impact of the channel. However, there is no filtering process at the relays and they are assumed to amplify and forward the transceivers' signals. Our goal is to minimize the total mean squared error (MSE) of the estimated received signals at both transceivers under the assumption that the total transmit power is limited. To do so, the relay beamforming weight vector and the transceivers' powers are optimally obtained and the pre-channel block equalizers are designed. Such a design is proved to lead to a relay selection scheme, where only the relays contributing to one tap of the end-to-end channel impulse response are turned on and the remaining relays are switched off. We introduced two optimization problems for sufficiently large and small amount of the available total transmit power of the network. The simulation results compare the performance of our proposed algorithm with the method of Chapter 4 for various total power budgets and noise powers at the relays and transceivers.

Chapter 6

Conclusion and Future work

6.1 Conclusion

In this thesis we focused on cooperative communication networks. We considered an asynchronous bi-directional relay network, where the relay paths are subject to different relaying and/or propagation delays. Such a network can be viewed as a multipath end-to-end channel which causes inter-symbol-interference at the two transceivers, when the data rates are sufficiently high. For such a two-way relay network, we studied multi-carrier and single-carrier communication schemes.

In the multi-carrier communication scheme, we deployed OFDM to diagonalize the end-to-end channel. For the sake of simplicity at the relays, we assumed simple amplify-and-forward relaying, thereby implementing a bi-directional network beamformer in a distributed manner. For such a two-way collaborative scheme, we proposed two different max-min design approaches to optimally obtain the subcarrier power loading at the transceivers as well as the relay beamforming weights.

In the first approach, for any given pair of transceivers' transmit powers, we first obtained a set of relay beamforming weight vectors such that each member of this

set maximizes the power-normalized SNR at one of the transceivers on one of the subcarriers, subject to per-relay power constraints. This set has twice as many members as the number of subcarriers, each of which corresponds to one possible impulse response for the end-to-end multipath channel. To obtain the transceivers' subcarrier powers, we then maximized the smallest subcarrier SNR at both transceivers for all such possible choices of the end-to-end channel impulse response.

In the second approach, the worst SNR across all transceivers' subcarriers is maximized, subject to a total power constraint, by properly adjusting the transceiver's transmit powers as well as the relay beamforming coefficients. We rigorously proved that this approach leads to a relay selection solution where only the relays corresponding to one of the taps of the multipath end-to-end channel are turned on and the other relays do not participate in the communication scheme. A semi-closed-form solution is then presented that can be used to obtain the relay beamforming weights.

In the single-carrier communication scheme, to combat the IBI introduced at the both transceivers, cyclic prefix is added to the transmitted signal blocks at the transceivers. Considering post-channel block equalization at the transceivers, we obtained the relay beamforming weights, the transmit power of the transceivers, and the transceivers block equalizers such that the total mean squared error (MSE) of the symbol estimates at the output of the block equalizers are minimized subject to a total power budget constraint. We rigourously proved that our proposed approach leads to a relay selection scheme, where only the relays, which contribute to one tap of the end-to-end channel impulse response, are turned on and the remaining relays are all turned off. To determine which tap of the end-to-end channel impulse response has to be non-zero, we presented a simple search procedure. Deploying post-channel

block equalization and assuming only a certain tap of the end-to-end channel impulse response is non-zero while all other taps are zero, we presented a semi-closed-form solution for the corresponding relay beamforming weight vector and the respective minimum total MSE of the symbol estimates. Such MSEs are calculated for all possible non-zero taps of the end-to-end channel impulse response. The only non-zero tap which yields the smallest total MSE, introduces the relays which have to be turned on.

Finally, we studied the asynchronous two-way relay network in a single-carrier communication scheme using pre-channel equalizers at the both transceivers. Under the assumption of the limited total power of the network, we aimed to optimally obtain the beamforming weight vector as well as the transceivers' powers in order to minimize the total MSE at the both transceivers. We proved that this design leads to a single tap communication scheme and compared the performance of this scheme with that of a post-channel equalization scheme introduced in Chapter 4.

6.2 Future Work

Some possible future work directions are listed below:

- In this thesis, we assumed that the channel state information is perfectly known and developed our data model based on this information. Studying asynchronous bi-directional relay networks with unknown or uncertain channel state information for both multi-carrier and single-carrier communication schemes can be an interesting topic.

- This work was done under the assumption that there is no direct link between

the transceivers. Existing such a direct link between the transceivers changes the signal model and hence, leads to another challenging problem which needs to be studied in detail. Note that assuming direct link between the both transceivers, instead of MABC, the TDBC communication scheme should be considered.

- Deploying both pre- and post-channel block equalizers for a single-carrier communication scheme is another challenging problem which can be studied in the future. It seems that applying both pre- and post-channel equalization blocks at the same time is equivalent to deploying OFDM at the transceivers. The details of the data model and the optimal design of the communication scheme is an open area of research.

- In our single-carrier communication scheme, we deployed both pre- and post-channel block equalization for an asynchronous two-way relay network. Utilizing linear or decision feedback equalization seems to be another challenging open area in this field.

- This thesis focuses on a single-input and single-output communication scheme and assumed that the transceivers are equipped with a single antenna. Extending this work and designing an OFDM-based and single carrier communication scheme for a multiple-input and multiple-output (MIMO) system is another interesting topic which can be investigated in the future work.

- Sum-rate maximization for our developed multi- and single-carrier communication schemes can be studied in the future and the results can be compared with our work where we have minimized the mean squared error for such a communication network.

Appendices

Appendix A

Proof of Lemmas in Chapter 3

A.1 Proof of (3.2.18)

Here, we prove that matrix $\mathbf{D}_q$ is diagonal and then find its elements. Let us define $\mathbf{V} \triangleq \mathbf{R}_{\rm cp}\mathbf{\Gamma}_q = [\mathbf{v}_1 \;\; \mathbf{v}_2 \;\; \cdots \;\; \mathbf{v}_L]$, where $\mathbf{v}_l$ is the lth column of the matrix $\mathbf{V}$. Then, we can write

$$\mathbf{V} = \mathbf{R}_{\rm cp}\mathbf{\Gamma}_q = \begin{bmatrix} \gamma_1(T_{\rm s} - \tau'_{1q}) & \cdots & \gamma_L(T_{\rm s} - \tau'_{Lq}) \\ \gamma_1(2T_{\rm s} - \tau'_{1q}) & \cdots & \gamma_L(2T_{\rm s} - \tau'_{Lq}) \\ \vdots & \ddots & \vdots \\ \gamma_1(NT_{\rm s} - \tau'_{1q}) & \cdots & \gamma_L(NT_{\rm s} - \tau'_{Lq}) \end{bmatrix}. \tag{A.1.1}$$

Now, we can rewrite $\mathbf{D}_q$ as

$$\begin{aligned} \mathbf{D}_q &= \mathrm{E}\{\mathbf{G}_q^H\mathbf{\Gamma}_q^H\mathbf{R}_{\rm cp}^H\mathbf{f}_i\mathbf{f}_i^H\mathbf{R}_{\rm cp}\mathbf{\Gamma}_q\mathbf{G}_q\} \\ &= \mathbf{G}_q^H\mathrm{E}\{\mathbf{V}^H\mathbf{f}_i\mathbf{f}_i^H\mathbf{V}\}\mathbf{G}_q\,. \end{aligned}$$

Let us also define $\mathbf{b} \triangleq \mathbf{V}^H\mathbf{f}_i$. The lth element of vector $\mathbf{b}$ is given by $b_l = \mathbf{v}_l^H\mathbf{f}_i$. Therefore, the expectation of (l,k)th element of the matrix $\mathbf{b}\mathbf{b}^H$ is

$$\mathrm{E}\{b_l b_k^*\} = \mathrm{E}\{\mathbf{v}_l^H\mathbf{f}_i\mathbf{f}_i^H\mathbf{v}_k\} = \mathbf{f}_i^H\mathrm{E}\{\mathbf{v}_l\mathbf{v}_k^H\}\mathbf{f}_i\,. \tag{A.1.2}$$

Note that

$$\mathbf{v}_l\mathbf{v}_k^H = \begin{bmatrix} \gamma_l(T_\mathrm{s}-\tau'_{lq}) \\ \gamma_l(2T_\mathrm{s}-\tau'_{lq}) \\ \vdots \\ \gamma_l(NT_\mathrm{s}-\tau'_{lq}) \end{bmatrix} \times \begin{bmatrix} \gamma_k(T_\mathrm{s}-\tau'_{kq}) & \gamma_k(2T_\mathrm{s}-\tau'_{kq}) & \cdots & \gamma_k(NT_\mathrm{s}-\tau'_{kq}) \end{bmatrix}$$

$$= \begin{bmatrix} \gamma_l(T_\mathrm{s}-\tau'_{lq})\gamma_k(T_\mathrm{s}-\tau'_{kq}) & \cdots & \gamma_l(T_\mathrm{s}-\tau'_{lq})\gamma_k(NT_\mathrm{s}-\tau'_{kq}) \\ \gamma_l(2T_\mathrm{s}-\tau'_{lq})\gamma_k(T_\mathrm{s}-\tau'_{kq}) & \cdots & \gamma_l(2T_\mathrm{s}-\tau'_{lq})\gamma_k(NT_\mathrm{s}-\tau'_{kq}) \\ \vdots & \vdots & \\ \gamma_l(NT_\mathrm{s}-\tau'_{lq})\gamma_k(T_\mathrm{s}-\tau'_{kq}) & \cdots & \gamma_l(NT_\mathrm{s}-\tau'_{lq})\gamma_k(NT_\mathrm{s}-\tau'_{kq}) \end{bmatrix}. \quad \text{(A.1.3)}$$

As we assumed that $\gamma_l(t)$ is spatially and temporally white, the expectation in (A.1.2), when applied to the entries of the matrix $\mathbf{v}_l\mathbf{v}_k^H$, yields non-zero values only if $j = k$ and if correlation is calculated between the same samples of $\gamma_l(t)$. Hence $\mathrm{E}\{\mathbf{v}_l\mathbf{v}_k^H\} = 0$ holds true for $k \neq j$ and

$$\mathrm{E}\{\mathbf{v}_l\mathbf{v}_l^H\} = \begin{bmatrix} \sigma^2 & 0 & \cdots & 0 \\ 0 & \sigma^2 & \cdots & 0 \\ \vdots & \vdots & \ddots & \vdots \\ 0 & 0 & \cdots & \sigma^2 \end{bmatrix}. \quad \text{(A.1.4)}$$

As a result, $\mathrm{E}\{b_l b_l^*\} = \sigma^2$ and $\mathrm{E}\{\mathbf{\Gamma}_q^H\mathbf{R}_{\mathrm{cp}}^H\mathbf{f}_i\mathbf{f}_i^H\mathbf{R}_{\mathrm{cp}}\mathbf{\Gamma}_q\} = \mathrm{diag}\{\sigma^2, \sigma^2, \cdots, \sigma^2\}$ for $l = 1, 2, \ldots, L$, and hence, we conclude that $\mathbf{D}_q = \mathrm{diag}\{\sigma^2|g_{1q}|^2, \sigma^2|g_{2q}|^2, \ldots, \sigma^2|g_{Lq}|^2\}$.

A.2 Proof of Lemma 3.3.1

To prove this lemma, we present the solution to the maximization in (3.3.1). Using (3.2.15), (3.2.17), (3.2.19), and (3.2.23), the optimization problem (3.3.1) can be

written as

$$\begin{aligned} \max_{\mathbf{w}} \quad & \frac{P_{ip}|\mathbf{f}_i^H\mathbf{B}\mathbf{w}|^2}{\mathbf{w}^H\mathbf{D}_q\mathbf{w}+\sigma^2} \\ \text{s.t.} \quad & |w_l|^2\left(|g_{l1}|^2\mathbf{1}^T\mathbf{p}_1+|g_{l2}|^2\mathbf{1}^T\mathbf{p}_2+N\sigma^2\right) \le NP_{l,\max}, \\ & \text{for } l=1,2,\ldots,L. \end{aligned} \tag{A.2.1}$$

where $p \neq q$. To solve (A.2.1), we use the assumptions that $\mathbf{1}^T\mathbf{p}_1 = NP_{\text{Tx1,max}}$ and $\mathbf{1}^T\mathbf{p}_2 = NP_{\text{Tx2,max}}$ to simplify the L inequality constraints in (A.2.1) as $|w_l| \le \lambda_l$, for $l = 1, 2, \ldots, L$, where $\lambda_l \triangleq \left(\frac{P_{l,\max}}{\sigma^2+|g_{l1}|^2P_{\text{Tx1,max}}+|g_{l2}|^2P_{\text{Tx2,max}}}\right)^{\frac{1}{2}}$. For any pair of i and q, we can rewrite the maximization in (A.2.1) as

$$\begin{aligned} \Theta_{iq} = \max_{\mathbf{w}} \quad & \frac{|\mathbf{f}_i^H\mathbf{B}\mathbf{w}|^2}{\mathbf{w}^H\mathbf{D}_q\mathbf{w}+\sigma^2} \\ & \text{subject to} \;\; |w_l| \le \lambda_l \qquad l=1,2,\ldots,L\,. \end{aligned} \tag{A.2.2}$$

Let us define $\boldsymbol{\rho} \triangleq [\rho_1 \;\; \rho_2 \;\; \cdots \;\; \rho_L]^T$ and $\boldsymbol{\psi} \triangleq [\psi_1 \;\; \psi_2 \;\; \cdots \;\; \psi_L]^T$, where ρ_l and ψ_l stand for the amplitude and the phase of w_l, respectively. Taking into account that the denominator of the objective function in (A.2.2) does not depend on $\boldsymbol{\psi}$, we can write the maximization in (A.2.1) as

$$\max_{\boldsymbol{\rho}} \;\; \frac{\delta_{iq}(\boldsymbol{\rho})}{\boldsymbol{\rho}^T\mathbf{D}_q\boldsymbol{\rho}+\sigma^2} \;\; \text{subject to} \;\; \rho_l \le \lambda_l, \qquad l=1,2,\ldots,L \tag{A.2.3}$$

where

$$\delta_{iq}(\boldsymbol{\rho}) \triangleq \max_{\boldsymbol{\psi}} |\mathbf{f}_i^H\mathbf{B}\mathbf{w}|^2 = \max_{\boldsymbol{\psi}} \left|\sum_{l=1}^{L}\rho_l\beta_{li}^q e^{j(\psi_l-\xi_{li}^q)}\right|^2 = \left|\sum_{l=1}^{L}\rho_l\beta_{li}^q\right|^2 = \left|\boldsymbol{\rho}^T\boldsymbol{\beta}_i^q\right|^2 . \tag{A.2.4}$$

In (A.2.4), $p \neq q$ and β_{li}^q and ξ_{li}^q are the amplitude and the phase of the lth entry of $\mathbf{B}^H\mathbf{f}_i$, respectively, and $\boldsymbol{\beta}_i^q \triangleq [\beta_{1i}^q \;\; \beta_{2i}^q \;\; \cdots \;\; \beta_{Li}^q]^T$. It follows from (3.2.6) that $\mathbf{B}_{12} = \mathbf{B}_{21}$, and hence, for any subcarrier index i, we have that $\beta_{li}^1 = \beta_{li}^2$ and $\xi_{li}^1 = \xi_{li}^2$.

Consequently, for any subcarrier index i, $\boldsymbol{\beta}_i^1 = \boldsymbol{\beta}_i^2$, and therefore, $\delta_{i1}(\boldsymbol{\rho}) = \delta_{i2}(\boldsymbol{\rho})$. Hereafter, with a small abuse of notation, we replace $\boldsymbol{\beta}_i^q$, ξ_{li}^q, and $\delta_{iq}(\boldsymbol{\rho})$ with $\boldsymbol{\beta}_i$, ξ_{li}, and $\delta_i(\boldsymbol{\rho})$, respectively. That is, we drop the superscript or the subscript q from these quantities. The maximization in (A.2.4) is achieved when $\psi_l = \xi_{li}$, which means that the phases of different entries of $\mathbf{w}_{iq}^{\mathrm{o}}$ do not depend on the transceiver index q. This completes the proof of part (a).

Using (A.2.4), the maximization in (A.2.2) can be written as

$$\begin{aligned} \max_{\boldsymbol{\rho}} \quad & \frac{|\boldsymbol{\rho}^T \boldsymbol{\beta}_i|^2}{\boldsymbol{\rho}^T \mathbf{D}_q \boldsymbol{\rho} + \sigma^2} \\ \text{subject to} \quad & \rho_l \leq \lambda_l, \qquad l = 1, 2, \ldots, L \end{aligned} \tag{A.2.5}$$

or, equivalently, as

$$\begin{aligned} \max_{\mathbf{y}} \quad & \frac{\langle \mathbf{c}_i^q, \mathbf{y} \rangle^2}{1 + \|\mathbf{y}\|^2} \\ \text{subject to} \quad & \mathbf{y} \preceq \boldsymbol{\alpha}_q \end{aligned} \tag{A.2.6}$$

where the following definitions are used: $\mathbf{y} \triangleq \sigma^{-1} \mathbf{D}_q^{\frac{1}{2}} \boldsymbol{\rho}$, $\mathbf{c}_i^q \triangleq \sigma^{-1} \mathbf{D}_q^{-\frac{1}{2}} \boldsymbol{\beta}_i$, $\boldsymbol{\alpha}_q \triangleq \sigma^{-1} \mathbf{D}_q^{\frac{1}{2}} \boldsymbol{\lambda}$, $\boldsymbol{\lambda} \triangleq [\lambda_1 \ \cdots \ \lambda_L]^T$. The maximization problem in (A.2.6) can be efficiently solved using the approach proposed in [51], and thus, the values of Θ_{iq}, defined as in (3.3.2), can be obtained for $i = 1, 2, \ldots, N$ and $q = 1, 2$. We now show that due to the specific structure of the optimization problem in (A.2.6), the corresponding optimal values of $\boldsymbol{\rho}$ are the same for different subcarrier indices i. To show this, note that as defined in (3.2.6), for $p \neq q$, the matrix $\mathbf{B}^H$ has only one non-zero element in its lth row. This non-zero element is equal to $g_{lp}^* g_{lq}^*$. Hence, using the fact that the magnitudes of all elements of $\mathbf{f}_i$ in (3.2.16) are equal to $\frac{1}{\sqrt{N}}$, we obtain that $\beta_{li} = \frac{|g_{lp} g_{lq}|}{\sqrt{N}}$. This leads us to

$$\boldsymbol{\beta}_1 = \boldsymbol{\beta}_2 = \ldots = \boldsymbol{\beta}_N = \frac{1}{\sqrt{N}} \Big[|g_{1p} g_{1q}| \ \ |g_{2p} g_{2q}| \ \ \cdots \ \ |g_{Lp} g_{Lq}| \Big]^T. \tag{A.2.7}$$

In light of (A.2.7), $\boldsymbol{\beta}_i$ does not depend on i. Hence, $\delta_i(\boldsymbol{\rho})$ and consequently, Θ_{iq} do not depend on i, i.e., $\Theta_{iq} = \Theta_{1q}$ for $i = 1, 2, \ldots, N$. This means that Θ_{iq} is the same for all subcarriers, so are the corresponding optimal values of $\boldsymbol{\rho}$. Therefore, the corresponding optimal values of $\boldsymbol{\rho}$, which achieve $\Theta_{iq} = \Theta_{1q}$, are the same for all subcarrier indices but different for $q = 1, 2$ and this completes the proof of part (b) of the lemma. We have already proven part (c) as $\Theta_{iq} = \Theta_{1q}$ holds true for any i.

A.3 Proof of Lemma 3.3.2

We first show that $\vartheta_{i'q'}^{iq}$, defined as in (3.3.3), depends on $(i - i')\text{mod}N$. To do so, let $\boldsymbol{\rho}_q^{\text{o}}$ denote the vector of the amplitudes of $\mathbf{w}_{iq}^{\text{o}}$. Note that, as we proved in Lemma 3.3.1, $\boldsymbol{\rho}_q^{\text{o}}$ does not depend on the subcarrier index i. Using the fact that the optimal value of the phase of the lth entry of $\mathbf{w}_{iq}^{\text{o}}$ does not depend on i and it is equal to ζ_{li} (as proved in parts (a) and (b) of Lemma 3.3.1), and denoting the lth entry of $\mathbf{w}_{iq}^{\text{o}}$ as $\hat{\rho}_{lq}e^{j\xi_{li}}$, where $\hat{\rho}_{lq}$ is the lth entry of $\boldsymbol{\rho}_q^{\text{o}}$, we can write (3.3.3) as

$$\begin{aligned}
\vartheta_{i'q'}^{iq} &= \frac{|\mathbf{f}_{i'}^H \mathbf{B}\mathbf{w}_{iq}^{\text{o}}|^2}{(\mathbf{w}_{iq}^{\text{o}})^H \mathbf{D}_{q'}\mathbf{w}_{iq}^{\text{o}} + \sigma^2} \\
&= \frac{1}{N}\frac{\left|\sum_{l=1}^{L} \hat{\rho}_{lq} g_{lp} g_{lq} e^{j(\xi_{li} - \xi_{li'})}\right|^2}{(\boldsymbol{\rho}_q^{\text{o}})^T \mathbf{D}_{q'}\boldsymbol{\rho}_q^{\text{o}} + \sigma^2} \\
&= \frac{\left|\sum_{l=1}^{L} \hat{\rho}_{lq} g_{lp} g_{lq} e^{j\frac{2\pi(i-i')}{N}n_l}\right|^2}{(\boldsymbol{\rho}_q^{\text{o}})^T \mathbf{D}_{q'}\boldsymbol{\rho}_q^{\text{o}} + \sigma^2}
\end{aligned} \tag{A.3.1}$$

where, n_l is the column index of the only non-zero entry of the lth row of $\mathbf{B}^H$. It follows from (A.3.1) that the set $\{\vartheta_{i'q'}^{i_1 q}\}_{i'=1}^{N}$ is a permutation of the set $\{\vartheta_{i'q'}^{i_2 q}\}_{i'=1}^{N}$.

A.4 Proof of the Equivalence of (3.3.8) and (3.3.9)

Substituting (3.2.19) in (3.3.8), the optimization problem (3.3.8) can be rewritten as

$$\begin{aligned} \max_{\mathbf{p}_1,\mathbf{p}_2\succeq\mathbf{0}} \quad & \max_{\mathbf{w}} \min_{i\in\{1,2,\ldots,N\}} \min_{q\in\{1,2\}} \frac{P_{ip}|\mathbf{a}_i^H\mathbf{w}|^2}{\mathbf{w}^H\mathbf{D}_q\mathbf{w}+\sigma^2}, \quad p\neq q \\ \text{subject to} \quad & \frac{\mathbf{1}^T\mathbf{p}_1}{N}+\frac{\mathbf{1}^T\mathbf{p}_2}{N}+\sum_{l=1}^{L}\tilde{P}_l \leq P_{\max} \end{aligned} \tag{A.4.1}$$

where $\mathbf{a}_i$ is an $L\times 1$ vector defined as $\mathbf{a}_i \triangleq \mathbf{B}^H\mathbf{f}_i$, for $i\in\{1,2,\ldots,N\}$. Note that without loss of optimality, all SNRs in (3.3.8) can be assumed to be balanced, that is

$$\mathrm{SNR}_{ip}=\mathrm{SNR}_{jq} \quad \text{for } p,q\in\{1,2\}\ ,\ i,j\in\{1,2,\ldots,N\}\,. \tag{A.4.2}$$

Otherwise, if, at the optimum, for any particular values of i, j, p, and q, $\mathrm{SNR}_{ip} > \mathrm{SNR}_{jq}$, then by reducing the optimal value of P_{iq}, (which does not affect the objective function and neither does it violate the total power constraint), we can ensure that $\mathrm{SNR}_{ip}=\mathrm{SNR}_{jq}$ is satisfied. Using (3.2.19) along with (A.4.2), we can easily show that for any transceiver index q, the following relationships between subcarrier transmit powers hold:

$$P_{iq} \;=\; \frac{P_{1q}|\mathbf{a}_1^H\mathbf{w}|^2}{|\mathbf{a}_i^H\mathbf{w}|^2} \quad \text{for } i=1,2,\ldots,N\,. \tag{A.4.3}$$

Also, for $i=j=1$, $p=1$, and $q=2$, we can use (3.2.19) along with (A.4.2) to obtain the following relationship between P_{11} and P_{12}:

$$\frac{P_{11}}{\mathbf{w}^H\mathbf{D}_2\mathbf{w}+\sigma^2} \;=\; \frac{P_{12}}{\mathbf{w}^H\mathbf{D}_1\mathbf{w}+\sigma^2}\,. \tag{A.4.4}$$

Let us define

$$\mathbf{u}(\mathbf{w}) \triangleq \left[\frac{1}{|\mathbf{a}_1^H\mathbf{w}|^2} \;\; \frac{1}{|\mathbf{a}_2^H\mathbf{w}|^2} \;\; \cdots \;\; \frac{1}{|\mathbf{a}_N^H\mathbf{w}|^2}\right]^T. \tag{A.4.5}$$

Using (A.4.3) and (A.4.5), vector $\mathbf{p}_q$ can be written as

$$\begin{aligned}\mathbf{p}_q &= [P_{1q} \;\; P_{2q} \;\; \cdots \;\; P_{Nq}]^T \\ &= \left[P_{1q} \;\; P_{1q}\frac{|\mathbf{a}_1^H\mathbf{w}|^2}{|\mathbf{a}_2^H\mathbf{w}|^2} \;\; \cdots \;\; P_{1q}\frac{|\mathbf{a}_1^H\mathbf{w}|^2}{|\mathbf{a}_N^H\mathbf{w}|^2}\right]^T = P_{1q}|\mathbf{a}_1^H\mathbf{w}|^2\mathbf{u}(\mathbf{w})\,. \end{aligned} \tag{A.4.6}$$

Now, using (3.2.23), and (A.4.2)-(A.4.6), the optimization problem (A.4.1) can be expressed as

$$\begin{aligned}\max_{\mathbf{p}_1,\,\mathbf{p}_2\succeq\mathbf{0}} \;\; &\max_{\mathbf{w}} \frac{P_{11}|\mathbf{a}_1^H\mathbf{w}|^2}{\mathbf{w}^H\mathbf{D}_2\mathbf{w}+\sigma^2} \text{ subject to} \\ &P_{ip} = \frac{P_{1p}|\mathbf{a}_1^H\mathbf{w}|^2}{|\mathbf{a}_i^H\mathbf{w}|^2}, \\ &\text{for } p\in\{1,2\} \;\text{ and } i\in\{1,\ldots,N\} \\ &\frac{P_{11}}{\mathbf{w}^H\mathbf{D}_2\mathbf{w}+\sigma^2} = \frac{P_{12}}{\mathbf{w}^H\mathbf{D}_1\mathbf{w}+\sigma^2} \\ &\frac{P_{11}|\mathbf{a}_1^H\mathbf{w}|^2\mathbf{1}^T\mathbf{u}(\mathbf{w})}{N} + \frac{P_{12}|\mathbf{a}_1^H\mathbf{w}|^2\mathbf{1}^T\mathbf{u}(\mathbf{w})}{N} + \\ \sum_{l=1}^{L}\frac{|w_l|^2}{N}&\left(|g_{l1}|^2\mathbf{1}^T\mathbf{p}_1 + |g_{l2}|^2\mathbf{1}^T\mathbf{p}_2 + N\sigma^2\right) \le P_{\max}\end{aligned} \tag{A.4.7}$$

or, equivalently, as

$$\begin{aligned}&\max_{P_{11}\succeq\mathbf{0}} \;\; \max_{\mathbf{w}} \;\; \frac{P_{11}|\mathbf{a}_1^H\mathbf{w}|^2}{\mathbf{w}^H\mathbf{D}_2\mathbf{w}+\sigma^2} \\ &\text{subject to} \;\; \frac{P_{11}}{\mathbf{w}^H\mathbf{D}_2\mathbf{w}+\sigma^2} = \frac{P_{12}}{\mathbf{w}^H\mathbf{D}_1\mathbf{w}+\sigma^2} \\ &\left[\left(1+\sum_{l=1}^{L}|w_l|^2|g_{l1}|^2\right)P_{11} + \left(1+\sum_{l=1}^{L}|w_l|^2|g_{l2}|^2\right)P_{12}\right] \\ &\frac{|\mathbf{a}_1^H\mathbf{w}|^2\mathbf{1}^T\mathbf{u}(\mathbf{w})}{N} + \sum_{l=1}^{L}|w_l|^2\sigma^2 \le P_{\max}\end{aligned} \tag{A.4.8}$$

where we have used the first $2N$ constraints in (A.4.7) to eliminate all subcarrier powers except P_{11} and P_{12}. Using (A.4.4) (i.e., the first constraint in (A.4.8)), we

rewrite the maximization problem (A.4.8) as

$$\begin{aligned}
&\max_{P_{11}\geq \mathbf{0}} \quad \max_{\mathbf{w}} \frac{P_{11}|\mathbf{a}_1^H\mathbf{w}|^2}{\mathbf{w}^H\mathbf{D}_2\mathbf{w}+\sigma^2} \\
&\text{s.t.} \left[\left(\sigma^2+\mathbf{w}^H\mathbf{D}_1\mathbf{w}\right)+\left(\sigma^2+\mathbf{w}^H\mathbf{D}_2\mathbf{w}\right)\left(\frac{\mathbf{w}^H\mathbf{D}_1\mathbf{w}+\sigma^2}{\mathbf{w}^H\mathbf{D}_2\mathbf{w}+\sigma^2}\right)\right] \\
&\times \frac{P_{11}|\mathbf{a}_1^H\mathbf{w}|^2\mathbf{1}^T\mathbf{u}(\mathbf{w})}{\sigma^2 N}+\sigma^2\mathbf{w}^H\mathbf{w}\leq P_{\max}\,. \qquad \text{(A.4.9)}
\end{aligned}$$

It can be shown that at the optimum, the constraint in (A.4.9) is satisfied with equality, i.e., all the total available power has to be consumed. Otherwise, one can always increase the optimal value of P_{11} such that this constraint is satisfied with equality and this further increases the cost function, thereby contradicting the optimality. Hence, we can write (A.4.9) as

$$\begin{aligned}
\max_{P_{11}\geq \mathbf{0}} \max_{\mathbf{w}} \quad & \frac{P_{11}|\mathbf{a}_1^H\mathbf{w}|^2}{\mathbf{w}^H\mathbf{D}_2\mathbf{w}+\sigma^2} \\
\text{subject to} \quad & P_{11}=\frac{N\sigma^2\left(P_{\max}-\sigma^2\mathbf{w}^H\mathbf{w}\right)}{2(\mathbf{w}^H\mathbf{D}_1\mathbf{w}+\sigma^2)|\mathbf{a}_1^H\mathbf{w}|^2\mathbf{1}^T\mathbf{u}(\mathbf{w})}
\end{aligned}$$

or, equivalently, as

$$\begin{aligned}
\max_{\mathbf{w}} \quad & \frac{N\sigma^2\left(P_{\max}-\sigma^2\mathbf{w}^H\mathbf{w}\right)}{2\left[\left(\mathbf{w}^H\mathbf{D}_1\mathbf{w}+\sigma^2\right)\left(\mathbf{w}^H\mathbf{D}_2\mathbf{w}+\sigma^2\right)\right]\mathbf{1}^T\mathbf{u}(\mathbf{w})} \\
\text{subject to} \quad & \mathbf{w}^H\mathbf{w}\leq\frac{P_{\max}}{\sigma^2}\,. \qquad \text{(A.4.10)}
\end{aligned}$$

The proof is now complete.

A.5 Proof of Lemma 3.3.3

We can rewrite the optimization problem (3.3.11) as

$$\begin{aligned}
\min_{\mathbf{w}} \quad & \frac{1}{N}\sum_{i=1}^{N}\frac{1}{\phi_i(\mathbf{w})} \\
\text{subject to} \quad & \|\mathbf{w}\|^2\leq\frac{P_{\max}}{\sigma^2}\,. \qquad \text{(A.5.1)}
\end{aligned}$$

Lemma A.5.1. *For any set of positive numbers* $\{\phi_i\}_{i=1}^N$*, the following inequality holds:*

$$\sum_{i=1}^{N} \frac{1}{\phi_i} \geq \frac{N^2}{\sum_{i=1}^{N} \phi_i} \tag{A.5.2}$$

where the equality holds iff $\{\phi_i\}_{i=1}^N$ *are all equal.*

Proof: The proof is based on the fact that the arithmetic mean of N positive numbers $\{\phi_i\}_{i=1}^N$ is larger or equal to their harmonic mean:

$$\frac{1}{N} \sum_{i=1}^{N} \phi_i \geq \frac{1}{\frac{1}{N} \sum_{i=1}^{N} \frac{1}{\phi_i}}$$

and equality holds if and only if $\phi_i = \phi_j$, for $i \neq j$. ■

Note that if $\{\phi_i\}_{i=1}^N$ have a certain structure described as $\phi_i = \phi_i(\mathbf{w})$, the equality holds iff one can find such structured $\{\phi_i(\mathbf{w})\}_{i=1}^N$ which are all equal, i.e., iff one can find a value for $\mathbf{w}$ such that all $\phi_i(\mathbf{w})$'s are all equal. Let $\mathcal{W}$ represent the set of such values of $\mathbf{w}$. Then, without any loss of optimality, we can rewrite the optimization in (A.5.1) as

$$\begin{aligned} \min_{\mathbf{w}} \quad & \frac{1}{N} \sum_{i=1}^{N} \frac{1}{\phi_i(\mathbf{w})} \\ \text{subject to} \quad & \|\mathbf{w}\|^2 \leq \frac{P_{\max}}{\sigma^2} \quad \text{and } \mathbf{w} \in \mathcal{W}\,. \end{aligned} \tag{A.5.3}$$

Note that the optimization problem (A.5.3) is feasible, (i.e., its feasible set is not empty) as its feasible set includes $\mathbf{w} = \mathbf{0}$. As for any $\mathbf{w} \in \mathcal{W}$, we have that $\sum_{i=1}^{N} \frac{1}{\phi_i(\mathbf{w})} = N^2 (\sum_{i=1}^{N} \phi_i(\mathbf{w}))^{-1}$, we can rewrite (A.5.3), equivalently, as

$$\begin{aligned} \min_{\mathbf{w}} \quad & N \left(\sum_{i=1}^{N} \phi_i(\mathbf{w}) \right)^{-1} \\ \text{subject to} \quad & \|\mathbf{w}\|^2 \leq \frac{P_{\max}}{\sigma^2} \quad \text{and } \mathbf{w} \in \mathcal{W}\,. \end{aligned} \tag{A.5.4}$$

or as

$$\begin{aligned} \max_{\mathbf{w}} \quad & \frac{\sigma^2\left(P_{\max}-\sigma^2\mathbf{w}^H\mathbf{w}\right)\sum_{i=1}^{N}|\mathbf{w}^H\mathbf{a}_i|^2}{2N\left(\mathbf{w}^H\mathbf{D}_1\mathbf{w}+\sigma^2\right)\left(\mathbf{w}^H\mathbf{D}_2\mathbf{w}+\sigma^2\right)} \\ \text{subject to} \quad & \|\mathbf{w}\|^2 \le \frac{P_{\max}}{\sigma^2} \quad \text{and } \mathbf{w}\in\mathcal{W}\,. \end{aligned} \tag{A.5.5}$$

Noting that

$$\sum_{i=1}^{N}|\mathbf{w}^H\mathbf{a}_i|^2=\sum_{i=1}^{N}|\mathbf{w}^H\mathbf{B}^H\mathbf{f}_i|^2=\|\mathbf{B}\mathbf{w}\|^2=\mathbf{w}^H\mathbf{B}^H\mathbf{B}\mathbf{w} \tag{A.5.6}$$

where the second equality follows from the Parseval's theorem, we can further simplify (A.5.5) as

$$\begin{aligned} \max_{\mathbf{w}} \quad & \frac{\sigma^2\left(P_{\max}-\sigma^2\mathbf{w}^H\mathbf{w}\right)\mathbf{w}^H\mathbf{B}^H\mathbf{B}\mathbf{w}}{2N\left(\mathbf{w}^H\mathbf{D}_1\mathbf{w}+\sigma^2\right)\left(\mathbf{w}^H\mathbf{D}_2\mathbf{w}+\sigma^2\right)} \\ \text{subject to} \quad & \|\mathbf{w}\|^2 \le \frac{P_{\max}}{\sigma^2} \quad \text{and } \mathbf{w}\in\mathcal{W}\,. \end{aligned} \tag{A.5.7}$$

We now characterize the set $\mathcal{W}$. In order for $\phi_i(\mathbf{w})$, $i=1,2,\ldots,N$, to be all equal, $\mathbf{w}\in\mathcal{W}$ should be such that, for any $i\neq j$, the following equation holds:

$$|\mathbf{w}^H\mathbf{a}_i|^2=|\mathbf{w}^H\mathbf{a}_j|^2\,. \tag{A.5.8}$$

The condition in (A.5.8) is equivalent to the following constraint on $\mathbf{w}$:

$$|\mathbf{f}_i^H\mathbf{B}\mathbf{w}|^2=|\mathbf{f}_j^H\mathbf{B}\mathbf{w}|^2\,. \tag{A.5.9}$$

Lemma A.5.2. *The condition in* (A.5.9) *implies that the discrete-time FIR end-to-end channel impulse response $h_{pq}[\cdot]$ must have a constant-amplitude discrete-time Fourier representation.*

Proof: The matrix $\mathbf{B}$ has only one non-zero element in each column. Let us say that for the lth column, this non-zero element is located at the m_lth row and its value

is equal to $g_{lp}g_{lq}$. Hence, we can write $|\mathbf{f}_i^H\mathbf{B}\mathbf{w}|^2 = \mathbf{w}^H\mathbf{B}^H\mathbf{f}_i\mathbf{f}_i^H\mathbf{B}\mathbf{w}$ as

$$\mathbf{w}^H \begin{bmatrix} g_{1p}^* g_{1q}^* e^{j\frac{2\pi}{N}(i-1)(m_1-1)} \\ \vdots \\ g_{Lp}^* g_{Lq}^* e^{j\frac{2\pi}{N}(i-1)(m_L-1)} \end{bmatrix} \begin{bmatrix} g_{1p}g_{1q}e^{-j\frac{2\pi}{N}(i-1)(m_1-1)} & \cdots & g_{Lp}g_{Lq}e^{-j\frac{2\pi}{N}(i-1)(m_L-1)} \end{bmatrix} \mathbf{w}$$

$$= \mathbf{w}^H \begin{bmatrix} g_{1p}^* g_{1q}^* g_{1p}g_{1q} & \cdots & g_{1p}^* g_{1q}^* g_{Lp}g_{Lq}e^{j\frac{2\pi}{N}(i-1)(m_1-m_L)} \\ \vdots & \ddots & \vdots \\ g_{Lp}^* g_{Lq}^* g_{1p}g_{1q}e^{j\frac{2\pi}{N}(i-1)(m_L-m_1)} & \cdots & g_{Lp}^* g_{Lq}^* g_{Lp}g_{Lq} \end{bmatrix} \mathbf{w}$$

$$= \sum_{l'=1}^{L}\sum_{l=1}^{L} g_{l'p}^* g_{l'q}^* g_{lp}g_{lq}w_{l'}w_l \left(e^{j\frac{2\pi}{N}(i-1)(m_{l'}-m_l)} + e^{-j\frac{2\pi}{N}(i-1)(m_{l'}-m_l)}\right)$$

$$= \sum_{l'=1}^{L}\sum_{l=1}^{L} g_{l'p}^* g_{l'q}^* g_{lp}g_{lq}w_{l'}w_l \cos\left(\frac{2\pi}{N}(i-1)(m_{l'}-m_l)\right). \quad \text{(A.5.10)}$$

In order for (A.5.10) to be independent of i, we need to have either $m_{l'} = m_l$, for $l', l = 1, \ldots, L$ or if $m_{l'} \neq m_l$ for any l and l', then $w_l w_{l'} = 0$. This means that only one set of the relays which all contribute to the same element of $\mathbf{B}\mathbf{w}$ should be turned on and the remainder of the relays have to be turned off. This condition on $\mathbf{B}\mathbf{w}$ implies that the multipath end-to-end channel turns into a frequency flat channel. The proof is now complete. ■

Lemma A.5.2 implies that $\mathbf{h}$ has only one non-zero element. The reason is that any allpass FIR filter has only one non-zero tap. Hence, the set $\mathcal{W}$ is such that only one of the entries of $\mathbf{h}$ is non-zero. The proof is now complete.

Appendix B

Derivations for Chapter 4

B.1 Calculating $\mathbf{R}_q(\mathbf{w})$

Using (4.2.11), we can also write

$$\begin{aligned}
\mathbf{R}_q(\mathbf{w}) &\triangleq \mathrm{E}\left\{\mathbf{r}_q(i)\mathbf{r}_q^H(i)\right\} \\
&= \mathrm{E}\left\{\left(\sqrt{P_{-q}}\widetilde{\mathbf{H}}(\mathbf{w})\mathbf{s}_{-q}(i)+\widetilde{\boldsymbol{\gamma}}_q(i)\right)\left(\sqrt{P_{-q}}\widetilde{\mathbf{H}}(\mathbf{w})\mathbf{s}_{-q}(i)+\widetilde{\boldsymbol{\gamma}}_q(i)\right)^H\right\} \\
&= P_{-q}\widetilde{\mathbf{H}}(\mathbf{w})\mathrm{E}\left\{\mathbf{s}_{-q}(i)\mathbf{s}_{-q}^H(i)\right\}\widetilde{\mathbf{H}}^H(\mathbf{w})+\mathrm{E}\left\{\widetilde{\boldsymbol{\gamma}}_q(i)\widetilde{\boldsymbol{\gamma}}_q^H(i)\right\} \\
&= P_{-q}\widetilde{\mathbf{H}}(\mathbf{w})\widetilde{\mathbf{H}}^H(\mathbf{w})+\mathbf{R}_{\mathrm{cp}}\mathrm{E}\left\{\overline{\boldsymbol{\gamma}}_q(i)\overline{\boldsymbol{\gamma}}_q^H(i)\right\}\mathbf{R}_{\mathrm{cp}}^H \\
&= P_{-q}\widetilde{\mathbf{H}}(\mathbf{w})\widetilde{\mathbf{H}}^H(\mathbf{w})+\mathbf{R}_{\mathrm{cp}}\mathrm{E}\left\{\left(\overline{\boldsymbol{\Upsilon}}_q(i)\mathbf{G}_q\mathbf{w}+\overline{\boldsymbol{\gamma}}_q'(i)\right)\left(\overline{\boldsymbol{\Upsilon}}_q(i)\mathbf{G}_q\mathbf{w}+\overline{\boldsymbol{\gamma}}_q'(i)\right)^H\right\}\mathbf{R}_{\mathrm{cp}}^H \\
&= P_{-q}\widetilde{\mathbf{H}}(\mathbf{w})\widetilde{\mathbf{H}}^H(\mathbf{w}) \\
&+ \mathbf{R}_{\mathrm{cp}}\mathrm{E}\left\{\overline{\boldsymbol{\Upsilon}}_q(i)\mathbf{G}_q\mathbf{w}\mathbf{w}^H\mathbf{G}_q^H\boldsymbol{\Upsilon}_q^H(i)\right\}\mathbf{R}_{\mathrm{cp}}^H+\mathbf{R}_{\mathrm{cp}}\mathrm{E}\left\{\overline{\boldsymbol{\gamma}}_q'(i)\overline{\boldsymbol{\gamma}}_q'^H(i)\right\}\mathbf{R}_{\mathrm{cp}}^H \\
&= P_{-q}\widetilde{\mathbf{H}}(\mathbf{w})\widetilde{\mathbf{H}}^H(\mathbf{w})+\mathbf{R}_{\mathrm{cp}}\mathrm{E}\left\{\overline{\boldsymbol{\Upsilon}}_q(i)\mathbf{G}_q\mathbf{w}\mathbf{w}^H\mathbf{G}_q^H\boldsymbol{\Upsilon}_q^H(i)\right\}\mathbf{R}_{\mathrm{cp}}^H+\sigma^2\mathbf{R}_{\mathrm{cp}}\mathbf{R}_{\mathrm{cp}}^H
\end{aligned} \tag{B.1.1}$$

Since $\mathbf{R}_{\mathrm{cp}}\mathbf{R}_{\mathrm{cp}}^H=\mathbf{I}_{N_s}$, we can write (B.1.1)

$$\mathbf{R}_q(\mathbf{w})=P_{-q}\widetilde{\mathbf{H}}(\mathbf{w})\widetilde{\mathbf{H}}^H(\mathbf{w})+\mathbf{R}_{\mathrm{cp}}\mathrm{E}\left\{\overline{\boldsymbol{\Upsilon}}_q(i)\mathbf{G}_q\mathbf{w}\mathbf{w}^H\mathbf{G}_q^H\boldsymbol{\Upsilon}_q^H(i)\right\}\mathbf{R}_{\mathrm{cp}}^H+\sigma^2\mathbf{I}_{N_s} \tag{B.1.2}$$

To further simplify (B.1.2), we now show that $\mathbf{Y}_q \triangleq \mathrm{E}\left\{\overline{\mathbf{\Upsilon}}_q(i)\mathbf{G}_q\mathbf{w}\mathbf{w}^H\mathbf{G}_q^H\mathbf{\Upsilon}_q^H(i)\right\}$ is equal to $\sigma^2\mathbf{w}^H\mathbf{G}_q^H\mathbf{G}_q\mathbf{w}\mathbf{I}_{N_t}$. To do so, we write $\overline{\mathbf{\Upsilon}}_q(i)\mathbf{G}_q\mathbf{w}$ as

$$\overline{\mathbf{\Upsilon}}_q(i)\mathbf{G}_q\mathbf{w} = \begin{bmatrix} \mathbf{v}_{iN_t,q} & \mathbf{v}_{iN_t+1,q} & \cdots & \mathbf{v}_{(iN_t+N_t-1),q} \end{bmatrix}^T \begin{bmatrix} g_{1q}w_1 \\ g_{2q}w_2 \\ \vdots \\ g_{Lq}w_L \end{bmatrix} =$$

$$\begin{bmatrix} \upsilon_1[iN_t - n'_{1q}] & \upsilon_2[iN_t - n'_{2q}] & \cdots & \upsilon_L[iN_t - n'_{Lq}] \\ \upsilon_1[iN_t + 1 - n'_{1q}] & \upsilon_2[iN_t + 1 - n'_{2q}] & \cdots & \upsilon_L[iN_t + 1 - n'_{Lq}] \\ \vdots & \vdots & \cdots & \vdots \\ \upsilon_1[iN_t + N_t - 1 - n'_{1q}] & \upsilon_2[iN_t + N_t - 1 - n'_{2q}] & \cdots & \upsilon_L[iN_t + N_t - 1 - n'_{Lq}] \end{bmatrix}$$

$$\times \begin{bmatrix} g_{1q}w_1 \\ g_{2q}w_2 \\ \vdots \\ g_{Lq}w_L \end{bmatrix} = \begin{bmatrix} \sum_{l=1}^{L} g_{lq}w_l\upsilon_l[iN_t - n'_{Lq}] \\ \sum_{l=1}^{L} g_{lq}w_l\upsilon_l[iN_t + 1 - n'_{Lq}] \\ \vdots \\ \sum_{l=1}^{L} g_{lq}w_l\upsilon_l[iN_t + N_t - 1 - n'_{Lq}] \end{bmatrix} \tag{B.1.3}$$

Now, we can write $\mathbf{Y}_q$ as

$$\mathbf{Y}_q = \mathrm{E}\left\{ \begin{bmatrix} \sum_{l=1}^{L} g_{lq}w_l\upsilon_l[iN_t - n'_{Lq}] \\ \vdots \\ \sum_{l=1}^{L} g_{lq}w_l\upsilon_l[iN_t + N_t - 1 - n'_{Lq}] \end{bmatrix} \times \right.$$
$$\left. \begin{bmatrix} \sum_{l=1}^{L} g^*_{lq}w^*_l\upsilon^*_l[iN_t - n'_{Lq}] & \cdots & \sum_{l=1}^{L} g^*_{lq}w^*_l\upsilon^*_l[iN_t + N_t - 1 - n'_{Lq}] \end{bmatrix} \right\} \tag{B.1.4}$$

or, equivalently, as

$$\begin{aligned}
\mathbf{Y}_q &= \mathrm{diag}\Bigg\{ \mathrm{E}\Bigg\{ \left(\sum_{l=1}^{L} g_{lq} w_l \upsilon_l[iN_t + k - 1 - n'_{Lq}] \right) \\
&\qquad \left(\sum_{l=1}^{L} g_{lq} w_l \upsilon_l[iN_t + k - 1 - n'_{Lq}] \right) \Bigg\} \Bigg\}_{k=1}^{N_t} \\
&= \mathrm{diag} \left\{ \sum_{l=1}^{L} g_{lq} g_{lq}^* w_l w_l^* \mathrm{E} \left\{ \upsilon_l^*[iN_t + k - 1 - n'_{Lq}] \upsilon_l[iN_t + k - 1 - n'_{Lq}] \right\} \right\}_{k=1}^{N_t} \\
&= \sigma^2 \mathrm{diag} \left\{ \sum_{l=1}^{L} g_{lq} g_{lq}^* w_l w_l^* \right\}_{k=1}^{N_t} \\
&= \sigma^2 \mathrm{diag} \left\{ \mathbf{w}^H \mathbf{G}_q^H \mathbf{G}_q \mathbf{w} \right\}_{k=1}^{N_t} = \sigma^2 \mathbf{w}^H \mathbf{G}_q^H \mathbf{G}_q \mathbf{w} \mathbf{I}_{N_t}
\end{aligned} \tag{B.1.5}$$

Using (B.1.5), we can rewrite (B.1.2) as

$$\begin{aligned}
\mathbf{R}_q(\mathbf{w}) &= P_{-q} \widetilde{\mathbf{H}}(\mathbf{w}) \widetilde{\mathbf{H}}^H(\mathbf{w}) + \mathbf{R}_{\mathrm{cp}} \left(\sigma^2 \mathbf{w}^H \mathbf{G}_q^H \mathbf{G}_q \mathbf{w} \right) \mathbf{R}_{\mathrm{cp}}^H + \sigma^2 \mathbf{I}_{N_s} \\
&= P_{-q} \widetilde{\mathbf{H}}(\mathbf{w}) \widetilde{\mathbf{H}}^H(\mathbf{w}) + \sigma^2 \left(\mathbf{w}^H \mathbf{G}_q^H \mathbf{G}_q \mathbf{w} + 1 \right) \mathbf{I}_{N_s}
\end{aligned} \tag{B.1.6}$$

B.2 Deriving (4.3.10)

We can rewrite (4.3.8) as

$$
\begin{aligned}
\lambda(\mathbf{w}, P_1, P_2) &= \sum_{q=1}^{2} \left(N_s - P_{\bar{q}} \mathrm{tr}\left\{\mathbf{F}^H \mathbf{D}^H(\mathbf{w}) \mathbf{F} \mathbf{R}_q^{-1}(\mathbf{w}) \mathbf{F}^H \mathbf{D}(\mathbf{w}) \mathbf{F}\right\}\right) \\
&= \sum_{q=1}^{2} \left(N_s - P_{\bar{q}} \mathrm{tr}\left\{\underbrace{\mathbf{F}\mathbf{F}^H}_{\mathbf{I}} \mathbf{D}^H(\mathbf{w}) \mathbf{F} \mathbf{R}_q^{-1}(\mathbf{w}) \mathbf{F}^H \mathbf{D}(\mathbf{w})\right\}\right) \\
&= 2N_s - \sum_{q=1}^{2} P_{\bar{q}} \mathrm{tr}\left\{\mathbf{D}^H(\mathbf{w}) (\mathbf{F} \mathbf{R}_q(\mathbf{w}) \mathbf{F}^H)^{-1} \mathbf{D}(\mathbf{w})\right\} \\
&= 2N_s - \sum_{q=1}^{2} P_{\bar{q}} \mathrm{tr}\left\{\mathbf{D}^H(\mathbf{w}) \left(\mathbf{F} \left(P_{\bar{q}} \widetilde{\mathbf{H}}(\mathbf{w}) \widetilde{\mathbf{H}}^H(\mathbf{w}) + \sigma^2 \left(\|\mathbf{G}_q \mathbf{w}\|^2 + 1\right) \mathbf{I}_{N_s}\right) \mathbf{F}^H\right)^{-1} \mathbf{D}(\mathbf{w})\right\} \\
&= 2N_s - \sum_{q=1}^{2} P_{\bar{q}} \mathrm{tr}\left\{\mathbf{D}^H(\mathbf{w}) \left(P_{\bar{q}} \underbrace{\mathbf{F}\widetilde{\mathbf{H}}(\mathbf{w})}_{\mathbf{D}(\mathbf{w})\mathbf{F}^H} \underbrace{\widetilde{\mathbf{H}}^H(\mathbf{w}) \mathbf{F}^H}_{\mathbf{F}\mathbf{D}^H(\mathbf{w})} + \sigma^2 \left(\|\mathbf{G}_q \mathbf{w}\|^2 + 1\right) \underbrace{\mathbf{F}\mathbf{F}^H}_{\mathbf{I}}\right)^{-1} \mathbf{D}(\mathbf{w})\right\} \\
&= 2N_s - \sum_{q=1}^{2} P_{\bar{q}} \mathrm{tr}\left\{\mathbf{D}^H(\mathbf{w}) \left(P_{\bar{q}} \mathbf{D}(\mathbf{w}) \underbrace{\mathbf{F}\mathbf{F}^H}_{\mathbf{I}} \mathbf{D}^H(\mathbf{w}) + \sigma^2 \left(\|\mathbf{G}_q \mathbf{w}\|^2 + 1\right) \mathbf{I}_{N_s}\right)^{-1} \mathbf{D}(\mathbf{w})\right\} \\
&= 2N_s - \sum_{q=1}^{2} P_{\bar{q}} \mathrm{tr}\left\{\mathbf{D}^H(\mathbf{w}) \left(P_{\bar{q}} \mathbf{D}(\mathbf{w}) \mathbf{D}^H(\mathbf{w}) + \sigma^2 \left(\|\mathbf{G}_q \mathbf{w}\|^2 + 1\right) \mathbf{I}_{N_s}\right)^{-1} \mathbf{D}(\mathbf{w})\right\} .
\end{aligned}
\tag{B.2.1}
$$

B.3 The expression for T-SNR

Here, we derive the expression for T-SNR. To do so, we first obtain the noise power in (4.2.11) as

$$\begin{aligned} P_{\mathrm{n},q} &= \frac{1}{N_t}\mathrm{E}\left\{\overline{\boldsymbol{\gamma}}_q^H(i)\overline{\boldsymbol{\gamma}}_q(i)\right\} \\ &= \frac{1}{N_t}\mathrm{E}\left\{\left(\mathbf{w}^H\mathbf{G}_q^H\overline{\boldsymbol{\Upsilon}}_q^H(i)+\overline{\boldsymbol{\gamma}}_q^{'H}(i)\right)\left(\overline{\boldsymbol{\Upsilon}}_q(i)\mathbf{G}_q\mathbf{w}+\overline{\boldsymbol{\gamma}}_q^{'}(i)\right)\right\} \\ &= \frac{1}{N_t}\mathbf{w}^H\mathbf{G}_q^H\mathrm{E}\{\overline{\boldsymbol{\Upsilon}}_q^H(i)\overline{\boldsymbol{\Upsilon}}_q(i)\}\mathbf{G}_q\mathbf{w}+\frac{1}{N_t}\mathrm{E}\{\overline{\boldsymbol{\gamma}}_q^{'H}(i)\overline{\boldsymbol{\gamma}}_q^{'}(i)\} \\ &= \sigma^2(\mathbf{w}^H\mathbf{G}_q^H\mathbf{G}_q\mathbf{w}+1) \end{aligned} \tag{B.3.1}$$

The total power of the signal received at Transceiver q, corresponding to different information symbols, in a block can be obtained as

$$\begin{aligned} P_{\mathrm{s},q} &= \frac{1}{N_s}\mathrm{E}\left\{\left(\sqrt{P_{\bar{q}}}\widetilde{\mathbf{H}}(\mathbf{w})\mathbf{s}_{\bar{q}}(i)\right)^H\left(\sqrt{P_{\bar{q}}}\widetilde{\mathbf{H}}(\mathbf{w})\mathbf{s}_{\bar{q}}(i)\right)\right\} \\ &= \frac{P_{\bar{q}}}{N_s}\mathrm{E}\left\{\mathbf{s}_{\bar{q}}^H(i)\widetilde{\mathbf{H}}^H(\mathbf{w})\widetilde{\mathbf{H}}(\mathbf{w})\mathbf{s}_{\bar{q}}(i)\right\} \\ &= \frac{P_{\bar{q}}}{N_s}\mathrm{tr}\left[\widetilde{\mathbf{H}}(\mathbf{w})\mathrm{E}\left\{\mathbf{s}_{\bar{q}}(i)\mathbf{s}_{\bar{q}}^H(i)\right\}\widetilde{\mathbf{H}}^H(\mathbf{w})\right] \\ &= \frac{P_{\bar{q}}}{N_s}\mathrm{tr}\left[\widetilde{\mathbf{H}}^H(\mathbf{w})\widetilde{\mathbf{H}}(\mathbf{w})\right] = \frac{P_{\bar{q}}}{N_s}\mathrm{tr}\left[\mathbf{F}^H\mathbf{D}^H(\mathbf{w})\mathbf{D}(\mathbf{w})\mathbf{F}\right] \\ &= P_{\bar{q}}\sum_{k=1}^{N_s}|\mathbf{f}_k^H\mathbf{B}\mathbf{w}|^2 = P_{\bar{q}}\mathbf{w}^H\mathbf{B}^H\mathbf{B}\mathbf{w}\,. \end{aligned} \tag{B.3.2}$$

Hence, using the total received SNR at Transceiver q can be written as

$$\text{T-SNR}_q = \frac{P_{\mathrm{s},q}}{P_{\mathrm{n},q}} = \frac{P_{\bar{q}}\mathbf{w}^H\mathbf{B}^H\mathbf{B}\mathbf{w}}{\sigma^2(\|\mathbf{G}_q\mathbf{w}\|^2+1)}\,. \tag{B.3.3}$$

B.4 Expression for the SNR in the kth entry of $\mathbf{r}_q(i)$

In the kth entry of $\mathbf{r}_q(i)$, denoting the kth entries of $\overline{\boldsymbol{\gamma}}_q(i)$ and $\overline{\boldsymbol{\gamma}}'_q(i)$ as $\overline{\gamma}_{k,q}(i)$ and $\overline{\gamma}'_{k,q}(i)$, respectively, the received noise power can be obtained as

$$\begin{aligned} P_{\mathrm{n},k,q} &= \mathrm{E}\{\overline{\gamma}^*_{k,q}(i)\overline{\gamma}_{k,q}(i)\} \\ &= \mathrm{E}\{(\mathbf{w}^H\mathbf{G}_q^H\mathbf{v}^*_{iN_t+k-1,q} + \overline{\gamma}'^*_{k,q}(i))(\mathbf{v}^T_{iN_t+k-1,q}\mathbf{G}_q\mathbf{w} + \overline{\gamma}'_{k,q}(i))\} \\ &= \mathbf{w}^H\mathbf{G}_q^H\mathrm{E}\{\mathbf{v}^*_{iN_t+k-1,q}\mathbf{v}^T_{iN_t+k-1,q}\}\mathbf{G}_q\mathbf{w} + \mathrm{E}\{\overline{\gamma}'^*_{k,q}(i)\overline{\gamma}'_{k,q}(i)\} \\ &= \sigma^2(\mathbf{w}^H\mathbf{G}_q^H\mathbf{G}_q\mathbf{w} + 1)\,. \end{aligned} \tag{B.4.1}$$

Before being corrupted by the noise, the kth entry of $\mathbf{r}_q(i)$ can be written as

$$\grave{r}_{k,q}(i) = \sqrt{P_{\bar{q}}}\tilde{\mathbf{h}}_k^T\mathbf{s}_{\bar{q}}(i) \tag{B.4.2}$$

where $\tilde{\mathbf{h}}_k^T$ is the kth row of $\widetilde{\mathbf{H}}(\mathbf{w})$. The power of $\grave{r}_{k,q}(i)$ can be calculated as

$$\begin{aligned} P_{\mathrm{s},k,q} &= \mathrm{E}\left\{\grave{r}_{k,q}(i)\grave{r}^*_{k,q}(i)\right\} = P_{\bar{q}}\tilde{\mathbf{h}}_k^T\mathrm{E}\left\{\mathbf{s}_{\bar{q}}(i)\mathbf{s}^H_{\bar{q}}(i)\right\}\tilde{\mathbf{h}}_k^* \\ &= P_{\bar{q}}\tilde{\mathbf{h}}_k^T\tilde{\mathbf{h}}_k^* = P_{\bar{q}}\|\mathbf{h}\|^2 = P_{\bar{q}}\mathbf{w}^H\mathbf{B}^H\mathbf{B}\mathbf{w} \\ &= P_{\bar{q}}\sum_{n=0}^{N-1}\mathbf{w}_n^H\mathbf{b}_n\mathbf{b}_n^H\mathbf{w}_n\,. \end{aligned} \tag{B.4.3}$$

Therefore, at Transceiver q, the SNR of the kth entry of $\mathbf{r}_q(i)$ can be represented as

$$\mathrm{SNR}_{k,q} = \frac{P_{\mathrm{s},k,q}}{P_{\mathrm{n},k,q}} = \frac{P_{\bar{q}}\mathbf{w}^H\mathbf{B}^H\mathbf{B}\mathbf{w}}{\sigma^2(\|\mathbf{G}_q\mathbf{w}\|^2 + 1)}\,. \tag{B.4.4}$$

Appendix C

Proofs in Chapter 5

C.1 Proof of Lemma 5.3.1

The Lagrangian of the optimization problem (5.3.26) can be written as

$$\begin{aligned}\mathcal{L}_\zeta(\boldsymbol{\alpha}, \kappa_1, \kappa_2) \triangleq & \sum_{k=1}^{N_s} \left(\frac{\mu_1}{\alpha_k + \mu_1}\right)^2 + \sum_{k=1}^{N_s} \left(\frac{\mu_2}{\alpha_k + \mu_2}\right)^2 \\ & + \kappa_1 \left[\left(\sum_{k=1}^{N_s} \frac{\alpha_k}{(\alpha_k + \mu_1)^2}\right) - P_1 N_s\right] + \kappa_2 \left[\left(\sum_{k=1}^{N_s} \frac{\alpha_k}{(\alpha_k + \mu_2)^2}\right) - P_2 N_s\right]\end{aligned} \tag{C.1.1}$$

The derivative of Lagrange function with respect to α_k is

$$\frac{\partial}{\partial \boldsymbol{\alpha}} \mathcal{L}_\zeta(\alpha_k) = \frac{-2\mu_1^2 + \kappa_1(\mu_1 - \alpha_k)}{(\alpha_k + \mu_1)^3} + \frac{-2\mu_2^2 + \kappa_2(\mu_2 - \alpha_k)}{(\alpha_k + \mu_2)^3}. \tag{C.1.2}$$

Equating (C.1.2) to zero results in

$$\frac{-2\mu_1^2 + \kappa_1(\mu_1 - \alpha_k)}{(\alpha_k + \mu_1)^3} = -\frac{-2\mu_2^2 + \kappa_2(\mu_2 - \alpha_k)}{(\alpha_k + \mu_2)^3}. \tag{C.1.3}$$

Equation (C.1.3) holds true for any value of $k = 1, 2, \cdots, N_s$. That means α_k is independent of k and all α_k's are the same. The proof is complete. ■

C.2 Proving that the inequality constraint in (5.3.42) is satisfied with equality

Let us assume that $\mathbf{w} = \sqrt{\eta}\tilde{\mathbf{w}}$, where $\|\tilde{\mathbf{w}}\| = 1$. Then, the left hand side of the inequality constraint in (5.3.42) can be written as

$$\tilde{f}(\eta) \triangleq \frac{2 + \eta\tilde{\mathbf{w}}^H\mathbf{G}_1^H\mathbf{G}_1\tilde{\mathbf{w}} + \eta\tilde{\mathbf{w}}^H\mathbf{G}_1^H\mathbf{G}_1\tilde{\mathbf{w}}}{\eta\tilde{\mathbf{w}}^H\mathbf{B}^H\mathbf{B}\tilde{\mathbf{w}}} + \sigma^2\eta. \tag{C.2.1}$$

The derivative of this function with respect to η is

$$\frac{\partial\tilde{f}(\eta)}{\partial\eta} = \frac{-2}{\eta^2\tilde{\mathbf{w}}^H\mathbf{B}^H\mathbf{B}\tilde{\mathbf{w}}} + \sigma^2. \tag{C.2.2}$$

Equating (C.2.2) to zero, we can obtain the value of η as

$$\eta = \sqrt{\frac{2}{\sigma^2\tilde{\mathbf{w}}^H\mathbf{B}^H\mathbf{B}\tilde{\mathbf{w}}}}. \tag{C.2.3}$$

Note that $\tilde{f}(\eta)$ is a decreasing function of η for those values which are less than the one obtained in (C.2.3). This means that by decreasing the norm of $\mathbf{w}$, one can increase the left hand side of the constraint in (5.3.42). Hence, if at the optimum, the inequality constraint in (5.3.42) is not satisfied with equality, we can reduce the norm of the optimal $\mathbf{w}$ such that the left hand side of the inequality constraint in (5.3.42) is increased and it becomes equal to P_{max}. However, this so-obtained value of $\mathbf{w}$ will result in a smaller value of the objective function and this contradicts optimality. The proof is complete.

C.3 Relationship between MSE and SNR

The MSE for Transceiver q can be obtained as:

$$\begin{aligned}
\mathrm{MSE}_q &= \mathrm{E}\left\{\mathbf{e}_q^H(i)\mathbf{e}_q(i)\right\} \\
&= \mathrm{E}\left\{[\widetilde{\mathbf{H}}(\mathbf{w})\mathbf{F}_{\bar{q}}\mathbf{s}_{\bar{q}}(i)+\widetilde{\boldsymbol{\gamma}}_q(i)-\mathbf{s}_{\bar{q}}(i)]^H[\widetilde{\mathbf{H}}(\mathbf{w})\mathbf{F}_{\bar{q}}\mathbf{s}_{\bar{q}}(i)+\widetilde{\boldsymbol{\gamma}}_q(i)-\mathbf{s}_{\bar{q}}(i)]\right\} \\
&= \mathrm{E}\left\{[(\widetilde{\mathbf{H}}(\mathbf{w})\mathbf{F}_{\bar{q}}-\mathbf{I})\mathbf{s}_{\bar{q}}(i)+\widetilde{\boldsymbol{\gamma}}_q(i)]^H[(\widetilde{\mathbf{H}}(\mathbf{w})\mathbf{F}_{\bar{q}}-\mathbf{I})\mathbf{s}_{\bar{q}}(i)+\widetilde{\boldsymbol{\gamma}}_q(i)]\right\} \\
&= \mathrm{E}\left\{[\mathbf{s}_{\bar{q}}^H(i)(\widetilde{\mathbf{H}}(\mathbf{w})\mathbf{F}_{\bar{q}}-\mathbf{I})^H+\widetilde{\boldsymbol{\gamma}}_q^H(i)][(\widetilde{\mathbf{H}}(\mathbf{w})\mathbf{F}_{\bar{q}}-\mathbf{I})\mathbf{s}_{\bar{q}}(i)+\widetilde{\boldsymbol{\gamma}}_q(i)]\right\} \\
&= \mathrm{E}\left\{\mathbf{s}_{\bar{q}}^H(i)(\widetilde{\mathbf{H}}(\mathbf{w})\mathbf{F}_{\bar{q}}-\mathbf{I})^H(\widetilde{\mathbf{H}}(\mathbf{w})\mathbf{F}_{\bar{q}}-\mathbf{I})\mathbf{s}_{\bar{q}}(i)+\widetilde{\boldsymbol{\gamma}}_q^H(i)\widetilde{\boldsymbol{\gamma}}_q(i)\right\} \\
&= \mathrm{E}\left\{\mathrm{tr}[\mathbf{s}_{\bar{q}}^H(i)(\widetilde{\mathbf{H}}(\mathbf{w})\mathbf{F}_{\bar{q}}-\mathbf{I})^H(\widetilde{\mathbf{H}}(\mathbf{w})\mathbf{F}_{\bar{q}}-\mathbf{I})\mathbf{s}_{\bar{q}}(i)]\right\}+\mathrm{E}\left\{\widetilde{\boldsymbol{\gamma}}_q^H(i)\widetilde{\boldsymbol{\gamma}}_q(i)\right\} \\
&= \mathrm{E}\left\{\mathrm{tr}[(\widetilde{\mathbf{H}}(\mathbf{w})\mathbf{F}_{\bar{q}}-\mathbf{I})\mathbf{s}_{\bar{q}}(i)\mathbf{s}_{\bar{q}}^H(i)(\widetilde{\mathbf{H}}(\mathbf{w})\mathbf{F}_{\bar{q}}-\mathbf{I})^H]\right\}+N_s\sigma^2 \\
&= \mathrm{tr}\left[\mathrm{E}\left\{[(\widetilde{\mathbf{H}}(\mathbf{w})\mathbf{F}_{\bar{q}}-\mathbf{I})\mathbf{s}_{\bar{q}}(i)\mathbf{s}_{\bar{q}}^H(i)(\widetilde{\mathbf{H}}(\mathbf{w})\mathbf{F}_{\bar{q}}-\mathbf{I})^H\right\}\right]+N_s\sigma^2 \\
&= \mathrm{tr}\left[(\widetilde{\mathbf{H}}(\mathbf{w})\mathbf{F}_{\bar{q}}-\mathbf{I})\mathrm{E}\left\{\mathbf{s}_{\bar{q}}(i)\mathbf{s}_{\bar{q}}^H(i)\right\}(\widetilde{\mathbf{H}}(\mathbf{w})\mathbf{F}_{\bar{q}}-\mathbf{I})^H\right]+N_s\sigma^2 \\
&= \| \widetilde{\mathbf{H}}(\mathbf{w})\mathbf{F}_{\bar{q}}-\mathbf{I} \|^2+N_s\sigma^2
\end{aligned} \tag{C.3.1}$$

The received SNR at Transceiver q is calculated as:

$$\mathrm{SNR}_q = \frac{\mathrm{E}\left\{[\widetilde{\mathbf{H}}(\mathbf{w})\mathbf{F}_{\bar{q}}\mathbf{s}_{\bar{q}}(i)]^H[\widetilde{\mathbf{H}}(\mathbf{w})\mathbf{F}_{\bar{q}}\mathbf{s}_{\bar{q}}(i)]\right\}}{\mathrm{E}\left\{\widetilde{\boldsymbol{\gamma}}_q^H(i)\widetilde{\boldsymbol{\gamma}}_q(i)\right\}} = \frac{\| \widetilde{\mathbf{H}}(\mathbf{w})\mathbf{F}_{\bar{q}} \|^2}{N_s\sigma^2} \tag{C.3.2}$$

Comparing (C.3.1) and (C.3.2), we can conclude that

$$\mathrm{MSE}_q = \| \widetilde{\mathbf{H}}(\mathbf{w})\mathbf{F}_{\bar{q}}-\mathbf{I} \|^2+\frac{\| \widetilde{\mathbf{H}}(\mathbf{w})\mathbf{F}_{\bar{q}} \|^2}{\mathrm{SNR}_q} \tag{C.3.3}$$

Bibliography

[1] A. Sendonaris, E. Erkip, and B. Aazhang, "User cooperation diversity-part I: System description," *IEEE Transactions on Communications*, vol. 51, pp. 1927–1938, Nov. 2003.

[2] A. Sendonaris, E. Erkip, and B. Aazhang, "User cooperation diversity-part II: Implementation aspects and performance analysis," *IEEE Transactions on Communications*, vol. 51, pp. 1939–1948, Nov. 2003.

[3] T. Cover and A. E. Gamal, "Capacity theorems for the relay channel," *IEEE Transactions on Information Theory*, vol. 25, pp. 572–584, Sep. 1979.

[4] J. N. Laneman, *Cooperative diversity in wireless networks: algorithms and architectures*. Phd thesis, Masachusetts Institute of Technology, MA, USA, Sep. 2002.

[5] J. N. Laneman, D. N. C. Tse, and G. W. Wornell, "Cooperative diversity in wireless networks: Efficient protocols and outage behavior," *IEEE Transactions on Information Theory*, vol. 50, pp. 3062–3080, Dec. 2004.

[6] J. Yu, M. Li, "Is amplify-and-forward practically better than decode-andforward or vice versa?," in *Proc. IEEE International Conference on Acoustics, Speech, and Signal Processing (ICASSP), Philadelphia, USA*, vol. 3, Mar. 2005.

[7] R. Lusina, P. Schober and L. Lampe, "Diversity-multiplexing trade-off of the hybrid non-orthogonal amplify-decode and forward protocol," in *Proc. IEEE International Symposium on Information Theory (ISIT), Toronto, Canada*, Jul. 2008.

[8] J. N. Laneman and G. W. Wornell, "Distributed space-time-coded protocols for exploiting cooperative diversity in wireless networks," *IEEE Transactions on Information Theory*, vol. 49, pp. 2415–2425, Oct. 2003.

[9] Y. Jing and B. Hassibi, "Distributed space-time coding in wireless relay networks," *IEEE Transactions on Wireless Communications*, vol. 5, pp. 3524–3536, Dec 2006.

[10] Y. Jing and H. Jafarkhani, "Network beamforming using relays with perfect channel information," in *Proc. International Conference on Acoustics, Speech, and Signal Processing (ICASSP), Honolulu, HI,*, vol. 3, Apr. 2007.

[11] C. E. Shannon, "Two-way communication channels," in *Proc. 4th Berkeley Symposium on Mathematics, Statistics, and Probability*, pp. 611–644, 1961.

[12] R. Zhang, Y.-C. Liang, C. C. Chai, and S. Cui, "Optimal beamforming for two-way multi-antenna relay channel with analogue network coding," *IEEE Journal on Selected Areas in Communications*, vol. 27, pp. 699–712, June. 2009.

[13] M. Chen and A. Yener, "Interference management for multiuser two-way relaying," in *Proc. 42th Annual Conference on Information Sciences and Systems (CISS), Princeton, NJ*, pp. 246–251, Mar. 2008.

[14] J. Joung and A. H. Sayed, "Multiuser two-way relaying method for beamforming systems," in *Proc. IEEE International Workshop on Signal Processing Advances in Wireless Communications (SPAWC), Perugia, Italy*, pp. 280–284, June 2009.

[15] F. Roemer and M. Haardt, "Tensor-based channel estimation (tence) for two-way relaying with multiple antennas and spatial reuse," in *Proc. IEEE International Conference on Acoustics, Speech and Signal Processing, Taipei, Taiwan*, pp. 3641–3644, Apr. 2009.

[16] S. J. Kim, P. Mitran, and V. Tarokh, "Performance bounds for bidirectional coded cooperation protocols," *IEEE Transactions on Information Theory*, vol. 54, pp. 5235–5241, Nov. 2008.

[17] S. J. Kim, N. Devroye, P. Mitran, and V. Tarokh, "Achievable rate regions for bi-directional relaying," *http://arXiv/0808.0954*.

[18] S. J. Kim, N. Devroye, P. Mitran, and V. Tarokh, "Comparison of bi-directional relaying protocols," in *Proc. IEEE Sarnoff Symposium, Princeton, NJ*, pp. 1–5, Apr.

[19] R. Vaze and R. W. Heath, "Optimal amplify and forward strategy for two-way relay channel with multiple relays," in *Proc. IEEE Information Theory Workshop ITW, Volos, Greece*, pp. 181–185, June 2009.

[20] J. Joung and A. H. Sayed, "User selection methods for multiuser two-way relay communications using space division multiple access," *IEEE Transactions on Wireless Communications*, vol. 9, pp. 2130–2136, Jul. 2010.

[21] J. Joung and A. Sayed, "Multiuser two-way amplify-and-forward relay processing and power control methods for beamforming systems," *IEEE Transactions on Signal Processing*, vol. 58, pp. 1833–1846, Mar. 2010.

[22] F. Roemer and M. Haardt, "Tensor-based channel estimation and iterative refinements for two-way relaying with multiple antennas and spatial reuse," *IEEE Transactions on Signal Processing*, vol. 58, pp. 5720–5735, Nov. 2010.

[23] F. Roemer and M. Haardt, "Algebraic norm-maximizing (ANOMAX) transmit strategy for two-way relaying with MIMO amplify and forward relays," *IEEE Signal Processing Letters*, vol. 16, pp. 909–912, Oct. 2009.

[24] T. Oechtering, C. Schnurr, I. Bjelakovic, and H. Boche, "Broadcast capacity region of two-phase bidirectional relaying," *IEEE Transactions on Information Theory*, vol. 54, pp. 454–458, Jan. 2008.

[25] V. Havary-Nassab, S. Shahbazpanahi, and A. Grami, "Optimal distributed beamforming for two-way relay networks," *IEEE Transactions on Signal Processing*, vol. 58, pp. 1238–1250, Mar. 2010.

[26] S. Shahbazpanahi, "A semi-closed-form solution to optimal decentralized beamforming for two-way relay networks," in *Proc. IEEE International Workshop on Computational Advances in Multi-Sensor Adaptive Processing (CAMSAP), Aruba*, pp. 101–104, Dec 2009.

[27] S. Shahbazpanahi and M. Dong, "A semi-closed form solution to the SNR balancing problem of two-way relay network beamforming," in *Proc. IEEE International Conference on Acoustics, Speech and Signal Processing (ICASSP), Dallas, TX*, pp. 2514–2517, Mar. 2010.

[28] S. Shahbazpanahi and M. Dong, "Achievable rate region and sum-rate maximization for network beamforming for bi-directional relay networks," in *Proc. IEEE International Conference on Acoustics, Speech and Signal Processing (ICASSP), Dallas, TX*, pp. 2510–2513, Mar. 2010.

[29] Y.-U. Jang, E.-R. Jeong, and Y. Lee, "A two-step approach to power allocation for OFDM signals over two-way amplify-and-forward relay," *IEEE Transactions on Signal Processing*, vol. 58, pp. 2426–2430, Apr. 2010.

[30] M. Chen and A. Yener, "Power allocation for F/TDMA multiuser two-way relay networks," *IEEE Transactions on Wireless Communications*, vol. 9, pp. 546–551, Feb. 2010.

[31] T. Koike-Akino, P. Popovski, and V. Tarokh, "Optimized constellations for two-way wireless relaying with physical network coding," *IEEE Journal on Selected Areas in Communications*, vol. 27, pp. 773–787, June. 2009.

[32] H. Q. Ngo, T. Quek, and H. Shin, "Amplify-and-forward two-way relay networks: Error exponents and resource allocation," *IEEE Journal on Communications*, vol. 58, pp. 2653–2666, Sep. 2010.

[33] R. Vaze and R. Heath, "On the capacity and diversity-multiplexing tradeoff of the two-way relay channel," *IEEE Transactions on Information Theory*, vol. 57, pp. 4219–4234, Jul. 2011.

[34] M. Zeng, R. Zhang, and S. Cui, "On design of collaborative beamforming for two-way relay networks," *IEEE Transactions on Signal Processing*, vol. 59, pp. 2284 –2295, May. 2011.

[35] M. Zaeri-Amirani, S. Shahbazpanahi, T. Mirfakhraie, and K. Ozdemir, "Performance tradeoffs in amplify-and-forward bidirectional network beamforming," *IEEE Transactions on Signal Processing*, vol. 60, pp. 4196–4209, Aug. 2012.

[36] H. Chen, A. Gershman, and S. Shahbazpanahi, "Filter-and-forward distributed beamforming in relay networks with frequency selective fading," *IEEE Journal on Signal Processing*, vol. 58, pp. 1251–1262, Mar. 2010.

[37] H. Chen, A. Gershman, and S. Shahbazpanahi, "Filter-and-forward distributed beamforming for relay networks in frequency selective fading channels," in *Proc. IEEE International Conference on Acoustics, Speech and Signal Processing (ICASSP), Taipei, Taiwan*, pp. 2269–2272, Apr. 2009.

[38] H. Chen, A. Gershman, and S. Shahbazpanahi, "Filter-and-forward distributed beamforming for two-way relay networks with frequency selective channels," in *Proc. IEEE Global Telecommunications Conference (GLOBECOM), Miami, FL*, pp. 1–5, Dec. 2010.

[39] A. Schad, H. Chen, A. Gershman, and S. Shahbazpanahi, "Filter-and-forward multiple peer-to-peer beamforming in relay networkswith frequency selective channels," in *Proc. IEEE International Conference on Acoustics, Speech and Signal Processing (ICASSP), Dallas, TX*, pp. 3246–3249, Mar. 2010.

[40] Y. wen Liang, A. Ikhlef, W. Gerstacker, and R. Schober, "Cooperative filter-and-forward beamforming for frequency-selective channels with equalization," *IEEE Transactions on Wireless Communications*, vol. 10, pp. 228 –239, Jan. 2011.

[41] Y. wen Liang, A. Ikhlef, W. Gerstacker, and R. Schober, "Filter-and-forward beamforming for multiple multi-antenna relays," in *Proc. the 5th International ICST Conference on Communications and Networking in China (CHINACOM), Beijing, China*, pp. 1 –8, Aug. 2010.

[42] Y. wen Liang, A. Ikhlef, W. Gerstacker, and R. Schober, "Cooperative filter-and-forward beamforming with linear equalization," in *Proc. IEEE Global Telecommunications Conference (GLOBECOM), Miami, FL*, pp. 1–6, Dec. 2010.

[43] H. Chen, S. Shahbazpanahi, and A. Gershman, "Filter-and-forward distributed beamforming for two-way relay networks with frequency selective channels," *IEEE Transactions on Signal Processing*, vol. 60, pp. 1927–1941, Apr. 2012.

[44] M. Dong and S. Shahbazpanahi, "Optimal spectrum sharing and power allocation for OFDM-based two-way relaying," in *Proc. IEEE International Conference on Acoustics, Speech and Signal Processing (ICASSP), Dallas, TX*, pp. 3310–3313, Mar. 2010.

[45] Y. Chang and Y. Hua, "Application of space-time linear block codes to parallel wireless relays in mobile ad hoc networks," *in Proc. the 36th Asilomar Conference on Signals, Systems and Computers, Asilomar, CA*, pp. 1002–1006, Nov. 2003.

[46] R. U. Nabar, H. Bolcskei, and F. W. Kneubuhler, "Fading relay channels: performance limits and space-time signal design," *IEEE Journal on Selected Areas in Communications*, vol. 22, pp. 1099–1109, Aug. 2004.

[47] A. F. Dana and B. Hassibi, "On the power efficiency of sensory and ad hoc wireless networks," *IEEE Transactions on Information Theory*, vol. 52, pp. 2890–2914, Jul. 2006.

[48] M. Janani, A. Hedayat, T. E. Hunter, and A. Nosratinia, "Coded cooperation in wireless communications: space-time transmission and iterative decoding," *IEEE Transactions on Signal Processing*, vol. 52, pp. 362–371, Feb. 2004.

[49] Y. Jing and H. Jafarkhani, "Distributed differential space-time coding in wireless relay networks," *IEEE Transactions on Wireless Communications*, vol. 56, pp. 1092–1100, Jul. 2008.

[50] F. Oggier and B. Hassibi, "A coding strategy for wireless networks with no channel information," in *Proc. Allerton Conference on Communications, Control, and Computing, Monticello, IL*, pp. 113–117, Sep. 2006.

[51] Y. Jing and H. Jafarkhani, "Network beamforming using relays with perfect channel information," *IEEE Transactions on Information Theory*, vol. 55, pp. 2499–2517, June 2009.

[52] Y. Liang, V. Veeravalli, and H. Poor, "Resource allocation for wireless fading relay channels: Max-min solution," in *IEEE Transactions on Information Theory*, vol. 53, pp. 3432–3453, Oct. 2007.

[53] Y. Yao, X. Cai, and G. Giannakis, "On energy efficiency and optimum resource allocation of relay transmissions in the low-power regime," *IEEE Transactions on Wireless Communications*, vol. 4, pp. 2917 – 2927, Nov. 2005.

[54] A. Host-Madsen and J. Zhang, "Capacity bounds and power allocation for wireless relay channels," *IEEE Transactions on Information Theory*, vol. 51, pp. 2020 –2040, June. 2005.

[55] M. Hasna and M.-S. Alouini, "Optimal power allocation for relayed transmissions over rayleigh-fading channels," *IEEE Transaction on Wireless Communications*, vol. 3, pp. 1999 – 2004, Nov. 2004.

[56] Y.-W. Hong, W.-J. Huang, F.-H. Chiu, and C.-C. J. Kuo, "Cooperative communications in resource-constrained wireless networks," *IEEE Signal Processing Magazine*, vol. 24, pp. 47–57, May 2007.

[57] A. Abdelkader, S. Shahbazpanahi, and A. Gershman, "Joint subcarrier power loading and distributed beamforming in OFDM-based asynchronous relay networks," in *Proc. the 3rd IEEE International Workshop on Computational Advances in Multi-Sensor Adaptive Processing (CAMSAP), Aruba*, pp. 105–108, Dec. 2009.

[58] V. Havary-Nassab, S. Shahbazpanahi, A. Grami, and Z. Q. Luo, "Distributed beamforming for relay networks based on second-order statistics of the channel state information," *IEEE Transactions on Signal Processing*, vol. 56, pp. 4306–4316, Sep. 2008.

[59] V. Havary-Nassab, S. Shahbazpanahi, and A. Grami, "An snr balancing approach to two-way relaying," in *Proc. IEEE 10th Workshop on Signal Processing Advances in Wireless Communications (SPAWC), Perugia, Italy*, pp. 250 –254, June. 2009.

[60] W. Cheng, M. Ghogho, Q. Huang, D. Ma, and J. Wei, "Maximizing the sum-rate of amplify-and-forward two-way relaying networks," *IEEE Signal Processing Letters*, vol. 18, Nov. 2011.

[61] A. Schad, A. B. Gershman, and S. Shahbazpanahi, "Capacity maximization for distributed beamforming in one- and bi-directional relay networks," in *Proc. IEEE International Conference on Acoustics, Speech and Signal Processing (ICASSP), Prague, Czech Republic*, pp. 2804 –2807, May 2011.

[62] A. Stefanov and E. Erkip, "Cooperative coding for wireless networks," *IEEE Transactions on Communications*, vol. 52, pp. 1470 – 1476, Sep. 2004.

[63] P. Mitran, H. Ochiai, and V. Tarokh, "Space-time diversity enhancements using collaborative communications," *IEEE Transactions on Information Theory*, vol. 51, pp. 2041 – 2057, June. 2005.

[64] S. Nam, M. Vu, and V. Tarokh, "Relay selection methods for wireless cooperative communications," in *Proc. the 42nd Annual Conference on Information Sciences and Systems (CISS), Princeton, NJ*, pp. 859 –864, Mar. 2008.

[65] S. Wen-miao, L. Yong-qian, L. Bao-Gang, and H. Jian-dong, "Cooperative partners selection in the cooperative diversity ad-hoc network," in *Proc. the 2nd International Conference on Mobile Technology, Applications and Systems (ICMTAS)*, pp. 4 pp. –4, Nov. 2005.

[66] Z. Li and E. Erkip, "Relay search algorithms for coded cooperative systems," in *Proc. IEEE Global Telecommunications Conference (GLOBECOM), St Louis, MO*, vol. 3, p. 6 pp., Nov. 2005.

[67] V. Shah, N. Mehta, and R. Yim, "The relay selection and transmission trade-off in cooperative communication systems," *IEEE Transactions on Wireless Communications*, vol. 9, pp. 2505 –2515, Aug. 2010.

[68] Y. Jing and H. Jafarkhani, "Single and multiple relay selection schemes and their achievable diversity orders," *IEEE Transactions on Wireless Communications*, vol. 8, pp. 1414 –1423, Mar. 2009.

[69] D. Michalopoulos, G. Karagiannidis, T. Tsiftsis, and R. Mallild, "Wlc41-1: An optimized user selection method for cooperative diversity systems," in *Proc. IEEE Global Telecommunications Conference (GLOBECOM), San Francisco, CA*, pp. 1 –6, Dec. 2006.

[70] B. Gedik and M. Uysal, "Two channel estimation methods for amplify-and-forward relay networks," in *Proc. Canadian Conference on Electrical and Computer Engineering (CCECE), Niagara Falls, ON*, pp. 000615 –000618, May. 2008.

[71] A. Lalos, A. Rontogiannis, and K. Berberidis, "Channel estimation techniques in amplify and forward relay networks," in *Proc. IEEE 9th Workshop on Signal Processing Advances in Wireless Communications (SPAWC), Recife, Brazil*, pp. 446 –450, Jul. 2008.

[72] Y. Yan, G. M. Jo, S. Balakannan, and M. H. Lee, "Joint channel estimation in asynchronous amplify-and-forward relay networks based on OFDM signaling," in *Proc. the 9th International Symposium on Communications and Information Technology (ISCIT), Incheon, Korea*, pp. 871 –875, Sep. 2009.

[73] H. Yomo and E. de Carvalho, "A CSI estimation method for wireless relay network," *IEEE Communications Letters*, vol. 11, pp. 480 –482, June. 2007.

[74] A. Behbahani and A. Eltawil, "On channel estimation and capacity for amplify and forward relay networks," in *Proc. IEEE Global Telecommunications Conference (GLOBECOM), New Orleans, LA*, pp. 1 –5, Dec. 2008.

[75] S. Sun and Y. Jing, "Channel training and estimation in distributed space-time coded relay networks with multiple transmit/receive antennas," in *Proc. IEEE Wireless Communications and Networking Conference (WCNC), Sydney, Australia*, pp. 1 –6, Apr. 2010.

[76] F. Gao, R. Zhang, and Y.-C. Liang, "Optimal channel estimation and training design for two-way relay networks," *IEEE Transactions on Communications*, vol. 57, pp. 3024 –3033, Oct. 2009.

[77] B. Jiang, F. Gao, X. Gao, and A. Nallanathan, "Channel estimation and training design for two-way relay networks with power allocation," *IEEE Transactions on Wireless Communications*, vol. 9, pp. 2022 –2032, June. 2010.

[78] F. Gao, R. Zhang, and Y.-C. Liang, "Channel estimation for ofdm modulated two-way relay networks," *IEEE Transactions on Signal Processing*, vol. 57, pp. 4443 –4455, Nov. 2009.

[79] Y. Jia and A. Vosoughi, "Impact of channel estimation error upon sum-rate in amplify-and-forward two-way relaying systems," in *Proc. IEEE International Workshop on Signal Processing Advances in Wireless Communications (SPAWC), Marrakech, Morocco*, pp. 1 –5, June. 2010.

[80] Y. Jia and A. Vosoughi, "Sum-rate maximization of two-way amplify-and-forward relay networks with imperfect channel state information," in *Proc. IEEE International Conference on Acoustics, Speech and Signal Processing (ICASSP), Prague, Czech Republic*, pp. 2808 –2811, May. 2011.

[81] Y. Zhao, R. Adve, and T. Lim, "Improving amplify-and-forward relay networks: optimal power allocation versus selection," *IEEE Transactions on Wireless Communications*, vol. 6, pp. 3114 –3123, Aug. 2007.

[82] G. Zheng, K.-K. Wong, A. Paulraj, and B. Ottersten, "Collaborative-relay beamforming with perfect CSI: Optimum and distributed implementation," *IEEE Signal Processing Letters*, vol. 16, pp. 257 –260, Apr. 2009.

[83] S. ShahbazPanahi and M. Dong, "Achievable rate region under joint distributed beamforming and power allocation for two-way relay networks," *IEEE Transactions on Wireless Communications*, vol. 11, pp. 4026–4037, Nov. 2012.

[84] Z. Wang and G. Giannakis, "Wireless multicarrier communications," *IEEE Signal Processing Magazine*, vol. 17, pp. 29 –48, May. 2000.

[85] J. Mirzaee, S. ShahbazPanahi, and R. Vahidnia, "Sum-rate maximization for active channels," *IEEE Signal Processing Letters*, vol. 20, pp. 771–774, Aug. 2013.